PRACA DOKTORSKA

IChF

Warsaw-4-PhD
Warsaw Doctoral School
in Natural and BioMedical Sciences

PhD Thesis

Stabilization of bacteriophages against adverse conditions

Mateusz Wdowiak

Supervisor:
Dr hab. Jan Paczesny, prof. IChF

Doctoral dissertation prepared within
Warsaw PhD School in Natural and BioMedical Sciences
at the Institute of Physical Chemistry,
Polish Academy of Sciences
Marcina Kasprzaka 44/52,
01-224 Warszawa

March 2024

Acknowledgments

"*What's interesting, the chance meetings are the ones that influence our lives*" ~ Otis the Scribe, *Asterix & Obelix: Mission Cleopatra*

The completion of this PhD thesis wouldn't have been possible without the people who had offered me a helping hand in my hour of need. First, I thank my supervisor, Prof. Jan Paczesny, for a huge dose of freedom and trust in my experimental work and the possibility to perform the scientific projects of my design. The vivid discussions and his comments helped me shape my manuscripts, this thesis, and motivated me to keep "giving more" and become a better scientist.

Next, I'd like to thank:

Dr. Eng. Agnieszka Wiśniewska, my friend at the IPC PAS, for engaging talks, warm coffee, pieces of life wisdom, and her assistance with performing the DSC analysis.

Aneta Karpińska, for her support, kind words, and help with performing the cytotoxicity assay, which was particularly important at the final stages of my work.

Rafał Zbonikowski, for his help with the estimation of the binding constant, and a piece of chemist's point of view (which I still need to have supplemented).

Bartłomiej Bończak, for assistance with BOA surface modification.

Quy Ong Khac, for assistance with cryoSEM imaging.

Colleagues from Team 2, with an emphasis on Enkhlin Ochirbat and Natalia Szczepańska, for keeping me (occasionally) distracted from my office duties.

My greatest gratitude to my parents, who were there for me no matter how foolish a decision I made. Their support and care allowed me to make it through and carry forward.

Lastly, I'd like to thank all my friends and everyone who believed in me.
And those who didn't, for a motivation to eventually succeed.

Funding

This work was supported by:

1. The National Science Centre, Poland, within the SONATA BIS grant "*Modification of virion stability - stabilization and inactivation of viruses"* according to decision number 2017/26/E/ST4/00041,
2. The Foundation for Polish Science from the European Regional Development Fund within the project POIR.04.04.00-00-14D6/18-00 "*Hybrid sensor platforms for integrated photonic systems based on ceramic and polymer materials* (HYPHa)" (TEAM-NET program).

List of publications

Publications related to the thesis:

1. **Mateusz Wdowiak,** Enkhlin Ochirbat, Jan Paczesny, *Gold—Polyoxoborates Nanocomposite Prohibits Adsorption of Bacteriophages on Inner Surfaces of Polypropylene Labware and Protects Samples from Bacterial and Yeast Infections*
   Viruses 2021, 13(7): 1206; doi.org/10.3390/v13071206
2. **Mateusz Wdowiak**, Jan Paczesny, Sada Raza (2022), *Enhancing the Stability of Bacteriophages Using Physical, Chemical, and Nano-Based Approaches: A Review*. *Pharmaceutics* 14(9): 1936; doi.org/10.3390/pharmaceutics14091936
3. **Mateusz Wdowiak**, Patryk A. Mierzejewski, Rafał Zbonikowski, Bartłomiej Bończak, Jan Paczesny (2023), *Congo red protects bacteriophages against UV irradiation and allows for the simultaneous use of phages and UV for membrane sterilization*. *Environmental Science: Water Research & Technology* 9(3): 696-706; doi.org/ 10.1039/D2EW00913G
4. **Mateusz Wdowiak**, Magdalena Tomczyńska, Quy Ong Khac, Aneta Karpińska, Agnieszka Wiśniewska, Rafał Zbonikowski, Francesco Stellacci, Jan Paczesny, *Multi-functional phage-stabilizing formulation for the simultaneous protection from the UV irradiation and elevated temperature*, submitted
5. **Mateusz Wdowiak**, Yurika Nishimura, Patryk A. Mierzejewski, Krzysztof Bielec, Witold Adamkiewicz, Grzegorz Bubak, Agnieszka Wiśniewska, Bartłomiej Bończak, Ryesuke Takeuchi, Shinobu Sato, Toshinari Maeda, Shigeori Takenaka, Satomi Yano, Haruka Ohtani, Kazunori Matsuura, Jan Paczesny, *Stabilization of virions using acridinyl-flanked poly(ethylene glycol): A promising approach for enhanced viability and therapeutic efficacy*, manuscript in preparation

Other publications:

6. Jan Paczesny, **Mateusz Wdowiak**, Enkhlin Ochirbat (2022), Bacteriophage-based biosensors: detection of bacteria and beyond. Book chapter in Nanotechnology for Infectious Diseases, 439-473; doi.org/10.1007/978-981-16-9190-4_20
7. Sada Raza, **Mateusz Wdowiak**, Jan Paczesny (2023), *An Overview of Diverse Strategies To Inactivate Enterobacteriaceae-Targeting Bacteriophages*. *EcoSal Plus*;
   doi.org/10.1128/ecosalplus.esp-0019-2022
8. Sada Raza, **Mateusz Wdowiak,** Mateusz Grotek, Witold Adamkiewicz, Kostiantyn Nikiforow, Pumza Mente, Jan Paczesny (2023), *Enhancing the antimicrobial activity of silver nanoparticles against ESKAPE bacteria and emerging fungal pathogens by using tea extracts*.
   Nanoscale Advances 5: 5786-5798; doi.org/10.1039/D3NA00220A
9. Anna Kusior, Julia Mazurkow, Piotr Jeleń, Maciej Bik. Sada Raza, **Mateusz Wdowiak**, Kostiantyn Nikiforow, Jan Paczesny, *Copper oxide electrochemical deposition to create antiviral and antibacterial nanocoatings*, submitted

Patents and patent applications:

10. **Mateusz Wdowiak**, Patryk A. Mierzejewski, Jan Paczesny, Patent no. P.441359 (02.06.2022)
    Original title: *Zastosowanie barwnika absorbującego promieniowanie ultrafioletowe do ochrony bakteriofagów przed promieniowaniem ultrafioletowym, sposób sterylizacji urządzeń przemysłowych oraz zastosowanie bakteriofagów zawierających barwnik absorbujący promieniowanie ultrafioletowe do sterylizacji urządzeń przemysłowych w procesach biotechnologicznych.*
    Title in English: *The use of a dye absorbing ultraviolet radiation to protect bacteriophages against ultraviolet radiation, a method for sterilizing industrial equipment and the use of bacteriophages containing a dye absorbing ultraviolet radiation for sterilization of industrial equipment in biotechnological processes.*
11. **Mateusz Wdowiak,** Jan Paczesny, Patent application no. P.447692 (02.02.2024),
    Original title: *Zastosowanie kompozycji zawierającej barwnik i polimer do ochrony bakteriofagów przed promieniowaniem ultrafioletowym i wysoką temperaturą oraz sposób sterylizacji przy użyciu bakteriofagów i wymienionej kompozycji*.
    Title in English: *The use of a composition containing a dye and a polymer to protect bacteriophages against ultraviolet radiation and high temperature, and a sterilization method using bacteriophages and the said composition*.

Abstract

The spread of drug resistance among microbes has become the modern-day plague and forced the entire scientific community to search for alternative methods for bacteria elimination. Bacteriophages - a group of viruses that infect bacterial cells - came out of the depths of history and appeared as the light at the end of the tunnel for this struggle. Phages are natural antimicrobials. As biological beings, they can evolve as fast as pathogenic bacteria do, giving humanity a chance to catch up in this arms race. However, this property remains their weak point, for the components of bacteriophage's virion (proteins and nucleic acids) can be damaged by adverse conditions, such as temperature, radiation, or chemical compounds. Therefore, efficient methods for phage stabilization against adverse conditions are essential to fully embrace the potential of those exceptional viruses.

This thesis aims to combine molecular biology and physical chemistry methods to develop novel and more efficient methods for bacteriophage stabilization. Effectively stabilized, phages could be applied in laboratory, industrial, and environmental conditions to aid their applicability, e.g., in fighting bacterial infections.

The following chapters of this thesis describe the use of nanomaterials, small molecular dyes, and polymers against selected adverse conditions. An inorganic nanocomposite was used to improve long-term phage storage in plastic labware. The stabilization of bacteriophages from UV irradiation was provided using small molecular dyes. Polymers provided stabilization during the exposure to elevated temperature.

Along with the real-life applications of the described methods, I also explained the mechanism behind the stabilizing properties of each of the examined factors. In the case of dye-mediated UV stabilization, the results presented in this thesis are the first to deal with such an issue.

The methods proposed in this thesis are based on compounds that are harmless to animals and the environment or designed to reduce the release of harmful substances outside the experimental systems. Successfully applied, the methods proposed in this thesis would allow the introduction of bacteriophages to sterilize flow bioreactor systems, preserve food, and be used in agriculture.

Streszczenie

Rozprzestrzenianie się lekooporności pośród drobnoustrojów stało się plagą współczesności i zmusiło całą społeczność naukową do poszukiwania alternatywnych metod eliminacji bakterii. Bakteriofagi, wirusy infekujące komórki bakterii, wydają się idealnym narzędziem do tego celu. Fagi są bytami biologicznymi, dlatego są w stanie ewoluować równie szybko, jak bakterie chorobotwórcze, dając ludzkości szansę w tym wyścigu zbrojeń. Ta właściwość pozostaje jednak również ich słabym punktem, gdyż element składowe wirionów, białka i kwasy nukleinowe, mogą łatwo zostać uszkodzone przez niekorzystne warunki, takie jak temperatura, promieniowanie czy związki chemiczne. Dlatego aby w pełni wykorzystać potencjał tych wyjątkowych wirusów, niezbędne są skuteczne metody stabilizacji.

Celem niniejszej pracy było połączenie metod biologii molekularnej i chemii fizycznej w celu opracowania nowych i bardziej efektywnych metod stabilizacji bakteriofagów. Skutecznie stabilizowane fagi mogą znaleźć zastosowanie w warunkach laboratoryjnych, przemysłowych i środowiskowych.

W kolejnych rozdziałach pracy opisałem zastosowanie nieorganicznego nanokompozytu BOA do długotrwałego przechowywania fagów w plastikowych naczyniach laboratoryjnych, stabilizacji bakteriofagów przed promieniowaniem UV przy użyciu barwników drobnocząsteczkowych – czerwieni Kongo oraz wybranych barwników spożywczych (w szczególności błękitu brylantowego FCF), oraz stabilizację podczas ekspozycji na podwyższoną temperaturę, za pomocą termoresponsywnego polimeru (PVME).

Oprócz praktycznych zastosowań opisanych metod, wyjaśniłem także mechanizm stojący za stabilizującymi właściwościami każdego z badanych czynników. W przypadku stabilizacji UV opartej o barwniki drobnocząsteczkowe, zaprezentowane w niniejszej pracy wyniki są pierwszymi, które podejmują podobne zagadnienie.

Metody zaproponowane w tej pracy opierają się na nieszkodliwych dla zwierząt i środowiska związkach, lub zaprojektowane są w taki sposób, aby ograniczać uwalnianie szkodliwych substancji poza układy doświadczalne. Niniejsze metody, pomyślnie zastosowane, umożliwią m.in. wprowadzenie bakteriofagów do sterylizacji układów bioreaktorów przepływowych oraz do konserwacji żywności w warunkach przemysłowych i środowiskowych.

List of abbreviations

CFU/mL - colony-forming units per milliliter

PFU/mL - plaque-forming units per milliliter

DLA - double-layer agar assay

UV-Vis - ultraviolet - visible

SEM - scanning electron microscopy

CryoEM - electron cryomicroscopy

EDAX - energy-dispersive X-ray spectroscopy

CR - Congo red

BB - brilliant blue FCF

AZ - azorubine

TR - tartrazine

QY - quinoline yellow

SY - sunset yellow FCF

AR - Allura red

PC - Ponceau 4R

IC - indigocarmine

PEG - poly(ethylene glycol)

APEG - acridly-flanked poly(ethylene glycol)

PVP - polyvinyl pyrrolidone

PVME - poly(vinyl methyl ether)

WTAs - wall teichoic acids

AMR - antimicrobial resistance

MBR - membrane bioreactor

Table of content

CHAPTER 1

Introduction to bacteriophage stabilization

Parts of this chapter were previously presented as a review article:

"*Enhancing the Stability of Bacteriophages Using Physical, Chemical, and Nano-Based Approaches: A Review"*
Mateusz Wdowiak, Jan Paczesny, Sada Raza, *Pharmaceutics* 14(9), 2022, doi.org/10.3390/pharmaceutics14091936

1.1. The threat of bacterial infections

Bacteria are one of the most abundant and diverse organisms on Earth, and one of the oldest. It is generally believed that the last universal common ancestor (LUCA) combined the features of bacteria and archaea [1]. The traces of organic carbon in sedimentary rock suggest such an organism could have lived 3.95 billion years ago (Ga) [2]. Undoubtedly, the bacteria resided on Earth between 3.8 Ga and 3.4 Ga, which is suggested by the stromatolites - organo-sedimentary structures of bacterial mats [3]. Within over 3.5 Ga of evolution, bacteria adapted to the vast majority of extreme environments on Earth: the depths of the oceans [4], hot springs [5], polar regions [6], air [7], and even the upper parts of the stratosphere [8]. They also exist in anthropogenic environments, such as sewers [9] and animal farms [10]. Numerous bacterial communities also colonize the bodies of animals, including humans [11–13]. In total, over 10^{30} bacteria are estimated to be present in Earth's biosphere [14].

Even though most bacteria (about 95% among the known species) are free-living organisms and remain harmless to other living creatures [15], the remaining 5% are pathogens of animals and plants. These bacterial pathogens are a significant burden to the modern-day world. Bacterial diseases are the cause of about 13% of deaths annually [16]. The most frequent bacterial infections are related to the contamination of food and water, resulting in about 76 million infections and nearly 2 million casualties [17,18]. In 2018, the total cost of food-borne illnesses reached about 110 billion USD, including the treatment cost of 15 billion USD [19]. While foodborne pathogens are a burden mostly in developing countries, in developed countries, the bacterial pathogens related to nosocomial infections (NIs), also known as hospital-acquired infections (HAIs), pose a significant threat. HAIs are infections that occur within 48 hours of hospital admission, up to 30 days after receiving healthcare, or up to 90 days after surgery. The report from April 2023 suggests that about 2 million patients are affected by NIs annually (in the USA only), among which 80.000 cases are fatal, causing economic losses of more than 4.6 billion USD [20].

The most recent bacteria-related threat is the spread of antibiotic resistance among the bacterial strains. The USA alone faces an annual expense of 55 billion USD in fighting drug-resistant microorganisms, with 20 billion USD related to healthcare costs and $35 billion attributed to productivity losses [21]. This predicament arises from the excessive use of antibiotics in medical settings [22] and in agriculture [23], where they

stimulate livestock growth, rising to the antimicrobial resistance (AMR) epidemic. Approximately 154 million antibiotic prescriptions are issued annually, and around 30% are unnecessary [24]. Recognizing the severity of the situation, the United Nations designated AMR as a threat to health and human development in 2016.

Notably, bacteria can develop resistance mechanisms within only 10 hours of antibiotic exposure [25], and the resistance to certain drugs may persist in bacterial communities for even 30 - 40 years [26]. The transmission of drug resistance can be spread between bacterial species through various means, including horizontal gene transfer of antibiotic resistance genes (ARGs) [27] or transduction (bacteriophage-mediated gene transfer) [28].

Increased antibiotic resistance has led to bacterial strains resistant to multiple drugs, some of them coupable of withstanding antibiotics of more than three classes. The prevalence of extended-spectrum beta-lactamase (ESBL)-positive strains has dramatically reduced the efficacy of beta-lactam antibiotics such as penicillin, cephalosporins, and monobactams [29] against Gram-negative bacteria. Meanwhile, among Gram-positive bacteria, resistance to beta-lactam antibiotics typically arises from developing bacterial penicillin-binding proteins (PBPs) [30]. Several bacterial strains have already developed the resistance mechanism to the drugs considered the “drugs of last resort”, including vancomycin [31], carbapenems [32], and colistin [33]. The ESKAPE acronym categorizes and describes the most prevalent and challenging bacterial pathogens, including *Enterococcus faecium*, *Staphylococcus aureus*, *Klebsiella pneumoniae*, *Acinetobacter baumannii*, *Pseudomonas aeruginosa*, and *Enterobacter* spp. These opportunistic pathogens are significant in numerous hospital-acquired infections and contribute to the global spread of antimicrobial resistance [34].

Bacterial infections affect animals (including humans) and plants, especially fruits and vegetables. This issue directly impacts humans, as bacterial plant diseases are estimated to cause annual economic losses of approximately 220 billion USD worldwide [35]. Among the multitude of bacterial pathogens, *Erwinia amylovora* (the causative agent of fire blight disease in apple trees) [36], *Agrobacterium tumefaciens* [37], and *Pseudomonas syringae* [38] are responsible for, economically, the most significant bacterial diseases. Conventional approaches for treating bacterial diseases involve antibiotics and pesticides, but the drawback lies in their accumulation in the environment, posing potential harm to living organisms. Additionally, the release

of antibiotics into the environment raises concerns about escalating antibiotic resistance.

Hence, bacterial infections affect animals and plants alike, and there is an urgent need to identify biocompatible and environmentally friendly bactericides that are harmless to humans and the ecosystem. Such bactericides should also, preferably, be capable of self-improvement to catch up with the development of resistance among bacteria. Against such criteria, bacteriophages appear as the most promising alternative to drugs.

1.2. Bacteriophages and their applications

Bacteriophages (phages for short) are a polyphyletic group of viruses that specifically infect bacteria while remaining harmless to all known eukaryotic organisms – plants, protists, fungi, and animals (including humans) [39,40]. Their name is derived from Latin word “bacteria” and the Greek word φαγεῖν (*phagein*), meaning “to devour”. Most known bacteriophages belong to the Caudovirales order, and are characterized by a double-stranded DNA genome and an icosahedral, tailed capsid with fibers attached to the tail [41]. Typically, the virion size ranges from 50 to 200 nm, although filamentous phages like filamentous phage M13 can extend up to 400 nm in length [42]. Notably, larger bacteriophages reaching the sizes of 800 – 1800 nm were discovered in marine water [41,43].

Based on the structure of their genomes, bacteriophages belong to Groups I – IV of the Baltimore classification of viruses. That means known bacteriophages have their genome in the form of:

- double-stranded DNA (Group I),
- single-stranded DNA (Group II),
- double-stranded RNA (Group III),
- positive-sense single-stranded RNA (Group IV).

At the moment, no bacteriophages with the genome in the form of negative-sense single-stranded RNA ((-)ssRNA) (Group V) or phages expressing the reverse transcriptase (Groups VI and VII) are known.

The dominant structural design shared by the vast majority of bacteriophages (over 95% of all known types [41]) involves storing genetic information as the double-stranded DNA within an icosahedral capsid [41,44]. Such capsid is usually equipped with

a spike-tail adorned with fibers. The length and rigidity of the tail spike are dependent on the phage's species, such as belonging to the family *Straboviridae* (characterized by a long and contractile tail, as seen in T4), the *Caudoviricetes* class (featuring a long, noncontractile tail, as seen in λ phage), or the family *Autographiviridae* (possessing short, noncontractile tails; represented by T7). The tail fibers, attached to the tail, carry a positive charge, while the head exhibits a substantial negative charge [45]. This structural asymmetry results in a permanent dipole moment for the virion. Phages falling outside the most common *Caudoviricetes* class include filamentous types (e.g., M13, fd) or nearly spherical (isometric) phages (e.g., MS2). These capsid structures are, however, significantly less prevalent.

Bacteriophages are obligate parasites, relying on the host's molecular machinery to complete their life cycle. Inside a single bacterial cell, hundreds of progeny virions are assembled. In most instances, the bacterial cell is disrupted, releasing phages and the death of the host cell (lytic cycle). However, specific phages, such as filamentous phages f1, fd, or M13, follow a chronic pattern where progeny virions are continuously secreted from the bacterial cell [46]. Phages that exclusively undergo the lytic cycle are termed virulent, while those capable of lytic and lysogenic (latent) cycles are referred to as temperate [47]. In the lysogenic cycle, the viral genome integrates into the bacterial chromosome, remaining latent and replicating alongside the host [48]. This integrated semi-stable state is called a prophage [49]; when affected by stressors, such as chemicals, UV radiation, or damage to the host DNA, the initiation of the lytic cycle as a means for the phage to escape from the compromised host can be triggered [50]. The lytic and lysogenic lifecycles of bacteriophages are visualized in **Figure 1**.

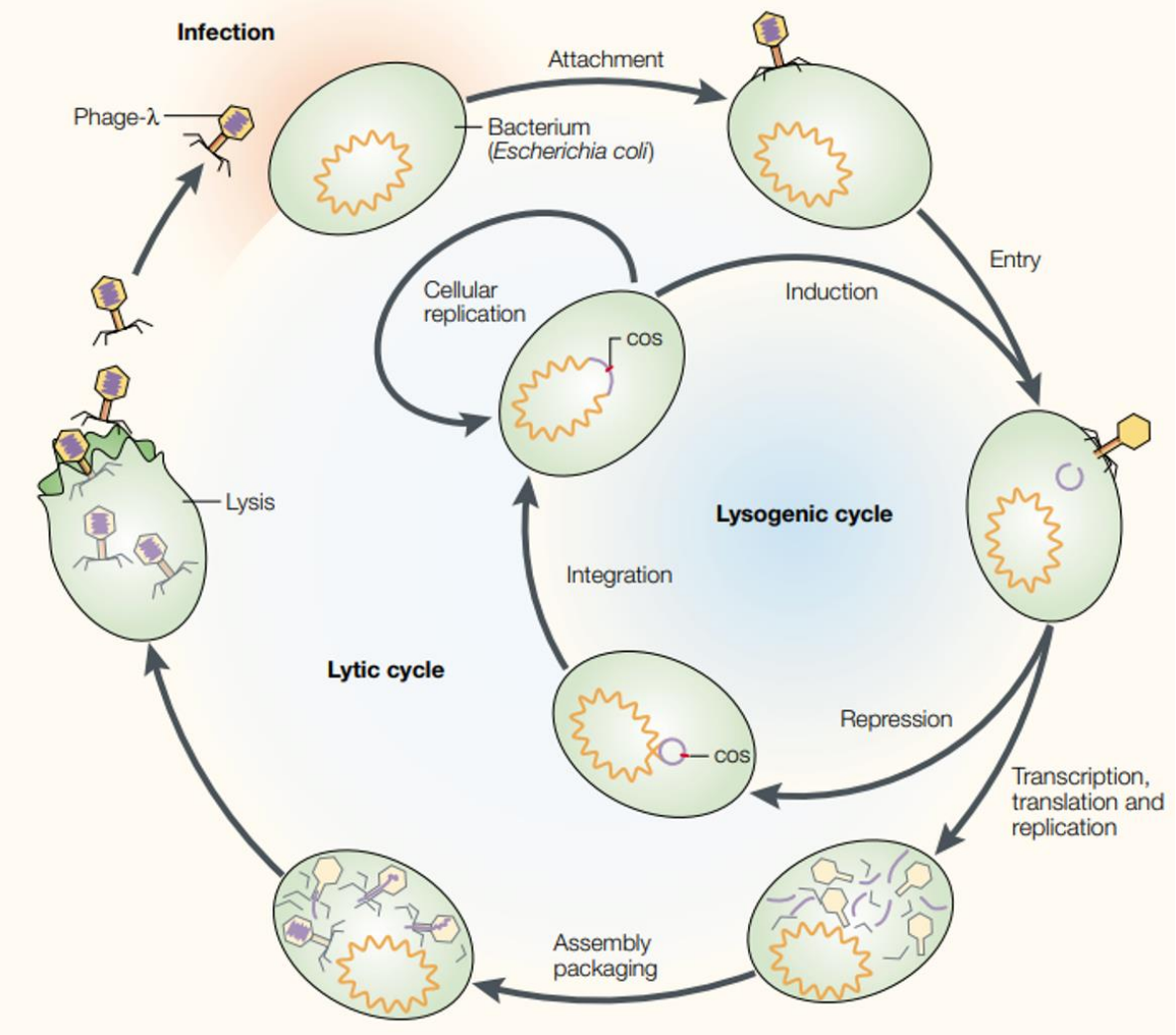

Figure 1. The life cycle of the template coliphage λ. Entering the lytic cycle, bacteriophage attaches to the receptor on the surface of the bacterial cell and introduces its genome inside the cell. The bacteriophage genome is replicated using the transcriptional and translational machinery, and proteins are produced. After the assembly, progeny virions leave the bacterial cell, simultaneously killing the cell. In the lysogenic cycle, the viral genome integrates into the bacterial chromosome and is replicated along with the bacterial genome. The graphic was adapted from Allan Campbell [51], based on Springer Nature License No. 5702441414289.

The successful multiplication of virions and completing the phage life cycle depend on accurately identifying a suitable and viable host. Consequently, a multi-step "identification" process is frequently employed. In the context of *Caudoviricetes*, the initial recognition relies on electrostatic interactions where positively charged tail fibers are drawn to the negatively charged surface of bacteria. Subsequent stages of host recognition involve specific receptor-binding proteins that differentiate and identify the suitable host. This specificity is crucial for further amplifying bacteriophages because certain bacterial receptors can be recognized by different bacteriophages (e.g., the LPS and OmpC of *E. coli* are recognized by both T4 phage and *Salmonella* phage

S16). Simultaneously, phage enzymes (such as hydrolases and depolymerases) are specific to bacterial host [52]. Therefore, non-specific binding would result in unsuccessful infection.

The specificity of bacteriophage recognition can be used for the sensing of bacteria [53]. Because the isolation of phages is rapid, cost-effective, and can be performed in any biological laboratory without requiring specific identification of the isolates [54] (generally), bacteriophages appear as the competitive alternative to "traditional" antibody-based sensors [55]. Simultaneously, the use of bacteriophages generates significantly less risk of false-positive recognition.

Facing the twilight of the antibiotic era, bacteriophages are gaining recognition for different applications in the fields of medicine, agriculture, industry, and food protection. Among bacteriophage's advantages, the most notable are:

- phages are highly specific to bacteria, posing minimal threats to humans [56],
- as "molecular parasites", phages require a viable host for multiplication through its transcriptional machinery. This characteristic enables the differentiation between living and dead bacteria, a crucial aspect in bacterial detection protocols [57],
- phages undergo self-amplification, simplifying and reducing the cost of their production compared to e.g., antibodies,
- due to their resilient nature against external factors, phages possess an extended shelf life. This resilience reduces environmental limitations and allows for the regeneration of sensor surfaces [58],
- being biological entities, phages evolve, enabling them to engage in an evolutionary arms race with bacteria and overcome developing resistance mechanisms. An intriguing example is the discovery of anti-CRISPR [59].

In the early 1900s, bacteriophages were considered for medical use [60]. However, due to a limited understanding of phages, concerns regarding formulation stability, and the emergence of antibiotics, phage therapies were largely ignored for decades [61]. The rise of drug-resistant superbugs and the shortage of new medicines has led to a resurgence of interest in bacteriophage-based antimicrobials [62]. Today, phages combat infections that do not respond to traditional antibiotics [63]. In some countries like Russia and Georgia, phage products are already available without a prescription [64,65]. In Western countries, phage-based treatments are progressing through clinical trials for conditions such as inner-ear infections [66], typhoid [67], and burn

wound infections (Phagoburn project) [68]. The first clinical trial in the USA was approved in 2019 [69].

Phage therapies are only a single aspect of bacteriophage-based methods. Phages undergo testing for biocontrol applications, particularly in the food industry and agriculture. Phage biocontrol is gaining recognition as an environmentally friendly and natural technology for precisely targeting pathogens [70]. As an alternative to antibiotics, phages have proven effective in safeguarding various food products, including dairy [71], fruits [72], vegetables [73], meat [74], and fish [75]. In 2020, fifteen more than fifty commercial entities providing phage-derived products were dedicated explicitly to biocontrol [76]. Currently, there are over ten approved products to improve food safety.

Finally, specific bacteriophages served as valuable surrogates for studying eukaryotic viruses, particularly those of potential risks. Examples included mostly coliphages (bacteriophages that target *Escherichia coli*), such as MS2 [77], ΦX174 [78], Qβ [79], and an enveloped phage Φ6 [80]. MS2 phages, for instance, are used in inactivation studies due to their UV resistance and similarity in inactivation profiles to certain enteric viruses, like the poliomyelitis virus [81]. Φ6, a unique enveloped bacteriophage belonging to the *Cystoviridae* family, has been utilized as a surrogate for SARS-CoV-2, e.g., in investigations regarding survival in evaporated saliva droplets on glass surfaces [80] and in tests evaluating surface disinfectants [82]. The similarity in the structure of Φ6 phage and the SARS-CoV-2 virus was presented in **Figure 2**. ΦX174 and Qβ are frequently employed as models in studies on virus deactivation [78,79].

Bacteriophages are biological objects that consist of proteins and nucleic acids, rendering them vulnerable to adverse environmental conditions such as electric fields, high temperatures, and radiation across various spectrums [83]. Therefore, sufficient stabilization protocols are essential to embrace the full applicative potential of bacteriophages.

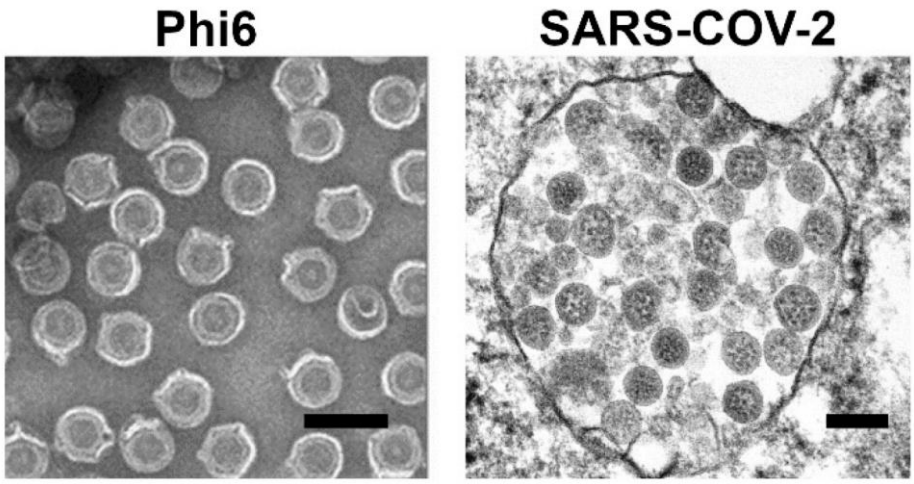

Figure 2. Using scanning electron microscopy imaging, the comparison of enveloped phage Φ6 and SARS-CoV-2 virus. The scale bar is 100 nm. The image of Φ6 phage was adapted from Block et al. [84] based on CC BY 3.0 Licence. The image of SARS-CoV-2 was adapted from Goldsmith et al. [85] based on Elsevier License No. 5740121326095. The collage was previously published in Wdowiak et al. [86] and is adapted here based on the CC BY 4.0 License.

1.3. The principles of bacteriophage stabilization

The primary challenge associated with using phages as antimicrobials lies in the stability of virions [87]. Critical criteria for assessing their viability include virulence, selectivity, host range, ease of manipulation, and modification. While phages can maintain their activity even after exposure to stress factors like high temperatures [88], pH variations [89], and organic solvents [90], this resilience serves as an additional consideration in exploring their potential medical applications [91].

The successful use of phages in treating diseases requires an additional stabilizing factor, since bacteriophages are recognized as alien, potentially hostile entities in the human body. Without stabilizing additives, phage formulation may trigger an inflammatory response by releasing pathogen-associated molecular patterns (PAMPs) from lysed bacteria (i.e., membrane proteins, LPS) [92] or directly impacting immunity. The direct response of the immunology system to the presence of phages relies on the modulation of the innate and adaptive immune response through phagocytosis, the cytokine response, and antibody production [93]. The anti-phage antibodies are a key factor hindering phage therapy's therapeutic efficacy [94]. Typically, they identify virions as antigens, rendering phages ineffective in infecting bacterial cells [95].

The stabilization during the storage of phage stocks is particularly important because improper preparation and storage of the phage suspension can significantly impact the effectiveness of the phage therapy approach [68].

From the point of view of industry and agriculture, phage-stabilization protocols against the adverse effects of UV irradiation [96], elevated temperatures [97], and drying [98] are essential. The stabilization methods developed for bacteriophages might also apply to stabilizing eukaryotic viruses, which is crucial for vaccine formulations. Various vaccine types utilize phages in distinct ways; they can carry the genomes of other viruses, bind eukaryotic virus antigens on the capsid's surface [99], or present virus antigens to selectively target factors through phage display [100].

Due to the enormous applicative potential of bacteriophages for medical and industrial purposes, phage stabilization has been of great interest in the past years. Different approaches were tested as protectants from several adverse conditions. These approaches included using polymeric compounds, novel protocols of encapsulation and lyophilization, and applying nanomaterials. The following sections describe the most promising ideas.

1.4. Polymer-based stabilization

According to the definition provided by Encyclopedia Britannica, a polymer is a substance or material with a large molecular mass consisting of repeating subunits. Due to the substantial number of these subunits, removing a single unit does not alter the properties of the entire molecule. Polymers are natural (including proteins, nucleic acids, and polysaccharides) and synthetic (polyethylene, polytetrafluoroethylene, and polypropylene) [101]. Even though the utilization of polymers for stabilizing phages and viruses is in its early stage, saccharides and polysaccharides have already taken the lead in this field.

The stabilizing effect of sugars against protein unfolding is well-established [102,103]. Sucrose, for instance, is used as a cryo-stabilizer in freeze-dried vaccines due to its capacity to stabilize against protein unfolding. However, it has been demonstrated that sucrose-induced stabilization of viral capsid proteins alone may not necessarily lead to stabilizing the virus capsid [104]. This suggests the stabilization *via* the addition of saccharides might be related to the modulation of the viscosity of the solution, providing a more favorable buffer solution. While the protein stabilization

effect is generally observed with many sugars, only sucrose and trehalose effectively stabilize viral capsids [105,106].

At molar concentrations, sucrose enhances protein-protein binding by modifying protein hydration properties [107], effectively stabilizing vaccines [105,108]. Moreover, other carbohydrates like agar or alginate can be employed to stabilize phage particles. Some studies proposed fifteen polymers with varying sodium alginate and calcium solution concentrations for storing bacteriophage DSM JG004, targeting *P. aeruginosa*. Hydrogel effectiveness was demonstrated in eliminating bacteria embedded on the surfaces of gel beads [109]. Another research group suggested using pullulan and trehalose films to protect the LISTEX P100 phage, targeting *Listeria monocytogenes*. While pullulan alone was not effective for phage stabilization after drying, the combination of pullulan and trehalose as a stabilizing matrix allowed the maintenance of about 7 log active phages after 60 days (from the initial concentration of 10 log). In comparison, only 3 log phages remained active in the trehalose matrix after the same duration [110].

Besides saccharides, more “traditional” polymers were also used for phage stabilization against drying. For instance, polyacrylamide was proposed for stabilizing phage particles dedicated to strictly research purposes, such as protein nuclear magnetic resonance spectroscopy. Trempe et al. documented the stabilization of a filamentous Pf1 phage using 5% polyacrylamide as a polymer-stabilized liquid crystal (PSLC). This innovative approach facilitated measurements of dipolar couplings with a single sample, enabling a more precise analysis of protein structure by comparing theoretical and experimental tensor parameters [111]. Another popular polymer, poly(ethylene glycol), was used in a buffer solution or for surface modification, and it is called PEGylation. PEGylation involves attaching poly(ethylene glycol) (PEG) groups to a target molecule, commonly used in food and drug formulation to enhance stability. PEG is biocompatible and reduces the immunogenicity of the molecule, although not degradable [112]. Similar to sucrose, PEG was known to influence protein-protein interactions by altering their hydration. Since phage capsids consist exclusively of proteins, PEGylation has been found to be a suitable phage stabilizer. This approach involved using a PEG polymer conjugate with phage proteins [113]. Kim et al. reported that two bacteriophages - Felix-O1 and A511 - modified with monomethoxypoly(ethylene glycol) (mPEG) exhibited prolonged presence in the bloodstream. After 24 hours, the quantity of non-modified phages was 2 log less than

that of mPEG-modified phages. However, the immunogenicity of the modified phages increased, indicated by a higher amount of IgG and IgM antibodies 12 days after injection [114]. PEGylated phage lysins are currently considered more promising [115]. In contrast, the PEGylation of phage endolysins resulted in the loss of their bactericidal properties *in vitro* [116].

Polymers are a popular stabilizing agent in solutions. However, without specific interactions between the polymer and bacteriophage, the local stabilizer concentration around the phage may be insufficient for effective protection. This drawback can be overcome using a modified and localized polymer-based method - encapsulation.

1.5. Encapsulation-based stabilization

Polymers serve as protective matrices in which phages are embedded, a process known as encapsulation. This method enhances stability and regulates the long-term release of active phage particles [117]. Various techniques, including emulsion, polymerization, spray-drying, and extrusion dripping, are employed for encapsulation [91]. When encapsulating bacteriophages for preservation and administration, it is crucial to consider potential stresses encountered by phages during and after the process. Maintaining the morphology of encapsulated particles and preventing aggregation or uncontrolled fusion with the surface of interest is essential [118]. The specific bacteriophage strain of interest defines the encapsulation conditions, making it challenging to develop universally applicable methods [91]. Encapsulation of phages also facilitates the transportation of samples at prescribed temperatures for extended periods. For instance, Menendez et al. demonstrated that microencapsulated phages could be maintained at 20°C for two months [119]. Dry encapsulation offers advantages over other liquid-based formulations, especially for transporting phages and ensuring a prolonged shelf-life [120].

Encapsulation has diverse applications, including the development of phage cocktails. For instance, a cocktail of three phages targeting *Salmonella* spp. was encapsulated within alginate microparticles containing calcium carbonate to extend their residence time in the gut [121]. Pacios-Michelena et al. combined alginate/chitosan-encapsulated phages with polyphenolic extracts, increasing phage persistence during UV exposure from about 5 minutes to at least 25 minutes [122]. Malik et al. listed various polymers used for phage encapsulation, such as agarose, alginate, chitosan, pectin, whey protein, gelled milk protein, hyaluronic acid methacrylate, hydroxypropyl

methylcellulose, poly(N-isopropyl acrylamide), poly(DL-lactide-co-glycolide), polyesteramide, polyvinyl pyrrolidone, polyethylene oxide/polyvinyl alcohol, cellulose diacetate, and polymethyl methacrylate [118]. Alginate was often chosen to encapsulate phages for applications requiring exposure to acidic media [121]. Tang et al. improved the release of phage particles from alginate microspheres by incorporating whey protein [91]. Alginate capsules can also be designed to immobilize phages, allowing storage at lower temperatures [119]. Additionally, bead encapsulation in chitosan-alginate multilayers enhances phage stability, even under harsh conditions like the intestine [123].

Liposomes (sometimes considered as biocompatible nanoparticles) are structures with a lipid bilayer surrounding therapeutic cargo, offering a promising approach for achieving directed delivery while surviving the extreme stomach and intestine conditions when administered orally [117]. Liposome-encapsulated phages are used to target *Salmonella* [91]. The “gastro-resistant” microparticles encapsulating anti-*Salmonella* phages were produced as pharmaceutical formulations to maintain elevated phage levels in the gut. Cationic liposome nanoparticles can also encapsulate anti-*Salmonella* phages, protecting them against the acidic conditions of the intestine [121]. This technique is commonly adopted to immobilize phage cocktails for treating burn infections [124]. However, liposome-encapsulated phages are less effective than phages alone, leading researchers to explore hydrogels (primarily polymers) as scaffolds for phage delivery [125].

In the pursuit of improvement, modifications in phage encapsulation approaches are gaining popularity. Microfluidic devices, for example, are used to produce calcium alginate capsules containing bacteriophages [126], with applications in sanitizing food surfaces. There is a continuous effort to refine these techniques to overcome challenges such as the immune system's exclusion of encapsulated phages and the cleavage of capsid proteins by gut proteases.

Encapsulation is an invaluable method for phage stabilization in moderate conditions of temperature, pH, or in the presence of enzymes for a relatively short time. However, several applications require bacteriophage formulations of constant titer to be stored for weeks or months. For such purposes, lyophilization appears significantly more efficient than encapsulation.

1.6. Lyophilization-based stabilization

Lyophilization is a dehydration process that involves freezing the substance in lower-pressure conditions. A method initially developed for food preservation has become widely employed for stabilizing and storing bacteriophages over the long term.

Initially, this process involved freezing the phage stock, reducing the pressure, and eliminating water through freeze-drying [127]. Currently, various methods have evolved within this category, including:

- spray-drying; involves atomizing the concentrated liquid and exposing it to hot air, leading to water evaporation, followed by drying and separation [127].
- hot-air-drying; the sample undergoes pre-treatment with ethyl oleate and potassium carbonate solutions before exposure to a temperature of approximately 50°C to 60°C [128].
- drum-drying; enhances hot-air-drying by placing the sample in a rotating drum to enhance heat transfer [129].

When storing phages, freeze-drying and spray-drying methods stand out as crucial. Freeze-drying is relatively the most cost-effective approach for preparing phage powders. In an early attempt involving mycobacteriophages, lyophilized phages stored in the dark remained active for over two years [130]. The average reduction in titer with such methods was approximately 1 log [131].

The viability of phages post freeze-drying is influenced by the drying time and the number of prior refrigeration cycles. The literature suggested that an extended drying duration (over 150 minutes) leads to three times higher phage survivability during freeze-drying than shorter durations (90 and 120 minutes). Moreover, each successive freezing event results in a titration decrease of about 3 log [132]. The efficacy of freeze-drying is also contingent on the size of phage powder grains during the procedure. A smaller bead formulation exhibits a lesser phage titer reduction than macro-beads.

The addition of cryoprotectants was proven effective in extending storage time. Merabishvili et al. suggested incorporating 0.5 M sucrose and trehalose solutions into *S. aureus* ISP phage. This resulted in a storage extension of up to 37 months with a titer loss of approximately 1 log [133]. Dini and Urraza corroborated this finding, emphasizing the importance of freeze-drying CA933P phage stocks in appropriate buffer solutions [134]. Moreover, in the M13 phage model, sugar solutions (sucrose and

trehalose) demonstrated superior cryoprotective qualities compared to polymers (PEG 6000), yielding a 2 log higher phage titer after seven days [135,136]. Recently, a combination of trehalose and whey protein isolate (WPI) facilitated the storage of freeze-dried *Salmonella* SPT 015 phage, even at room temperature [137]. Conversely, other sugars like lactose or mannose proved less efficient as cryoprotectants, as Chang et al. [138] indicated.

Spray-drying allows for a reduction in the decrease of the phage titer during procedure [139]. Still, adding certain carbohydrates to the phage solution seems to be crucial for the entire drying protocol. For instance, Vandenheuvel et al. compared the addition of dextran, lactose, and trehalose to phage-titer decrease during the spray-drying of phages, revealing that trehalose was the best cryoprotectant for such assays [140]. It was found that the stability of spray-dried phage formulation is dependent on the crystallization process of the saccharide matrix. A relatively new approach is atmospheric spray-freeze-drying (ASFD) - a combination of freeze-drying and spray-drying assays [141,142]. Preliminary results promised novel antibacterial formulations for medical purposes [143,144], but the method still requires optimization and more recognition from the scientific community for proper efficacy verification [145].

The unconventional approach for storing and stabilizing the tailed bacteriophages by freezing mature virions within bacterial cells is worth mentioning among freezing-related approaches. Bacteriophages, mixed with their host bacterium at an appropriate multiplicity of infection (MOI), undergo a brief incubation at 37°C. Subsequently, the infected cells are frozen and stored at -80°C. Upon revival and washing, the phages are released and exhibit active infection of bacterial cells. This method enables phage storage with minimal or no losses in phage titer for approximately ten months, depending on the specific phage involved [146].

1.7. Nano-assisted stabilization

Nanotechnology, according to the definition given by Encyclopedia Britannica, is “the manipulation and manufacture of materials and devices on the scale of atoms or small groups of atoms”. Therefore, nanomaterials are described as materials and structures manufactured in the “nanoscale”, i.e., having at least one geometrical dimension ranging from 1 nm to 100 nm.

The integration of nanotechnology in medicine offers a promising solution to stability challenges. Nanoparticles serve as carriers for drug solubilization,

effectively navigating through biological barriers within the body [147]. Associating phages with nanoparticles extends their detectability in the bloodstream by approximately 24 hours compared to control conditions [148]. Given that most bacteriophages align with the classical definition of nanomaterials (dimensions ranging from 1 nm to 100 nm), they synergize well with abiotic nanomaterials, ensuring heightened efficiency [149].

Nanoscience plays a pivotal role in immobilizing phages, allowing for chemical or genetic modifications that enable strong binding to nanomaterials [150]. Gold nanoparticles are commonly used to stabilize T4-like bacteriophages for *E. coli* cell detection [151]. Furthermore, phage probes modified and stabilized with gold nanoparticles effectively target the DNA of *Bacillus anthracis* [152]. Silica nanoparticles are popular for more cost-effective applications due to their ability to bind with phages [150]. Phage-engineered bio-functionalized silicon nanoparticles, produced in a single step, have been applied in optical biosensors. Nanoparticles have also demonstrated the ability to augment the performance of phage-based biosensors, enabling rapid and sensitive detection methods [153]. Carbon-based nanomaterials, in particular, have emerged as promising next-generation miniaturized biosensors for achieving sensitive and selective detection [154]. An illustrative example is the chemisorption of virions on a glassy carbon electrode decorated with gold nanoparticles, effectively reducing the limit of detection (LOD) to 14 CFU/mL within a 30-minute incubation period [155]. Alternatively, the durability of sensors can be extended by employing specific components of virions, such as receptor-binding proteins (RBPs), instead of the entire bacteriophage [156].

The combination of nanomaterials and bacteriophages is also of interest from the point of view of medicine and infection control. In vaccine formulations, experiments have utilized nanolayers of aluminum oxide to stabilize λ bacteriophages, ensuring controlled antigen release *in vivo* [157]. Moreover, the synergistic effect of phages and nanoparticles was also observed and examined. Such combinations were extensively applied in targeting biofilms and combating pathogenic infections [158]. For instance, pairing the C3 phage with gold nanoparticles (AuNPs) showed promise in treating both the planktonic and biofilm states of *P. aeruginosa*. This combination demonstrated high stability across a broad range of temperatures, pH levels, and salt concentrations [159]. In other experiments, polyvalent phages were affixed to magnetic colloidal nanoparticle clusters (CNCs) to enhance biofilm penetration [160]. Phage virions can serve

as stabilizing agents in synthesizing gold nanoparticles, endowing them with antibacterial and antibiofilm properties [161]. The collaborative action of metallic nanoparticles and bacteriophages exhibits a synergistic effect against pathogenic bacteria. For instance, combining phage ZCSE6 with zinc oxide nanoparticles effectively targeted *S. enterica*, causing the deformation of biofilms [162].

CHAPTER 2
Goals and objectives

Bacteriophages can be potentially introduced to most sectors of modern-day industry and medicine (infection control and therapeutics). This is due to their natural antibacterial activity, tremendous specificity and selectivity towards their host bacteria, low cost of operation, ease of preparation, and abundance in the environment. The bottleneck for introducing phages in these protocols is overcoming the difficulties related to the stability and variability of phage titers and formulations [121]. The number of reports on improving phage stability premises the protocols suitable against adverse conditions.

Currently, there's no sight of a universal stabilizer against multiple adverse conditions. Each method described in the Introduction (Chapter 1) has drawbacks and requires further improvements. Lyophilization frequently caused morphology distortions in phage capsids, impacting their activity [163]. The effectiveness of cryoprotectants in preserving lyophilized phages shows discrepancies, with reports of phages being unstable during one year of storage at room temperature when lyophilized with skim milk and sucrose [164]. Furthermore, studies indicate that phage solutions remain stable only up to 126 days after the rehydration of lyophilized virions [165]. Careful selection of excipients, tailored to the specific phage family, is essential. Phage encapsulation in liposomes has frequently resulted in undesired aggregation, fusion, or rupture, limiting the practical application and further development of such stabilizing methods [166]. While nano-based solutions for phage stabilization show promise, they are limited, necessitating further development.

Moreover, some adverse conditions still need to be overcome. Until now, efficient methods to protect phages from UV radiation are still sparse. For instance, natural extracts and astaxanthin offer protection against UV exposure (1 mW/cm^2), but this protection lasts only for up to 5 minutes [167]. This suggests that the method would be ineffective during the standard conditions of UV sterilization (6 mW/cm^2; 30 minutes). The lack of a method for simultaneous stabilization from UV irradiation and temperature limits the applicability of phages in the agriculture and food industries. Given these limitations, further research is essential to develop strategies that ensure phage stability during storage and preservation without compromising their activity.

The results presented in this dissertation aim to develop novel methods for bacteriophage stabilization against adverse conditions, such as uncontrollable absorption during long-term storage, UV irradiation, elevated temperatures, and

drying. In my work, I use a variety of chemical compounds, including small-molecular compounds, polymers, and inorganic nanomaterials, to achieve this goal.

Chapter 4 addresses the issue previously described by Richter et al. [168], which is the uncontrollable absorption of bacteriophages onto the surfaces of the labware. This leads to an uncontrolled decrease in phage titer. The study proved that the hydrophobicity of the labware material is a crucial factor in determining the absorption rate. In the case of bacteriophage virions, such absorption on certain materials may cause a decrease in bacteriophage titer by up to 5 log within only 4 hours. In my work, I verify whether the labware's surface modification using nanocomposite deposited on the inner walls of the tubes could solve this issue.

Chapter 5 addresses the difficulties of using bacteriophages and UV irradiation for sterilization purposes in industrial systems. Both bacteriophages and UV irradiation are non-corrosive, which is a significant advantage compared to the chemical treatment. However, currently known methods for phage-UV sterilization [169] require the separation of the phage- and UV-based sterilization, which prolongs the sterilization procedures. This is because UV radiation damages bacteriophage's genome, thus inactivating phages. I investigate the efficacy of phage protection against UV radiation using small-molecular compounds, including dyes, food colorants, and selected sulfonic compounds.

In Chapter 6, I verify the possibility of phage stabilization against the elevated temperature using various polymers. Virus stabilization during temperature exposure is important from the point of view of vaccine formulation. Currently, the majority of vaccines contain attenuated (inactivated) viruses. Heat inactivation is a cause for the necessity of the "cold chain" during vaccine transportation and storage. Evilevitch et al. [170] described the premature ejection of viral genome at temperatures of 65-70°C. This phenomenon affects bacteriophages (λ) and eukaryotic viruses (HSV). I selected poly(ethylene glycol), acridinyl-flanked poly(ethylene glycol), polyvinyl pyrrolidine, and poly(vinyl methyl ether) as potential temperature stabilizers.

Bacteriophage application in environmental conditions, e.g., for eliminating bacterial plant pathogens, requires efficient stabilization from the UV, temperature, and drying. Over 50% of the sunlight energy is carried within the range of near-infrared radiation, thus, indirectly, the heat [171]. However, the adverse effects of UV irradiation can't be neglected. In Chapter 7, I conclude the findings of Chapters 5 and 6 and

propose a dye-polymer formulation for stabilization during sunlight exposure (UV, elevated temperature and drying).

CHAPTER 3
Experimental section

3.1. Materials

$HAuCl_4 \cdot 3H_2O$ (99.8%, Aldrich, Saint Louis, Missouri, USA), $NaBH_4$ granules (99%, Fluka, Buchs, Switzerland), HCl (analytical grade, POCH, Gliwice, Poland), NaOH (99.8%, POCH, Gliwice, Poland), H_2SO_4 (min. 95%, POCH, Gliwice, Poland), H_2O_2 (30%, Chempur, Piekary Śląskie, Poland) were utilized as received. Ethanol 95% (POCH, Gliwice, Poland) and chloroform (Chempur, Piekary Śląskie, Poland) used for cleaning were of analytical grade. Ultra-pure water characterized by resistivity of 18.2 MΩ·cm was obtained from the Milli-Q water purification system.

Congo red (disodium 4-amino-3-[4-[4-(1-amino-4-sulfonato-naphthalen-2-yl)diazenylphenyl]phenyl] diazenyl-naphthalene-1-sulfonate), crystal violet (4-{Bis[4-(dimethylamino)phenyl]methylidene}-N,N-dimethylcyclohexa-2,5-dien-1-iminium chloride), eriochrome black T (sodium 1-[1-Hydroxynaphthylazo]-6-nitro-2-naphthol-4-sulfonate), methyl orange (sodium 4-{[4-(dimethylamino)phenyl]diazenyl}benzene-1-sulfonate), thymol blue (3,3-Bis[4-hydroxy-2-methyl-5-(propane-2-yl)phenyl]-2,1,6-benzoxathiole-1,1(3H)-dione) and phenol red (phenolsulfonphthalein) were obtained from POCh (Gliwice, Poland). TM buffer contained 10 mM Tris base, 5 μM $CaCl_2$, 10 mM $MgSO_4$, and distilled water (pH=7.4). All components were purchased from Sigma Aldrich (USA). Bacteria and yeasts were suspended in a 0.9% NaCl (ROTH, Germany). All solutions were sterilized by autoclaving before use. Ultrapure water characterized by 18.2 MΩ·cm resistivity was obtained from the Direct-Q water purification system.

The potential properties against UV radiation were evaluated by testing eight commonly available food dyes: brilliant blue FCF (BB; E133), azorubine (AZ; E122), tartrazine (TR; E102), quinoline yellow (QY; E104), sunset yellow FCF (SY; E110), Allura red (AR; E129), Ponceau 4R (PC; E124), and indigocarmine (IC; E132). All dyes, except Allura red, were supplied by Food Colours Perczak S.J. (Piotrków Trybunalski, Poland), while Allura red was provided by Sweetdecor S.C. (Radzików, Poland). Unless specified otherwise, all dyes were used at 0.5% (w/v) concentration.

To assess protective properties against exposure to high temperatures, solutions of poly (ethylene glycol) PEG 6000 (Sigma Aldrich, Saint Louis, Missouri, USA), PEG 20000 (Sigma Aldrich, Saint Louis, Missouri, USA), polyvinyl pyrrolidone (M = 20.000 Da), and poly(vinyl methyl ether) (50 wt. % in water) (Sigma Aldrich, Saint

Louis, Missouri, USA), with a molecular mass ranging from 4.000 to 6.500 Da were used. Unless stated otherwise, the polymers were used in a 0.1% (w/v) concentration.

LB-agar contained 15 g/L of agar, 10 g/L of NaCl, 10 g/L of tryptone, 5 g/L of yeast extract, and 15 g/L of agar (Carl Roth, Germany), and it was used as an instant mix (Carl Roth, Germany). LB Top-Agar had the same composition, except that the agar concentration was 5 g/L. Liquid LB-medium had the same composition except for lacking 15 g/L of agar (Carl Roth, Germany).

BHI-agar contained 10 g/L meat peptone, 5 g/L bovine heart extract, 12.5 g/L bovine brain extract, 5 g/L sodium chloride, 2.5 g/L dipotassium phosphate, 2 g/L glucose, and 15 g/L agar. Liquid BHI medium had the same composition except for the lack of 15 g/L of agar.

YPD-agar contained 20 g/L casein extract, 10 g/L yeast extract, 20 g/L glucose, and 15 g/L agar (Carl Roth, Germany). Liquid YPD medium had the same composition except for the lack of 15 g/L of agar.

TM buffer was formulated using 10 mM Tris base, 5 µM $CaCl_2$, 10 mM $MgSO_4$, and distilled water (pH = 7.4), with its components obtained from Sigma Aldrich (Saint Louis, Missouri, USA). All solutions underwent sterilization through autoclaving before use. A phosphate buffer (50 mM, pH 7.4) was prepared from NaH_2PO_4 and Na_2HPO_4, sourced from Carl Roth in Karlsruhe, Germany.

All the media, buffers, and the glassware were sterilized before the use by autoclaving (Prestige UK 9L class N autoclave, Venus Michał Matuszczak, Kalisz, Poland).

3.2. Surface modification with BOA nanocomposite

Gold nanoparticles were synthesized following a previously described procedure [172]. Initially, a 50 mM aqueous stock solution of the gold precursor was prepared by dissolving $HAuCl_4 \cdot 3H_2O$ with an equimolar amount of HCl. Simultaneously, $NaBH_4$ was dissolved with the same molar amount of NaOH (50 mM). In Eppendorf tubes, 50 µL of the $HAuCl_4$ solution was added to 1 mL of deionized water. Subsequently, 150 µL of $NaBH_4$/NaOH solution was introduced. The reaction mixture in the Eppendorf tubes was vigorously shaken for 1 minute until a noticeable color change occurred. Initially light-yellow, the solution turned to brown-orange immediately after adding $NaBH_4$/NaOH and then transitioned to a wine-red hue.

Sodium borohydride played a dual role: (*i*) function as a reductive agent and (*ii*) being the source of inorganic borate ligands that stabilized the nanoparticles. This protocol is scalable, allowing for preparing batches of potentially unlimited volumes. In this study, a 250 mL batch represented the maximum volume of the gold nanoparticle dispersion prepared.

The surface modification of the BOA was prepared following a previously described protocol [173], with minor modifications. Briefly, 10 mL polypropylene (PP) vials designated for coating were filled with the colloidal gold nanoparticles (AuNPs) suspension, reaching approximately two-thirds of their maximum volume. Subsequently, the solution's pH was reduced by adding 100 µL of 0.4 M HCl per 1 mL of the gold suspension to achieve optimal deposition.

The tubes containing the reaction mixture underwent mechanical agitation for one hour, ensuring the uniform coating of the interior of the bottles (previous procedures indicated that the use of argon had an insignificant effect on deposition efficiency). The colorless post-reaction liquid was removed, and the bottles were washed with deionized water. A fresh portion of the AuNPs suspension with an identical volume was introduced to the already coated bottles to prepare multiple-layer coatings, and the procedure was repeated. Both single- and triple-coated vials were examined. Finally, after the last water rinsing, the bottles were left to air-dry overnight.

3.3. Bacteriophages

3.3.1. Bacteriophage suspension preparation

In this thesis, bacteriophages T1 (*Tunaviridae*), T4 (*Tevenviridae*), T7 (*Studierviridae*), MS2 (*Leviviridae*), M13 (*Inoviridae*), LR1_PA01 (likely the *Pbunavirus* group) (obtained from the University of Gdańsk, Gdańsk, Poland), P22 (*Podoviridae*), Φ29 (*Salasmaviridae*), and Φ6 (obtained from the German Collection of Microorganisms and Cell Cultures, Braunschweig, Germany) were used. These phages were chosen to represent different virus groups with different genome organizations, including double-stranded DNA (dsDNA) represented by T1, T4, T7, P22, and Φ29; single-stranded DNA (ssDNA) represented by M13; and single-stranded RNA ((+)ssRNA) represented by MS2. As a representative of enveloped bacteriophages, *Pseudomonas* phage Φ6 was used in the experiment. Φ6 phage belongs to the *Cystoviridae* family. LR1_PA01 phage was an environmental isolate form the Baltic sea water, from the Gulf of Gdańsk.

Bacteriophages were amplified according to the protocol adapted from the Department of Molecular Virology, Faculty of Biology, University of Warsaw (Warsaw, Poland). In short, 100 µL of bacteriophage suspension was mixed with 100 µL of the host bacteria suspension in the PBS buffer solutions. After 10 minutes of incubation at 4°C, the mixture was added to 3 mL of LB Top agar and poured onto the LB plates. Plates were incubated overnight at 37°C. After the incubation, 4 mL of TM buffer solution was poured onto the plate, and the plates were incubated for 2 hours at 4°C. Later, the TM buffer solution, with the Top agar layer, was transferred to a 50 mL Falcon tube and incubated with shaking (220 RPM) for 15 minutes at room temperature (~22°C). Before the shaking, 50 µL was added to induce the lysis of bacterial cells. Next, the mixture was centrifuged (10 minutes, 8200 RPM), and the supernatant was transferred to the new 50 mL Falcon tube. The supernatant was additionally filtered using 0.45 µm Nylon66 syringe filters. Bacteriophage stocks were stored at 4°C.

3.3.2. Double overlay method

A droplet plaque counting test was conducted to evaluate phage activity and virulence. A 0.4 mL LB medium containing 0.5% agar was mixed with 200 µL of refreshed bacteria cultures. Depending on the type of phage, *E. coli* BL21 (T1, T4, T7), *E. coli* C3000 (M13 and MS2), *S. enterica* DSM 18522 (P22), *P. aeruginosa* PAO1 (LR1_PA01), *P. syringae* DSM (Φ6), or *B. subtilis* DSM 5547 (Φ29) were used. At least eight droplets (5 µL each) of adequately diluted phage suspensions were deposited onto the plate. Then, the plates were left to dry and incubated at 37°C for 24 hours afterward. In the phage long-term storage experiments, phage suspensions in TM buffer solution (10^5 PFU/mL) were incubated at room temperature for 24 hours with shaking (400 RPM) in polypropylene (PP) vials. Unusual shaking conditions were supposed to increase the number of collisions with the inner walls of the container in both pristine and BOA-modified vials. At specific time points (after 0, 1, 3, 6, and 24 hours of incubation), 100 µL of the solutions were transferred into the fresh Eppendorf tubes and then counted using the droplet test. After an overnight incubation, phage plagues were counted and converted to the PFU/mL according to the equation: PFU/mL = n × d × 200, where n was the number of plagues, and d was a dilution.

3.3.3. Bacteriophage exposure to UV

Investigated phages were suspended in a TM buffer solution, with or without adding the food dye at a given concentration (ranging from 0.001 – 2% depending on the experiment), to achieve an initial concentration of 10^5 PFU/mL. Each prepared sample was then incubated at 4°C for 24 hours. The concentration of CR was 1% (w/v); the solution was prepared by dissolving 10 mg of the dye powder in the TM buffer solution. For food dyes, the concentration was 0.5% (w/v). Following the 24-hour incubation period, titration was carried out through a droplet test on double-layer LB-agar plates. The top-agar layer consisted of the adequate host bacteria. After incubation with the dyes, the droplet test involved placing at least eight droplets (5 µL each) of each phage suspension on the top-agar layer. The remaining bulk of each sample was transferred to sterile glass Petri dishes (90 mm diameter) due to potential concerns about plastic dishes generating oxygen radicals and causing uncontrolled phage adsorption, which could impact experimental results.

For UV-C radiation exposure, the Petri dishes were positioned inside a UV chamber (CL-1000 Ultraviolet Crosslinker, UVP; 5 × 8 W, 254 nm UV) for 1 minute at a distance of 15 cm from the radiation source. The second titration was performed after UV-C radiation exposure for 1 minute, and the total bacteriophage count was determined after an overnight incubation (approximately 16 hours).

3.3.4. Bacteriophage exposure to elevated temperature

T4 bacteriophages (10^5 PFU/mL) were incubated in the polymer solution in the temperature stabilization assay. I've selected the following polymers: poly(ethylene glycol) (PEG), acridinyl-flanked poly(ethylene glycol) (APEG), polyvinyl pyrrolidone (PVP), and poly (vinyl methyl ether) (PVME). PEG is a polymeric compound frequently used for stabilizing cosmetic requisites and vaccines. PVP is a compound commonly used as a binder in pharmaceutical tablets. For this study, PEG with a molecular mass of 6.000 Da, PEG with a molecular mass of 20.000 Da, APEG with a molecular mass of 20.000 Da, PVP with a molecular mass of 20.000 Da (Sigma-Aldrich, Saint Louis, Missouri, USA), PVME (with a molecular mass of about 6.500 Da) were tested. The concentrations of polymers were 100 nM, 1 µM, 100 µM, and 200 µM. Polymers were suspended in the TM buffer solution. A TM buffer solution served as a control for the polymer's effect on the phages. After a 24-hour incubation at 4°C, the vials were transferred to a Bath thermostat with a stainless steel bath (Peter Huber

Kältemaschinenbau SE, Offenburg, Germany) and incubated for 3 hours at 65°C. Additional phage suspensions without PVME or with 10 mg/mL PVME were incubated at room temperature (about 22°C) as a control. Subsequently, the quantitative analysis of bacteriophage activity was performed using the droplet test.

In further tests, PVME solutions at concentrations ranging from 1 ng/mL to 10 mg/mL were used. The protocol was similar to the PEG, APEG, PVP, and PVME experiments.

3.4. Bacteria and yeasts

3.4.1. Bacteria and yeasts storage and culturing

In this thesis, *E. coli* BL21, *E. coli* C3000, *P. aeruginosa* PAO1 (obtained from the Institute of Biochemistry and Biophysics in Warsaw, Poland), *S. enterica* DSM 18522, *P. syringae* DSM 21482 (sourced from the German Collection of Microorganisms and Cell Cultures, Braunschweig, Germany), and *A. baumannii* ATCC BAA-1605 (sourced from the Pomeranian Medical University, Szczecin, Poland) were used as models for Gram-negative bacteria. Among tested Gram-positive bacteria were *L. monocytogenes* EGDe (sourced from the University of Warsaw Biological and Chemical Research Centre), *S. aureus* ATCC 29213, *E. durans* PCM 1857 (sourced from the collection of the Institute of Physical Chemistry PAS), *S. aureus* ATCC 43300 sourced from the Pomeranian Medical University, Szczecin, Poland), and *B. subtilis* DSM 5547 (sourced from the German Collection of Microorganisms and Cell Cultures, Braunschweig, Germany). Vastly, all the bacteria were cultures using the LB medium. BHI medium and agar were only used for *L. monocytogenes* culturing.

In antibacterial tests, bacterial cultures were prepared following a standard protocol. Initially, a single colony from the agar plate was inoculated into an appropriate medium at 37°C in an orbital shaker. For *P. syringae*, the incubation temperature was 28°C. Subsequently, bacterial cultures were diluted with the liquid medium to achieve the proper optical density within the range of OD_{600} = 0.5 - 1.0. Then, bacteria were diluted with the PBS buffer solution to the initial concentration of 10^5 CFU/mL. After applying sufficient antibacterial protocol, 100 µL of suspension was cultured onto the LB agar plates (BHI agar for *L. monocytogenes*). The plates were incubated overnight at 37°C (28°C for *P. syringae*). After an overnight incubation, bacterial colonies were counted and converted to the CFU/mL according to the equation: CFU/mL = n × d × 10, where n was the number of colonies, and d was a dilution.

In the long-term storage protocol, bacteria were incubated at room temperature for 24 hours with shaking (400 RPM). At specific time points (after 0, 1, 3, 6, and 24 hours of incubation), 100 µL of the solution was cultured onto LB-agar plates.

In the UV inactivation protocol, bacteria were suspended in either PBS buffer solution with 1% Congo red (w/v) or 0.5% of the food dye (BB, AZ, TR, QY, SY, AR, PC, IC) to achieve an initial concentration of about 10^5 cells per mL. Following the 24-hour incubation at 4°C, 100 µL of the bacterial suspension was cultured on LB or BHI, agar plates to assess whether adding the dyes impacted their growth. The remaining suspensions were transferred to sterile glass plates and exposed to UV-C radiation for a specific duration (1 minute) inside the UV chamber (CL-1000 Ultraviolet Crosslinker, UVP; 5 × 8 W, 254 nm UV). After the exposure, 100 µL of each solution was cultured on LB or BHI. Additionally, to verify the selectivity of CR-mediated protection against UV irradiation, a mixture of LR1_PA01 bacteriophage and *E. coli* BL21 bacteria was prepared. Both bacteria and phages were suspended in the TM buffer solution. The LR1_PA01 phage's initial concentration was approximately 10^5 PFU/mL), and the initial concentration of *E. coli* was about 10^5 CFU/mL. Further experiments were similar to the established UV exposure protocol.

Saccharomyces cerevisiae wild type (WT) strain (obtained from the Institute of Biochemistry and Biophysics in Warsaw, Poland) was used as a yeast model. Yeast cultures were prepared following a standard protocol that is similar to bacteria. The only modification was that YPD agar plates with yeasts were incubated for 48 hours instead of 16 hours (overnight incubation). For yeast culturing, the YPD medium and agar were used.

3.4.2. Sterilization of model membranes

The experiments were performed according to a previously established protocol [174], involving representative pairs of bacteriophages and their host bacteria, encompassing Gram-positive and Gram-negative types. A simplified model for membrane surface sterilization in flow bioreactors utilized Nylon66 syringe filters.

First, refreshed bacteria were suspended in TM buffer to achieve a concentration of approximately 10^5 CFU/mL. Nylon66 filters were flushed with 5 mL of bacterial cultures diluted in TM buffer using a syringe. This procedure was repeated twice with the same sample of bacterial culture. Then, the filters were filled with 1 mL

of the samples. The experimental design for applying CR was slightly different from the BB-PVME formulation. In the CR-based protocol, the samples were as follows:

1. Control (TM buffer only),
2. TM buffer with 15 minutes of UV exposure,
3. TM buffer with T4/LR1_PA01 phages (10^3 PFU/mL),
4. TM buffer with Congo red,
5. TM buffer with T4/LR1_PA01 phages and UV,
6. TM buffer with Congo red and UV,
7. TM buffer with T4/LR1_PA01 phages and Congo red,
8. TM buffer with T4/LR1_PA01 phages, Congo red, and UV.

In the BB-PVME formulation protocol, the samples were:

1. Control (TM buffer),
2. TM buffer with 10 minutes of UV exposure,
3. TM buffer with T4/Φ29 phages,
4. BB-PVME formulation,
5. TM buffer, T4/Φ29, and UV,
6. BB-PVME formulation and UV,
7. T4/Φ29 and BB-PVME formulation,
8. T4/Φ29, BB-PVME formulation, and UV.

The final concentrations were approximately 10^4 PFU/mL of bacteriophage, containing 0.1% CR or 0.1% BB + 0.1% PVME. The samples were incubated for 20 minutes at room temperature and then exposed to 10 minutes of UV radiation within a laminar hood (Thermo Scientific MSC-ADVANTAGE; 36 W, 254 nm UV). After the exposure, bacteria were recovered from the filters by counterflow washing with 1 mL of TM buffer solution. The number of bacteria was estimated using the plating method. 100 µL of each bacterial solution (diluted 1 and 10 times) was cultured overnight on LB-agar plates containing kanamycin (10 mg/mL) at 37°C.

After the incubation, the colonies were counted. For both control samples, with a targeted concentration of about 5×10^4 CFU/mL (equivalent to 5 ml of a 10^4 CFU/mL suspension), approximately 4.8×10^4 CFU were recovered (i.e., around 96%).

3.4.3. Food preservation experiments

To validate the efficacy of the BB-PVME formulation in phage-related food preservation, an experiment was performed to simulate bacterial contaminations on the surface of lettuce leaves. *E. coli* BL21 and *S. enterica* DSM 18522 were chosen, as these bacterial species are plant-based food's most common bacterial contaminants. Lettuce leaves were cut into 1.5 cm × 1.5 cm square pieces using a sterile scalpel, then a 100 µL suspension of 10^5 CFU/mL of bacterial cells (*E. coli* or *S. enterica*) was applied to the surface of the lettuce pieces. The leaves were then left at room temperature until the bacterial suspension dried. Subsequently, 100 µL of T4/P22 phage suspension (approximately 10^6 PFU/mL) in TM buffer solution, 0.5% BB solution in TM buffer, or BB-PVME formulation (0.5% BB + 0.1% PVME) was applied to the surface of the lettuce pieces. As a control, 100 µL of TM buffer solution was used. The samples were incubated for 25 minutes at room temperature and then exposed to 5 minutes of UV radiation within a laminar hood (Thermo Scientific MSC-ADVANTAGE; 36 W, 254 nm UV). Following exposure, the lettuce pieces were homogenized using a kitchen mortar. Homogenized samples were suspended in 1 mL of fresh TM buffer solution, and 100 µL of each suspension was cultured overnight on LB-agar at 37°C. The experiment was performed in triplicate.

3.4.4. Bacteria and bacteriophages stabilized in environmental conditions

To assess the efficacy of the BB-PVME formulation in the natural environmental conditions, *E. coli* BL21 bacteria and T4 bacteriophages were suspended in various solutions: TM buffer, 0.5% BB in TM buffer, 0.1% PVME in TM buffer, or the formulation (0.5% BB and 0.1% PVME in TM buffer) to achieve a concentration of approximately 10^6 PFU/mL. Following overnight incubation, 1.98 mL of each suspension was transferred to quartz cuvettes (10 × 10 mm, Hellma) or 60 mm glass Petri dishes (only for the solar simulator). Subsequently, 20 µL of *E. coli* suspension was added to attain a final bacteria concentration of 10^5 CFU/mL.

Quartz cuvettes were chosen to minimize radiation absorption from glass and plastic, especially in the UV range. The phage suspensions were exposed to artificial sunlight using the Wavelabs LS-2 AAA, 160 × 160 mm^2 LED solar simulator (Wavelabs, Hyderabad, India) with a pulse duration of 3600 seconds and an intensity of 100%. Alternatively, natural sunlight conditions (T = 25°C, pressure = 1021 mbar, humidity = 67%, and 42% by the end of the experiment; UV index = 3 and 4 – approximately

75 and 100 mW/m^2, respectively) were replicated. These conditions resembled sunlight exposure during a typical summer day. Bacteriophages were exposed to both artificial and natural sunlight for 1 hour.

At the start of the experiment (0'), after 30 minutes of exposure (30'), and after the experiment (60'), 300 µL of each solution was transferred to fresh Eppendorf tubes. Each sample was titrated using the droplet test on double-layer LB agar plates for phage quantification or onto LB agar plates for bacterial quantification, followed by overnight incubation. The experiment was performed in triplicate.

3.5. Cytotoxicity assay

Cytotoxicity tests were performed using MTT proliferation/metabolic activity assays with two distinct cancer cell lines: HeLa (cervical cancer) and A549 (lung cancer). Approximately 10,000 cells/well for both cell lines were counted using the Countess II Cell Counter and seeded into a 96-well plate (Greiner Bio-One). The cells were then incubated for 6 hours at 37°C. Subsequently, the medium was removed, and a tested formula containing a dye and a polymer at five different concentrations (*via* double dilutions) was added to the fresh cell medium. Each concentration was tested in five repeated experiments.

After a 6-hour incubation, the medium was replaced with a culture medium containing 1 mM 3-(4,5-dimethylthiazol-2-yl)-2,5-diphenyltetrazolium bromide (MTT reagent, Thermo Fischer Scientific). The cells were incubated with the MTT reagent for 3 hours at 37°C. The solutions were then replaced with dimethyl sulfoxide (DMSO) and incubated for 10 minutes. The absorbance in each well was measured at 540 nm using a SpectraMax i3x MultiMode Microplate Reader with injectors (Molecular Devices). Each experiment included negative and positive controls, where negative controls contained 1% Triton-X 100, and positive controls consisted of cells cultured without the tested formula.

3.6. Instrumentation

Scanning electron microscopy observations were performed using the FEI Nova NanoSEM 450 (Hillsboro, Oregon, USA) with an accelerating voltage ranging from 5 kV to 10 kV under high vacuum conditions. The microscope was equipped with an EDAX (Energy Dispersive X-ray Spectroscopy) spectrometer, enabling chemical composition analysis in micro areas.

A thin gold layer was sputtered using K550X equipped with a Quorum Technologies LTD. Sputtering was performed at 10 mA for 600 seconds, resulting in a layer thickness of approximately 10 nm. This gold layer was essential for SEM imaging, as polypropylene is non-conductive and tends to charge upon exposure to an electron beam.

Dynamic light scattering (DLS) measurements were carried out using a Zetasizer Nano ZS apparatus (Malvern Instruments Ltd., Malvern, UK) equipped with a dynamic light scattering module (He−Ne laser 633 nm, max 4 mW).

UV-Vis spectra were obtained using an Evolution 220 UV-visible spectrophotometer (Thermo Scientific, Waltham, Massachusetts, USA). All samples containing CR or other dyes were diluted 100 times before the measurement. Measurements were performed in quartz cuvettes (10 × 10 mm, Hellma), with the wavelengths from 200 nm to 800 nm examined and incremented by 1 nm.

The morphology of bacteriophages was investigated using cryogenic electron microscopy (CryoSEM) (Gemini500 SEM, Carl Zeiss). Heated and non-heated samples were mixed thoroughly before vitrification. For the heated samples, a vial of the liquid sample was heated at 65°C while being shaken at 500 rpm for 3 hours in an Eppendorf ThermoMixer F1.5. A similar vial was kept in ambient condition for the same duration. Electron microscopy grids (lacey carbon, copper, 200 mesh from Electron Microscopy Sciences, USA) were made hydrophilic prior to the vitrification by glow discharging by 60 volts, 3 mA, and for 60 seconds. A 3.5 ul sample aliquot was placed on a grid, and a piece of Whatman filter paper (Sigma-Aldrich) was applied to blow away excessive liquid. The resulting thin film of the sample was plunge-freezed immediately into liquid ethane in a homemade device. The vitrified grid was transferred to a cryogenic holder Gatan 626 (Gatan, USA) and then to a transmission electron microscope F20 (Thermofisher, USA) under cryogenic temperature. All Images were recorded in a low-dose mode at a magnification of 50000X at 4096 × 4096 pixels, giving a pixel size of 0.2 nm. Post-image processing, including format conversion, cropping, and auto-contrast adjustment, was carried out in ImageJ (Version 1.54H, NIH-USA). The cryo-SEM was used to minimize the effects of sample preparation on the integrity of bacteriophages. P22 bacteriophages in the TM buffer, or TM buffer containing 0.1% PVME, were used for imaging. Phages were visualized after a 3-hour of incubation at room temperature (about 22°C) or 65°C in the water bath.

Differential scanning calorimetry (DSC) analysis was performed using MICROCAL VP-CAPILLARY DSC (Malvern, Worcestershire, UK). The range of temperature was from 25°C to 80°C. All samples were measured under the same conditions in the same series of experiments. Sample P1 and P2 were taken from the same batch of solution (not heated – PVME, heated once - PVME ×1, or heated twice – PVME ×2) and put into two different holes on the plate to check the repeatability of measurement. The concentration of PVME in all the samples was 0.1% (app. 150 mM). Before the analysis, we performed one (PVME × 1) or two (PVME ×2) cycles of incubation in the water bath (65°C, 3 hours).

3.7. Statistical analysis

All the experiments were performed in triplicate. Statistical analysis was performed using the Student's t-test to determine if the observed differences were statistically significant (* $p < 0.05$; ** $p < 0.01$; *** $p < 0.001$). The error bars on the graphs marked the standard deviations (SD).

CHAPTER 4
Bacteriophage stabilization during long-term storage

Parts of this chapter were previously presented as a research article:

"*Gold—Polyoxoborates Nanocomposite Prohibits Adsorption of Bacteriophages on Inner Surfaces of Polypropylene Labware and Protects Samples from Bacterial and Yeast Infections"*
Mateusz Wdowiak, Enkhlin Ochirbat, Jan Paczesny, *Viruses*, 2021 13(7), doi.org/10.3390/v13071206

4.1. The principles of long-term storage of bacteriophage formulations

Bacteriophages have become of great interest for therapeutic purposes and as surrogates of eukaryotic viruses. Modified phages can be used as carriers of antigens, becoming an alternative to commonly used vaccines. Even though mRNA-based vaccines have been desired and examined [175] and became of great recognition due to the recent SARS-CoV-2 pandemic [176], a number of vaccines nowadays still contain inactivated pathogens or antigens. In the case of such vaccines, their stability is defined by three parameters:

- its ability to retain its properties,
- the duration of maintaining its properties,
- and parameters indicating its stability [177].

This means that phage-based vaccines would have to meet the same criteria.

The situation is different when applying bacteriophages for therapeutic purposes (phage therapy). Generally, the main factor for asserting the value of phages for medical purposes is not primarily their resistance to external conditions. More commonly, their virulence, selectivity, ease of manipulation, and/or modification are considered, even though the stability of phages is equally essential. As described previously, such attitude may be misleading due to the susceptibility of bacteriophages to external conditions, such as chemical substances, alterations in pH, temperature fluctuations (freezing or heat), exposure to UV light, and general preparation and formulation [83,91]. However, the effect of physical factors on the stability of phage formulations turned out to be much more than these frequently considered factors.

In 2021, it was found that phages can adhere to surfaces when stored in plastic containers, leading to a significant decrease in the number of active virions in the bulk [168] (**Figure 3**). This effect is influenced by the frequency of collisions between virions and the container surface, which can be accelerated by mixing (introduction of active transport) or an increase in temperature. The hydrophobic/hydrophilic interactions between the surface, water molecules, and virions determine the efficiency of these collisions. If the water wetting angle (WA) inside the container exceeds a certain threshold (for T4 phages this threshold was approximately 95°), it becomes more favorable for virions to “cover” the hydrophobic surface. This reduces the overall energy of the system as it minimizes contact between water molecules and hydrophobic surface [168]. This explanation aligns with findings from other studies

concerning biomolecules. Biomolecules may adopt a conformation where their hydrophobic segments contact the hydrophobic surface, while more hydrophilic regions are exposed to the surrounding bulk (and water) [173].

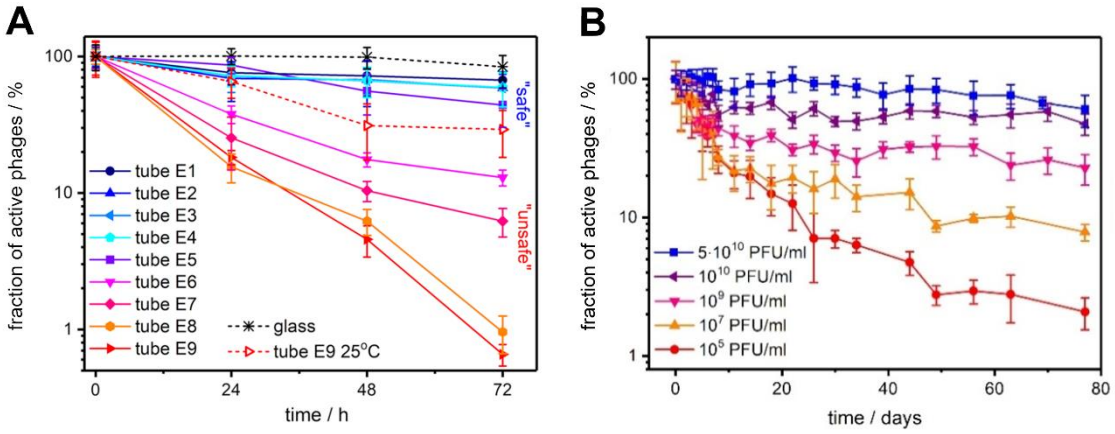

Figure 3. The rate of absorption of bacteriophages on the surfaces of plastic labware. A) The effects of elevated temperature (50°C) on the activity of T4 bacteriophages incubated for 72 hours in polypropylene Eppendorf-type tubes from different vendors (E1-E9). The tubes were categorized as „safe" and "unsafe" depending on the absorption rate. B) Concentration-dependent decrease in T4 bacteriophage titer during 80 days of incubation in the "unsafe" Falcon-like tube. In phage stocks of lower concentration (10^5) the decrease of about 2 log was observed, while no significant decrease was observed in highly concentrated stock (5×10^{10}). The graphs were adapter from Richter et al. [173] based on the CC BY 4.0 License. These results were also a part of PhD dissertation by Łukasz Richter, performed and defended at the Institute of Physical Chemistry PAS in 2019.

Consequently, a tube with a WA higher than the threshold is considered "unsafe" for phages. In such a container, the phage suspension titer may experience a substantial decrease by several orders of magnitude. This phenomenon seemed to be much more than the laboratory-scale observation and might directly affect human lives. In the *Phagoburn* project – an initiative for dealing with *P. aeruginosa* infections from burn wounds - inadequate storage led to a thousand-fold reduction in phage titers within 15 days after stock preparation. As a result, patients received a significantly lower phage dosage (10^2 PFU/mL daily instead of 10^5 PFU/mL daily) than what was intended [68]. Due to the generally good handling of phage formulations, the unexpected absorption on the surface of the labware might be the reason behind the undoing of the *Phagoburn* project.

The surface modification of the labware that decreased the absorption rate seems to be an approachable solution to the problem. Preferably, such modification should combine the absorption limitation with antibacterial and antifungal properties. The gold-oxoborate (BOA) nanocomposite could provide both.

4.2. BOA Nanocomposite

Gold-oxoborate (BOA) nanocomposite responded to the need for novel antibacterial nanocoatings. The significant advantage of gold nanoparticles (AuNPs) is that their antimicrobial activity relies on contact killing instead of ion release (which is responsible for the toxicity of, e.g., silver nanoparticles). Gold-based nanomaterials exhibit different activity towards mostly mammalian cells, depending on the shape of nanoparticles and the type of the cell; however, they're generally considered harmless to mammalian cells. Gold-based nanomaterials also feature increased durability compared to other metal-based nanomaterial [178].

The major drawback related to the use of nanoparticles to be overcome is the tendency of the nanoparticles to agglomerate. Hence, the antimicrobial activity of the nanoparticles is proportional to their size (smaller nanoparticles present better biocidal activity compared to the large ones, which is related to their active surface). The agglomeration is an unfavorable phenomenon leading to the decrease of the NPs activity. Capping agents are frequently used to synthesize nanoparticles to avoid agglomeration. Capping agents (e.g., thiols derivatives) are (usually) charged molecules that are immobilized on the surface of nanoparticles. Due to the charge, they prohibit further agglomeration by electric repelling [179].

In the case of BOA nanocoating, sodium borate ($NaBH_4$) acts as a reducing agent, as a capping agent (in the reduced, borate, form) and a matrix to embed AuNPs. At concentrations below 25 mM, both boric acid and borate typically exist as monomers. The presence of planar BO_3^- and tetrahedral BO_4^- moieties is pH-dependent [180]. In higher concentration solutions, an equilibrium is established between the boric acid and polynuclear complexes such as $B_3O_3(OH)_4^-$, $B_4O_5(OH)_4^{2-}$, $B_3O_3(OH)_5^{2-}$, $B_5O_6(OH)_4^-$, and $B(OH)_4^-$. Changes in pH induce condensation, leading to the formation of more complex polyanions. Under acidic pH conditions, planar nets stacked together are formed [181].

In the presence of gold nanoparticles, metallic cores become embedded in the polyoxoborate matrix. This results in the formation of a nanocomposite coating known as BOA. The building blocks of BOA are amphiphilic, with amphiphilicity stemming from charge delocalization and the reduction in the formal charge of polymerized oxoborate anions (imparting hydrophobic properties). Additionally, the presence of accessible -OH groups at the edges contributes to the hydrophilic properties of BOA. This

amphiphilic nature allows BOA to be effectively deposited on hydrophilic surfaces (often through condensation with surface OH groups) and hydrophobic surfaces [178]. When present in the reaction vial, AuNPs are embedded within the oxoborate matrix on the surface of the modified container.

BOA was developed earlier by Paczesny and coworkers. The antibacterial activity of the BOA nanocomposite was verified earlier in the cotton-based materials [178] and orthodontic appliances [182]. BOA-modified materials appeared to be effective against both planktonic Gram-positive and Gram-negative bacteria and the prevention of biofilm formation by the oral cavity bacteria. At the same time, the nanocomposite was harmless to mammalian cells (18LN, BTC-6, HepG2, SVF cell lines) and presented an insignificant release of gold to the solution [178]. However, in laboratory practice, the contaminations are frequently caused by yeasts [183], so there was a need to verify the antifungal activity of BOA nanocomposite as well. Moreover, preliminary results suggested that the surface modification with BOA may increase the hydrophobicity of the surface, allowing it to limit the absorption of the phages onto the labware surfaces.

4.3. Results and discussion

4.3.1. Characterization of BOA-modified vials

At first, AuNPs and polypropylene (PP) vials modified with BOA nanocomposite were characterized. DLS measurement was used to estimate the size of synthesized AuNPs (**Figure 4A**). The diameter measurement confirmed using UV-Vis (**Figure 4B**) indicated the size of the nanoparticles of about 4.5 ± 1 nm. The EDAX elemental analysis detected large amounts of carbon, most probably from the vial (made of polypropylene) – 93.19% of the sample's weight. The remaining 6.81% was gold. Boron, oxygen, and hydrogen shares were insignificant (**Figure 4C**).

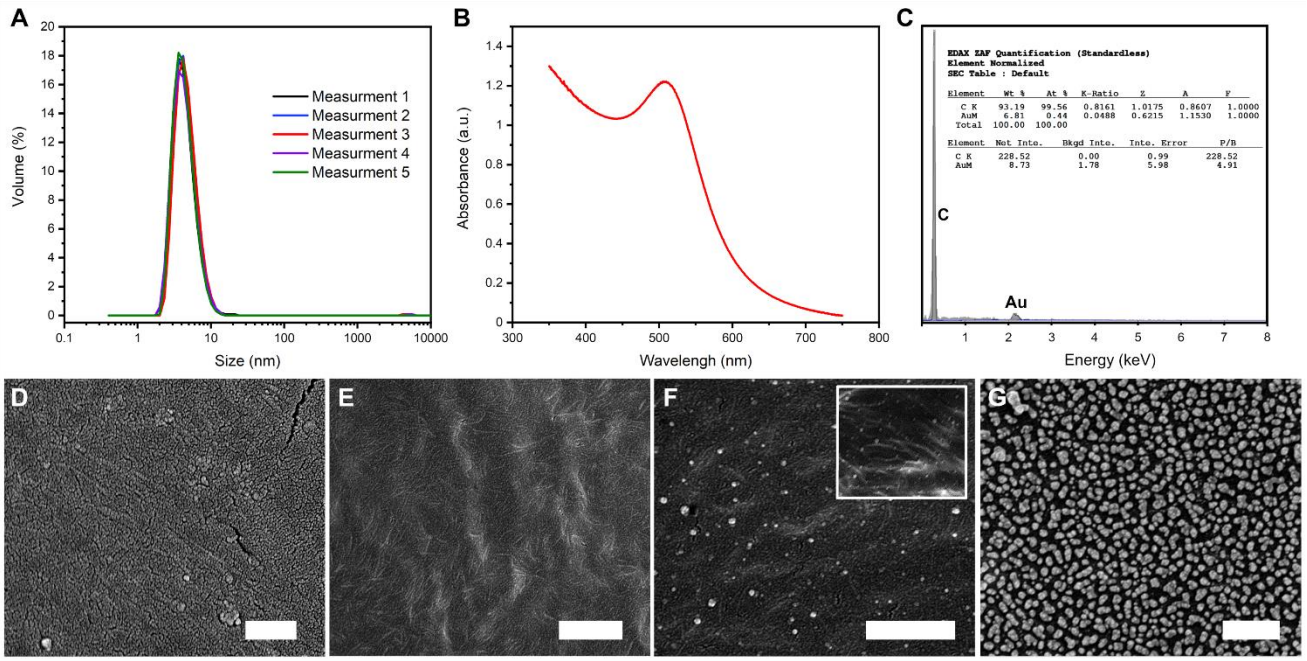

Figure 4. A) DLS measurements show the hydrodynamic diameter of the initial AuNPs equal to 4.5 ± 1 nm. B) UV-Vis measurement of the initial AuNPs. C) The EDX spectrum of BOA was deposited onto the polypropylene surface, proving gold's presence within the coating. SEM pictures of D) pristine polypropylene vial used in the study; E) pristine vial after 24 hours incubation with M13 phages. Visible fiber-like features are virions. F) The inner surface of the vial after single deposition of BOA, and G) triple deposition of BOA. The inset in C) shows the same surface as the main picture in C) but without an additional thin layer of gold-sputtered to facilitate SEM observations. Scale bars correspond to 500 nm.

Scanning electron microscopy examinations revealed the distinction between single (**Figure 4F**) and triple (**Figure 4G**) BOA deposition. Following a single deposition, sparsely distributed bright objects, sized around 30 to 50 nm (significantly larger than the initial nanoparticles with a diameter of approximately 4.5 nm), were evident on the surface (**Figure 4F**). After multiple deposition processes, a densely packed and uniform layer of similar bright objects was observed (**Figure 4G**). In the case of pristine vials (**Figure 4D**), only cracks in the sputtered gold layer were noted. The inset in **Figure 4F** displays the surface of the same sample as the main picture but with lower resolution, as this sample was not sputtered. Comparable morphological features were observed in both sputtered and non-sputtered samples, ruling out the possibility that the discussed bright objects are artifacts originating from sample post-processing.

4.3.2. Improved bacteriophage storage

To demonstrate the effectiveness of BOA in stabilizing phage suspensions, three representative phages we investigate: MS2, M13, and T4, which belong to three major phage types—symmetrical, filamentous, and tailed phages, respectively.

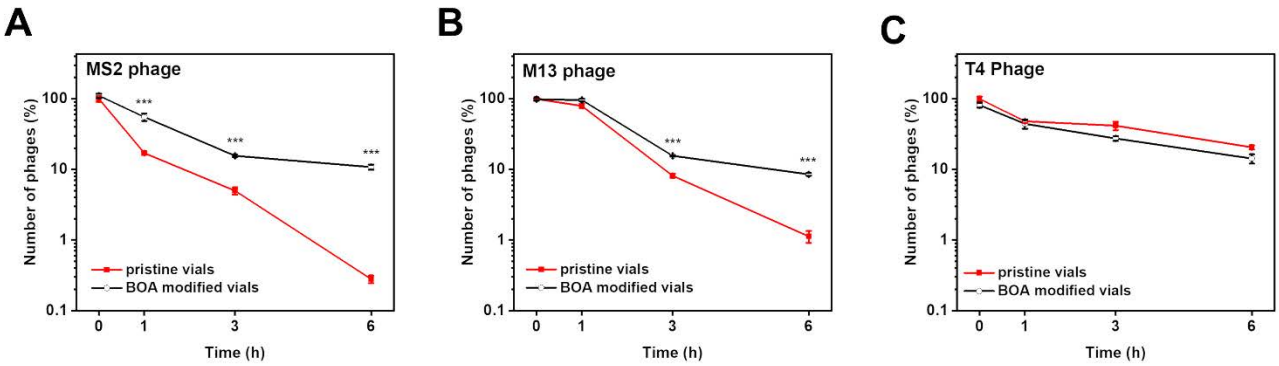

Figure 5. Comparison of the number of bacteriophages presented as a percent of concentration, respectfully to the concentration of phages at 0 h. The initial concentrations were A) $3.75 \times 10^3 \pm 3.74 \times 10^2$ PFU/mL for MS2, B) $5.08 \times 10^3 \pm 1.60 \times 10^2$ PFU/mL for M13, and C) $6.60 \times 10^5 \pm 5.01 \times 10^4$ PFU/mL for T4. The decrease was visible in pristine vials in M13 and MS2 but not in T4. BOA showed statistically significant protection against the phage titer decrease in the case of M13 and MS2 and did not show any adverse effect on T4 suspensions (*** $p < 0.001$).

After the 24-hour incubation, a significant decrease in bacteriophage titer was observed in pristine vials. For MS2 bacteriophage, a reduction of over 99.9% was observed (**Figure 5A**). For the M13 phage, the decrease was about 99% (**Figure 5B**). Simultaneously, it was smaller than 1 log in BOA-modified vials, which suggested that BOA-modified surfaces effectively reduced the decrease in phage titer during the incubation. For T4 phage, a decrease of about 50% was observed in both pristine and BOA-modified vials (**Figure 5C**). The results suggested that the BOA nanocomposite had no significant effect on T4 bacteriophage.

4.3.3. Antibacterial and antifungal activity

Antibacterial efficacy of BOA nanocomposite was performed by incubating representatives of Gram-negative bacteria (*E. coli*) and Gram-positive bacteria (*S. aureus*) in both pristine and BOA-modified polypropylene containers. Remarkably, even a single deposition of BOA significantly impacted bacteria.

The experiments involving *E. coli* demonstrated an increase in the number of bacterial cells in non-modified vials (**Figure 6A**). After 24 hours, the cell count in the suspension increased by approximately tenfold. This phenomenon aligns with Garvie's

findings in the 1950s, where it was noted that "*E. coli will grow when cell suspensions are inoculated into phosphate buffer*" [184]. Only three cell division cycles were needed to achieve an eightfold increase, closely matching the observed rise. The number of *E. coli* cells remained relatively constant throughout the experiment in BOA-covered vials. Two potential explanations for this phenomenon are considered: (*i*) BOA effectively inhibits replication, or (*ii*) it kills bacteria at a rate comparable to their replication. After 24 hours, the bacterial count in the control sample was roughly ten times higher than in BOA-protected vials.

In the case of the Gram-positive bacterium, *S. aureus*, a substantial decrease (approximately 99%) was observed in BOA-modified vials after only 3 hours of incubation (**Figure 6B**), while the number of bacterial cells changed marginally in the non-modified containers.

The observed difference in the magnitude of BOA's effect between Gram-positive and Gram-negative bacteria aligns with prior research, indicating that Gram-positive bacteria are more sensitive to physical and chemical factors than Gram-negative bacteria [185].

In the case of the Gram-positive bacterium, *S. aureus*, a substantial decrease (approximately 99%) was observed in BOA-modified vials after only 3 hours of incubation (**Figure 6B**), while the number of bacterial cells changed marginally in the non-modified containers.

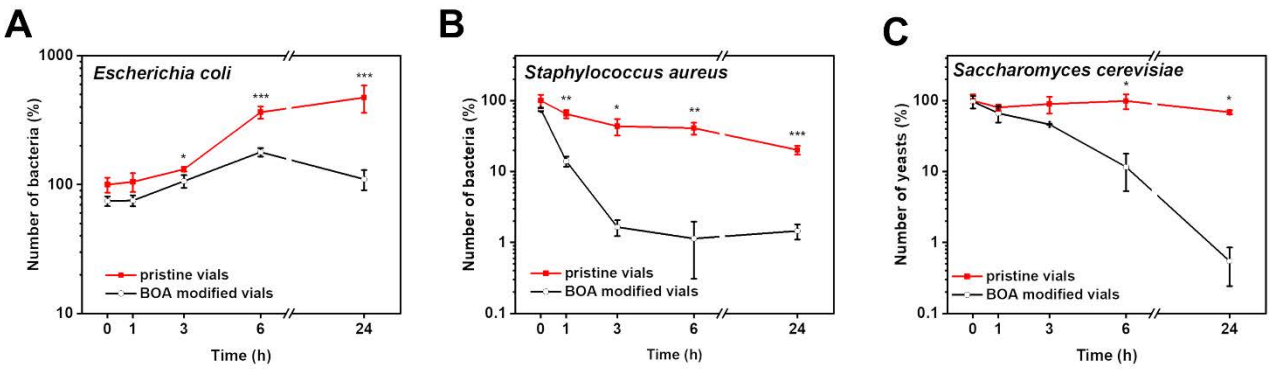

Figure 6. Comparison of growth rate of A) *E. coli* BL21 (DE3) (initial concentration of $1.78 \times 10^3 \pm 2.38 \times 10^2$ CFU/mL), B) *S. aureus* (initial concentration of $1.53 \times 10^4 \pm 3.28 \times 10^3$ CFU/mL), and C) *S. cerevisiae* (initial concentration of $8.25 \times 10^4 \pm 1.84 \times 10^4$ CFU/mL) in pristine vials and BOA-modified vials. In all cases, BOA caused a decrease in the number of viable cells compared to pristine vials (* $p < 0.05$; ** $p < 0.01$; *** $p < 0.001$).

For the representative of yeasts, *S. cerevisiae*, the 24-hour incubation in BOA-modified vials resulted in a 99% decrease in the titer. At the same time, in pristine vials,

the number of yeast cells remained approximately the same throughout the experiment (**Figure 6C**). The results suggest highly antifungal and antibacterial activity against Gram-positive bacteria and at least bacteriostatic activity against Gram-negative bacteria.

4.3.4. Mechanism of improved long-term storage

Previous research has established that the adsorption of phages is influenced by the water-wetting angle (WA). When the WA surpasses a specific threshold value, phages tend to adsorb onto plastic surfaces. SEM observations confirmed the presence of M13 virions on the surface of non-modified vials after 24 hours of incubation (**Figure 4E**), indicating successful adsorption. For T4 phages, the threshold WA was around 95° [168]. Here, the wetting angle of pristine vials was approximately 93.2° ± 0.2°. This explains why there was no decrease in T4 titer in pristine vials.

A single deposition of BOA did not exhibit phage protection (data not shown). However, a notable stabilization of MS2 and M13 suspensions was observed upon triple deposition of BOA onto the inner surface of the containers (**Figure 5A-B**). The saturation of the surface with BOA led to a reduction in the wetting angle (WA) from approximately 93.2° ± 0.2° to around 83.8° ± 1.3°. After 6 hours of incubation with mixing, the MS2 and M13 suspensions titers were more than an order of magnitude higher than in the pristine vials. BOA effectively prevented the adsorption of virions on polypropylene surfaces, transforming the vials from “unsafe” to “safe” by decreasing the WA.

4.4. Summary

The quality of labware is an uncontrollable variable, and it may impact the reproducibility of phage-related studies or the effectiveness of phage therapies. Hence, it’s known that virions may adhere to the inner walls of plastic containers when the water-wetting angle goes beyond a certain threshold. This phenomenon may significantly affect the reproducibility of phage-related research. However, modifying plastic labware with the BOA nanocomposite can overcome such adverse effects. The BOA nanocomposite reduced the uncontrollable sticking of virions to plastic surfaces and provided protection against bacteria and fungi. The process of depositing BOA is simple and aligns with the principles of “green chemistry” since it uses a water-based protocol that minimizes waste. These findings are a step toward improving the

reproducibility of phage-related research. Additionally, BOA could be employed to store phage cocktails for phage therapies and biocontrol applications.

CHAPTER 5

Bacteriophage stabilization from the UV irradiation using small-molecular dyes

Parts of this chapter constitute research articles:

1. "*Congo red protects bacteriophages against UV irradiation and allows for the simultaneous use of phages and UV for membrane sterilization"*
   Mateusz Wdowiak, Patryk A. Mierzejewski, Rafał Zbonikowski, Bartłomiej Bończak, Jan Paczesny, *Environmental Science: Water Research & Technology*, 2023, 9(3), 696-706,

   Figures 7-11, **22-25**, and **29-32** were adapted from this paper, referenced as [174] based on CC BY NC 4.0 License.

2. "*Multi-funtional phage-stabilizing formulation for simultaneous protection from UV irradiation and elevated temperature"*
   Mateusz Wdowiak, Magdalena Tomczyńska, Quy Ong Khac, Aneta Karpińska, Agnieszka Wiśniewska, Rafał Zbonikowski, Francesco Stellacci, Jan Paczesny, submitted

5.1. Bacterial contaminations in the industry

Bacteria, the most abundant organisms on Earth, affect almost every aspect of human life, including the industrial environment. The food-producing industry, one of the fastest-growing sectors, is particularly vulnerable to bacterial infections. According to the Food and Agriculture Organization (FAO), the AMR foodborne pathogens "increases costs of both health care and food production", and the AMR *Salmonella* contaminations cause the annual burden of $50 billion [186]. In this case mostly human pathogens are considered. Among poultry, *Salmonella* spp. *Campylobacter* spp., and *Clostridium perfringens* are the most frequent pathogens that can be both fatal for animals and result in food contamination. In the USA alone, nearly 90% of poultry flocks were affected by *Salmonella* or *Campylobacter* [187]. Aquaculture aquatic animals (including fish, shellfish, and shrimps) are exposed to pathogens, such as *Vibrio* spp. and *Aeromonas* spp. [188]. Hence, there are over 30 different foodborne pathogens, so efficient methods for eliminating bacteria seem essential for the modern-day food industry.

However, not only the food industry is affected by bacterial contaminations. The fuel ethanol industry, utilizing almost 10% of the total corn crop and producing 15 billion liters of fuel ethanol, is affected by lactic acid bacteria (LAB) contamination. LAB, mostly *Lactobacillus fermentum*, *Lactobacillus salivarius*, and *Lactobacillus casei*, are disturbing the growth of *S. cerevisiae* by overgrowing and producing acetic and lactic acids that are harmful to yeasts [189,190]. The main reservoirs for bacterial contaminations are, however, water-based facilities, including bioreactors and membrane systems.

5.1.1. Membrane biofouling and bioreactors

The global market for membrane bioreactors is projected to reach 4.9 billion USD, experiencing a compound annual growth rate (CAGR) of 8.3% by 2026 [191]. Notably, from 2018 to 2023, the market demonstrated rapid growth, increasing from 1.9 billion USD to 3.8 billion USD in just five years, with a remarkable CAGR of 14.7%. In 2019, another report estimated the sector's value to be 3.0 billion USD [192].

Despite its growth, the membrane bioreactor industry faces significant challenges, including biofouling, which is considered one of its primary threats. The cost of cleaning fouled membranes is 50 to 100% higher than standard maintenance procedures, and using fouled membranes can elevate energy costs or lead to equipment malfunctions. Biofouling is most commonly treated with chemicals [193].

However, they are often corrosive and might impact the membrane's integrity. Additionally, disposing of used chemicals and by-products poses health, safety, and environmental risks [194].

UV light is another sterilization agent, though its application is constrained by bioreactor geometry and limited access to cloudy media [195]. Alternative methods, such as antibiotics, antifungal drugs, temperature sterilization [196], and ozonation [197], are expensive, time-consuming, or require specialized equipment with corrosion-resistant properties [198]. Hence, there is a pressing need to develop new methods to combat membrane fouling, preferably using mild agents that don't generate toxic waste. Hence, bacteriophages are specific towards their bacterial hosts and biodegradable, so they seem to be a promising solution for bioreactor sterilization.

5.1.2. Agriculture

Bacterial infections significantly threaten not only humans but also plants (particularly fruit plants and vegetables). This issue directly affects humans, as bacterial plant diseases are estimated to cause annual economic losses of around 220 billion USD globally [35]. Among the numerous bacterial pathogens, *E. amylovora* [36] (causing Fire blight disease in apple trees), *Agrobacterium tumefaciens* [37], and *P. syringae* [38] are responsible for economically significant diseases. Conventional methods for treating bacterial diseases involve the use of antibiotics and pesticides. However, both approaches contribute to environmental accumulation and potentially harm living organisms [199]. Notably, the release of antibiotics into the environment raises concerns about fueling antibiotic resistance [200]. Consequently, there is an urgent need to identify biocompatible and environmentally friendly bactericides, such as bacteriophages, to address these challenges.

Plenty of commercially available bacteriophage-based products are designed to deal with bacterial infections in food products, including crops [201] and contamination by food-borne pathogens [202]. Even though the majority of obstacles related to phage application in the food industry and agriculture are related to the law and regulations [203], the stability of phage-based products in the food industry is equally important [204]. Introducing bacteriophage in the plant-growing industry would meet additional challenges, such as exposure to UV irradiation. The stabilization challenge during UV exposure can be overcome using protein-binding dyes (e.g., Congo red or trypan blue) [174,205].

5.2. Simultaneous usage of bacteriophages and the UV

The application of bacteriophages is an intriguing solution for eliminating fouling agents like bacterial cells, holding significant promise for industrial applications. However, current research in this area is in its early stages. The specificity of certain phages targeting specific bacteria necessitates combining bacteriophage sterilization with less specific bactericidal factors, such as UV radiation.

A report from 2021 by Scarascia et al. suggested a two-step sterilization protocol using UV and bacteriophages for efficient bioreactor membrane sterilization. The method, as described, had a notable advantage in terms of speed, taking about 3 to 6 hours. The authors compared the efficacy of simultaneous UV and bacteriophage use for different durations (3 and 6 hours) and bacteriophage exposure following UV exposure. Significant differences in bacteria elimination efficacy were observed between independent UV-C + bacteriophage and simultaneous UV-C + bacteriophage exposure. This made the protocol significantly faster than chemical-based sterilization methods, such as 96 hours for chlorine and up to a few days for ozonation while maintaining comparable efficacy to chemical treatment. For instance, the alive/dead cell ratio after chemical treatment was approximately 0.25; after UV-C + bacteriophage treatment, it was around 0.35 [169]. However, a drawback of this method is that UV deactivates bacteria and phages alike. The reason might be that ultraviolet radiation targeted the viral genome [96], particularly the pyrimidine bases, causing damage and mutations. Even though some coliphages (e.g., T2, ΦX174, MS2, fr) were known for developing UV resistance, this process was considered “prolonged and inefficient” [206]. Understanding the adverse impact of UV radiation on bacteriophages underscores the urgency of developing protection mechanisms against this highly energetic radiation [202]. The concurrent use of UV radiation and bacteriophages, with stabilizers that would shield the phages from the detrimental effects of UV, could lead to an even more efficient and potentially faster sterilization protocol. Fortunately, the candidate for such a UV-stabilizing factor was already proposed in the 80s.

The reports from 1989, 1991, and 2008 suggested the application of Congo red (CR) and trypan blue dyes to protect certain baculoviruses (a family of insect-targeting, eukaryotic viruses), namely *Lymantria dispar* (L.) nuclear polyhedrosis virus (LdMNPV), *Lymantria dispar* (L.) cypovirus (LdCPV), and *Heliothis zea* nuclear polyhedrosis virus (HzMNPV), from the adverse effects of UV irradiation. According

to the authors, at the CR concentration of 1% (w/v), the viruses remained at 100% of their original activity after 60 minutes of irradiation [205,207,208]. However, their results were inconsistent with CR's reported effects on the representatives of enveloped viruses, such as human immunodeficiency virus (HIV) [209], Newcastle disease virus (NDV) [210], influenza virus, fowl plague virus, and Sindbis virus [211]. In these cases, CR was shown to have an adverse effect on virions.

The inconsistency of the CR effect on different viruses and the fact that these effects weren't verified on bacteriophage models were a motivation to prove the potential UV-protective properties of CR dye to non-enveloped and enveloped bacteriophages. The successful introduction of dye-mediated protection might solve the problem of efficacy limitation in combined phage-UV sterilization protocols.

Congo red, a representative of azo dyes, has been recognized for over a century as a staining agent. It is commonly used to stain amyloids and aggregated proteins in the medical field. Its toxicity to rats is estimated at an LD_{50} of 15.2 g per kilogram of body mass. For humans, a lethal dose is approximated to be around 143 mg per kg of body mass [212], similar to caffeine, with an LD_{50} ranging from 150 to 200 mg per kg [213]. However, some studies suggest that CR might be hazardous, with potential harm to the environment and animals [214]. Consequently, the application of Congo red protocols is restricted to procedures that do not involve living organisms, and it is only viable when the dye can be recovered from aqueous solutions. This underscores the urgent need to identify alternative dyes that exhibit similar properties but are non-hazardous in nature.

The dyes already approved as food additives seem to be promising alternatives. Several food dyes, including brilliant blue FCF (E132), Allura red (E129), and sunset yellow FCF (E110), are recognized for their interactions with diverse proteins [215,216] or even bacteriophages [217,218]. Notably, brilliant blue FCF resembles brilliant blue R-250 (Coomassie blue), commonly used for protein staining in gel electrophoresis. While this connection has yet to be confirmed, the possibility of dye-phage interactions might be a premise for a suitable and non-hazardous alternative for CR. One of the goals was to verify the potential UV-protective properties of several frequently used food dyes – tartrazine, quinoline yellow, sunset yellow FCF, Allura red, Ponceau 4R, azorubine, brilliant blue FCF, and indigocarmine. Applying food dyes as UV-protectants would solve the problem of bio-accessibility and improve the sterilization protocols combining bacteriophages and UV irradiation in the food industry.

5.3. Results and discussion

5.3.1. Congo red

Initially, the study aimed to determine the effect of UV irradiation (254 nm, approximately 360 mJ/cm^2) on investigated bacteriophages (T1, T4, T7, MS2, Φ6, M13, and LR1_PA01). The energy level used in this experiment was comparable to that of the standard sterilization protocol. In the control samples containing only bacteriophage suspensions in the TM buffer solution, virtually all bacteriophages were inactivated after 1 minute of irradiation (**Figure 7**). This means the bacteriophage amount was below the method's detection limits, i.e., 25 PFU/mL (**Figure 7A**). The complete inactivation was observed regardless of the initial phage concentration (ranging from 10^5 PFU/mL to 10^8 PFU/mL; data not shown).

It was observed that bacteriophage Φ6 was already inactivated during incubation with CR before irradiation. Φ6 is representative of enveloped phages.

Upon adding CR to the phage suspensions and 1 minute of UV irradiation, a minor phage titer drop was observed for T4 and T7, while no decrease was observed for T1, LR1_PA01, MS2, and M13. The LR1_PA01 phage exhibited the most significant reduction in titer, approximately 1 log, among all examined phages.

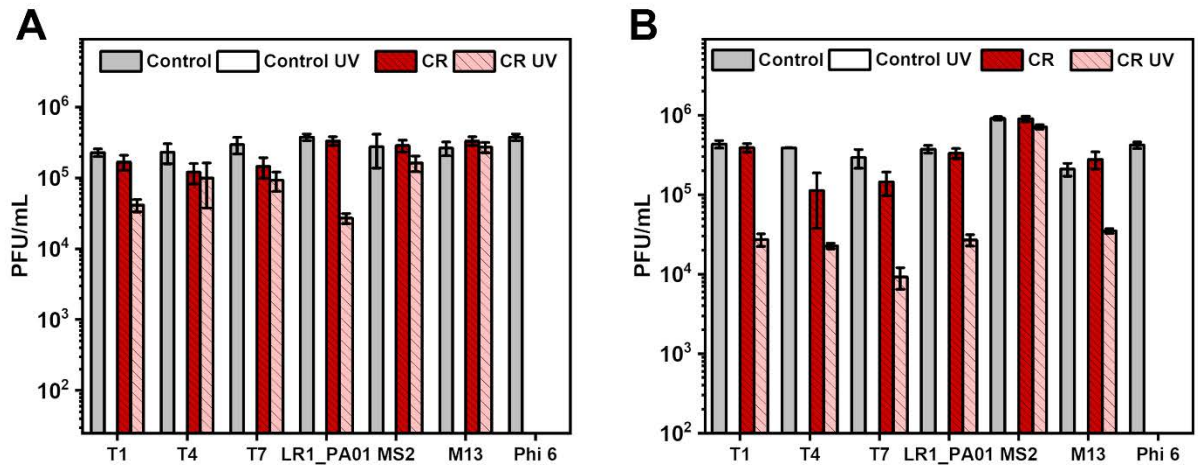

Figure 7. The effect of UV, Congo red (1%), and both UV and Congo red on (A) T1, T4, T7, LR1_PA01, MS2, M13, and Φ6, (B) *E. coli, P. aeruginosa, L. monocytogenes, E. durans*, and *S. cerevisiae*. CR protected non-enveloped phages against UV but deactivated Φ6 even without UV irradiation. The time of the UV irradiation was A) 1 minute and B) 60 minutes. Please note that bars corresponding to "Control UV" samples are not drawn, as in all cases, all phages were inactivated, and the titer was below the detection limit of the method.

The survival rate was similar when the UV exposure was extended to 60 minutes. In such conditions, the T7 phage exhibited the most significant decrease

in titer (almost 2 log), while other dsDNA bacteriophages (T1, T4, LR1_PA01) presented similar survival rates (decrease by about 1.5 log). Just like during 1-minute exposure, the reduction in the tier of MS2 phage was minimal (< 0.5 log). The addition of CR allowed for maintaining specific activity in the case of all examined non-enveloped bacteriophages after 60 minutes of exposure (**Figure 7B)**.

For all six examined non-enveloped bacteriophages, the lowest effective dose of CR, allowing for protection against UV irradiation, was estimated. Bacteriophages were pre-incubated with CR concentrations varying from 0.001% to 2%. The samples were exposed to UV radiation for 1 minute (the same parameters as in previous experiments) (**Figure 8)**. Data were fitted using the Hill equation to find EC_{50}, i.e., the concentration that provides 50% protection in the given conditions.

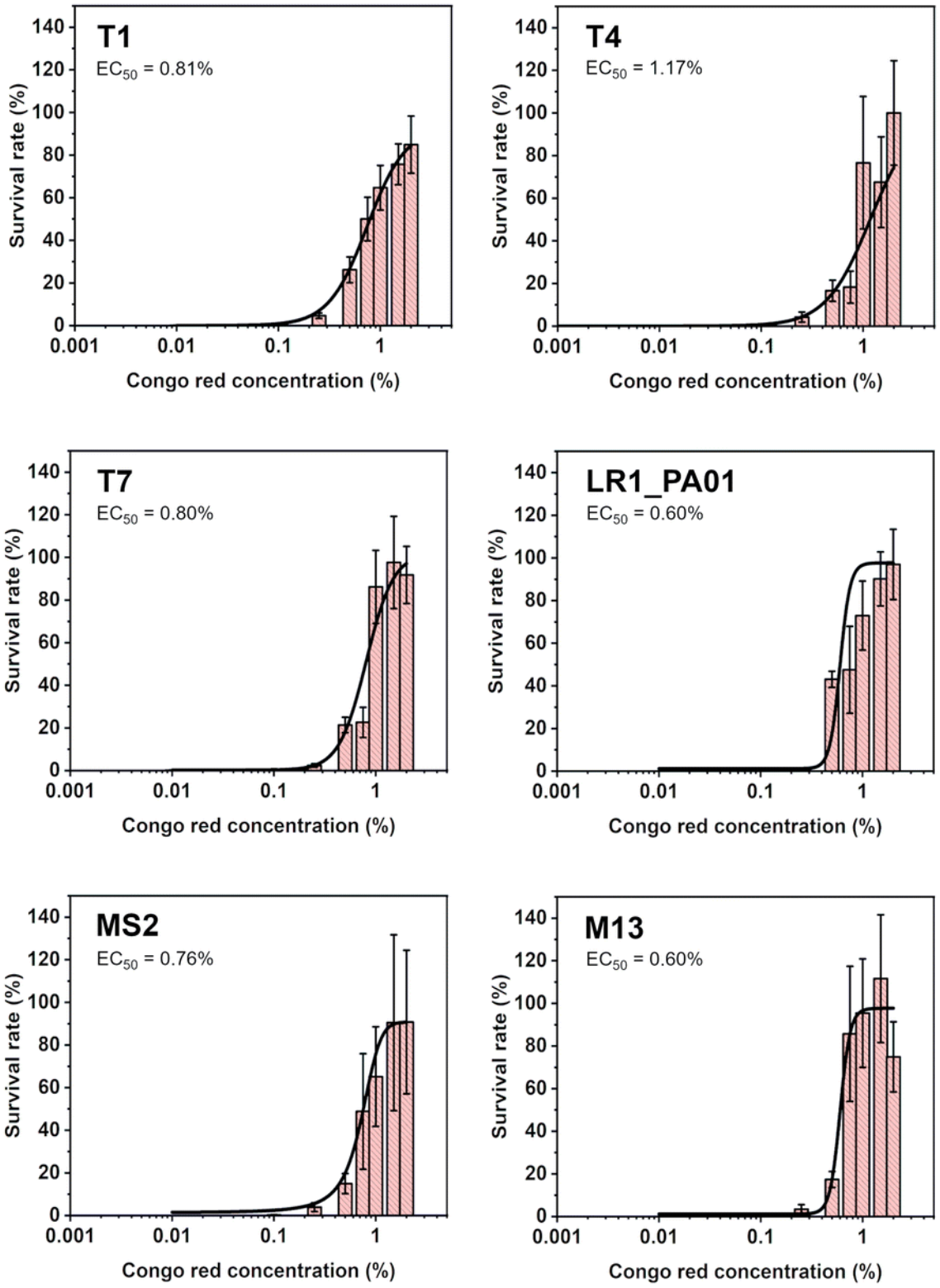

Figure 8. The survival rate of T1, T4, T7, LR1_PA01, M13, and MS2 bacteriophages after 1 minute of UV irradiation as a function of the CR concentration is presented. Data were fitted using the Hill equation. The lower-limiting concentration turned out to be 0.1%.

The calculated EC_{50} values ranged between 0.60% and 1.17%, depending on the type of bacteriophage. Filamentous M13 phage and LR1_PA01 phage were characterized with the lowest EC_{50} concentration of 0.60%.

The selectivity of CR protection was verified towards Gram-negative bacteria (*E. coli, P. aeruginosa*), Gram-positive bacteria (*L. monocytogenes, E. durans*), and yeast (*S. cerevisiae*). CR alone did not impact the various bacterial species, whether Gram-negative or Gram-positive. Interestingly, the incubation in CR alone led to the elimination of *S. cerevisiae* even without UV exposure.

P. aeruginosa exhibited higher UV resistance than the other microorganisms studied. A 1-minute UV irradiation (without CR) resulted in approximately a 3 log deactivation of *P. aeruginosa*, whereas complete deactivation (5 to 6 log decrease) was observed for *E. coli, L. monocytogenes, E. durans*, and *S. cerevisiae*.

CR did not protect against UV for Gram-negative bacteria, as the UV irradiation effect was similar with or without CR. However, CR offered almost complete protection against UV for the Gram-positive bacteria, both *L. monocytogenes* and *E. durans* (**Figure 9**).

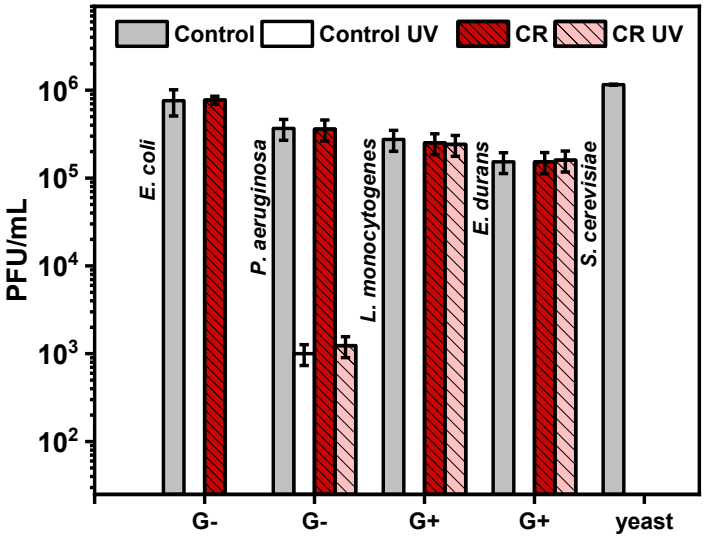

Figure 9. The verification of CR protective properties towards bacteria and yeasts. Gram-negative bacteria (*E. coli, P. aeruginosa*) were unprotected against UV. *L. monocytogenes* and *E. durans* could survive UV exposure when CR was added. For *S. cerevisiae*, the presence of the dye itself was lethal.

To confirm that the phage protection was caused by the uniqueness of CR and not by the presence of any additional molecule in the system, five more dyes were

tested. In the experiment, two additional azo dyes (eriochrome black T and methyl orange) and three representatives of triphenylmethane dyes (crystal violet, thymol blue, and phenol red) were selected. These dyes are commonly used as pH indicators in cell biology laboratories. In another experimental set, popularly used staining compounds (rhodamine B, eosin Y, SYBR green, crystal violet) and quinine were used. Titration tests indicated that only CR exhibited bacteriophage protective properties against UV. In contrast, thymol blue and phenol red led to a decrease in viral titers after 24 hours of incubation compared to the control sample and other tested compounds (**Figure 10**).

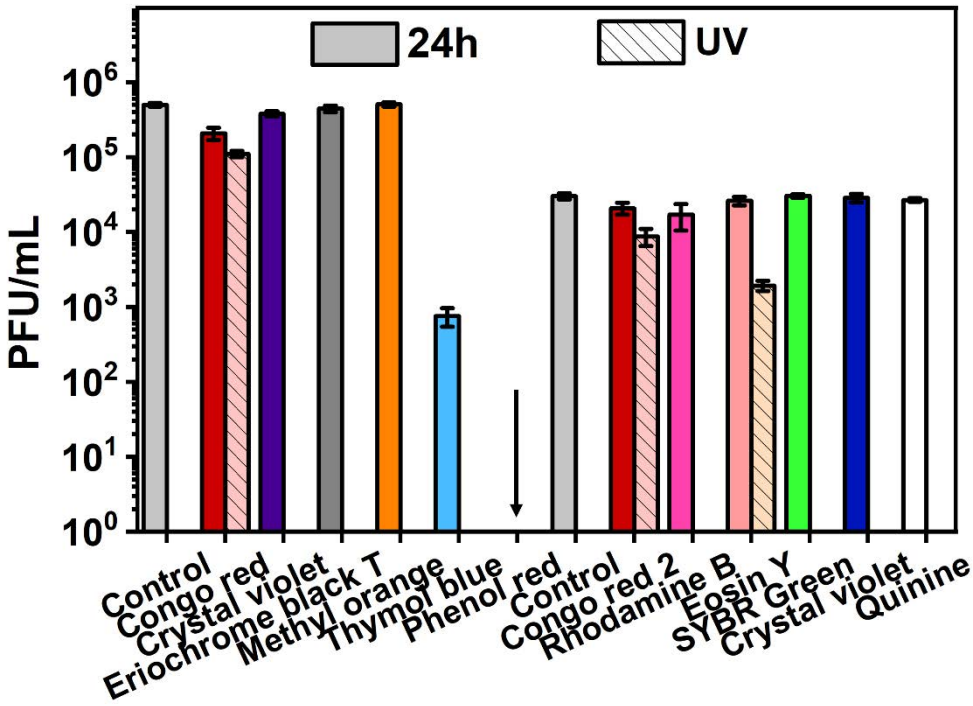

Figure 10. The comparison of UV protective properties of CR to other dyes. Comparison with various pH indicators (including crystal violet, eriochrome black T, methyl orange, thymol blue, and phenol red), and popularly used staining or UV absorbing compounds (rhodamine B, eosin Y, SYBR green, crystal violet, and quinine). The experiments were performed with two sets of samples. In one of them the initial concentration of phages was 10^6 PFU/mL, in the other - 10^5 PFU/mL. Among all the examined compounds, only the addition of CR to T4 phage suspension was protected during UV irradiation.

Among other tested dyes and compounds, only the protein-binding dye Congo red exhibited satisfactory efficacy, displaying a decrease in phage titer of less than 0.5 log after UV exposure (**Figure 10)**. Eosin Y demonstrated a certain level of protection against UV, resulting in a decrease in phage titer of approximately 1 log, which was below the desired stabilization level. It is plausible that eosin Y may be excited by light

in the visible spectrum, leading to non-obvious and yet-to-be-described phenomena [219].

In contrast, the other examined compounds (rhodamine B, SYBR green, crystal violet, and quinine) did not exhibit significant UV-protective properties. After 1 minute of UV exposure, the decrease in bacteriophage titer was to below the detection limits of the plating method (<200 PFU/mL). These findings strongly suggest that binding to the proteins of the viral capsid is crucial for protection against UV irradiation. Both rhodamine B and crystal violet bind to the cell membrane or bacterial cell wall, structures that are absent in bacteriophage virions, explaining their lack of efficacy. The inefficacy of SYBR green and quinine indicates that binding to DNA is unlikely to be related to stabilization against UV irradiation.

The selectivity of CR protection towards phages was verified by preparing the mixture of bacteriophage (LR1_PA01) and its non-host bacteria (*E. coli* BL21). Another goal of such an experiment was to confirm that adding CR to protect phages wouldn't affect the efficacy of eliminating bacteria by UV. Fortunately, the experimental design allowed for the observation that the UV irradiation resulted in the complete deactivation of all bacterial cells (by about 5 log), both with and without CR addition. UV deactivated LR1_PA01 in the absence of CR, but its activity was fully preserved in the presence of CR. The quantity of active LR1_PA01 phages was approximately the same as before irradiation (**Figure 11**).

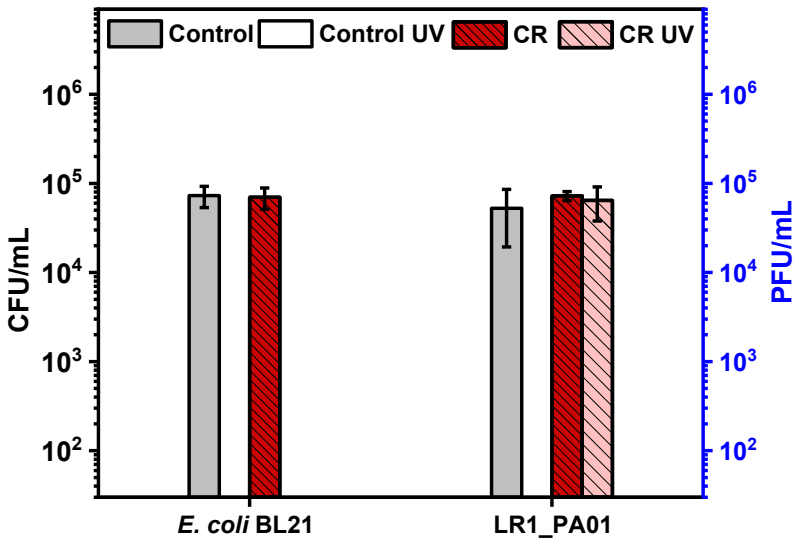

Figure 11. CR provides selective protection against UV to bacteriophages but not Gram-negative bacteria. A mixture of the LR1_PA01 bacteriophage and non-host bacteria (*E. coli*)

was exposed to UV (1 minute), CR (1%), and the mixture of UV and CR. After the exposure, bacterial cells presented a 100% mortality, while the number of active LR1_PA01 phages did not change.

5.3.2. Food dyes

To assess the UV protective properties of selected food dyes, a range of bacteriophages representing diverse capsid morphology and genetic material (T4, MS2, M13, P22; 10^5 PFU/mL), along with representatives of Gram-positive and Gram-negative bacteria (*S. aureus*, *B. subtilis*, *E. coli*, *A. baumannii*; 10^5 CFU/mL), were incubated in 0.5% (w/v) solutions of food dyes. After overnight incubation and a 1-minute exposure to UV irradiation (~360 mJ/m^2), bacteria and bacteriophage were quantified using plating or double-layer agar methods, respectively.

The results revealed that all selected food dyes substantially protected phages against UV exposure. This is very different comparing to other dyes and molecules (cf. **Figure 10** in section 5.3.1). The reduction in phage titer in the dye-containing samples was minimal (below 0.5 log). In contrast, the control sample (TM buffer solution) experienced a significant decline in phage titer, dropping below the detection limits of the employed method (approximately 25 PFU/mL) (**Figure 12**).

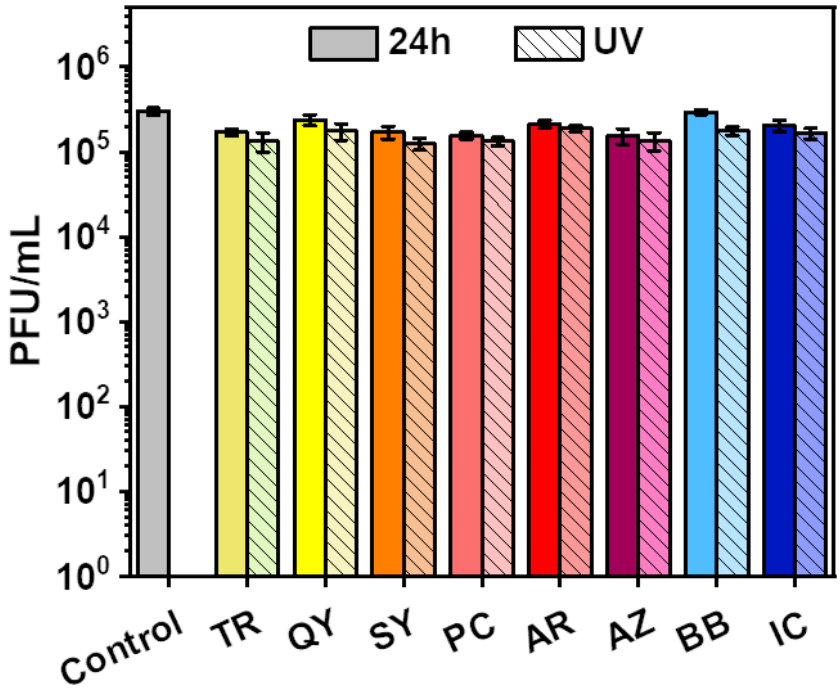

Figure 12. The evaluation of UV-protective properties of the food dyes performed on the T4 bacteriophage. A) The decrease in the titer of T4 bacteriophage caused by 1 minute UV exposure after overnight incubation in 0.5% solutions of tartrazine (TR), quinoline yellow (QY), sunset yellow FCF (SY), Ponceau 4R (PC), Allura red (AR), azorubine (AZ), brilliant blue FCF (BB) and indigocarmine (IC).

Knowing that all examined food dyes could protect T4 bacteriophage against UV irradiation, the next step was to verify if bacteriophages of different capsid morphology - MS2, M13, P22 - would also be protected. At the same time, the minimal concentration of each dye required to protect 50% of each examined bacteriophage in the solution (EC_{50}) was estimated.

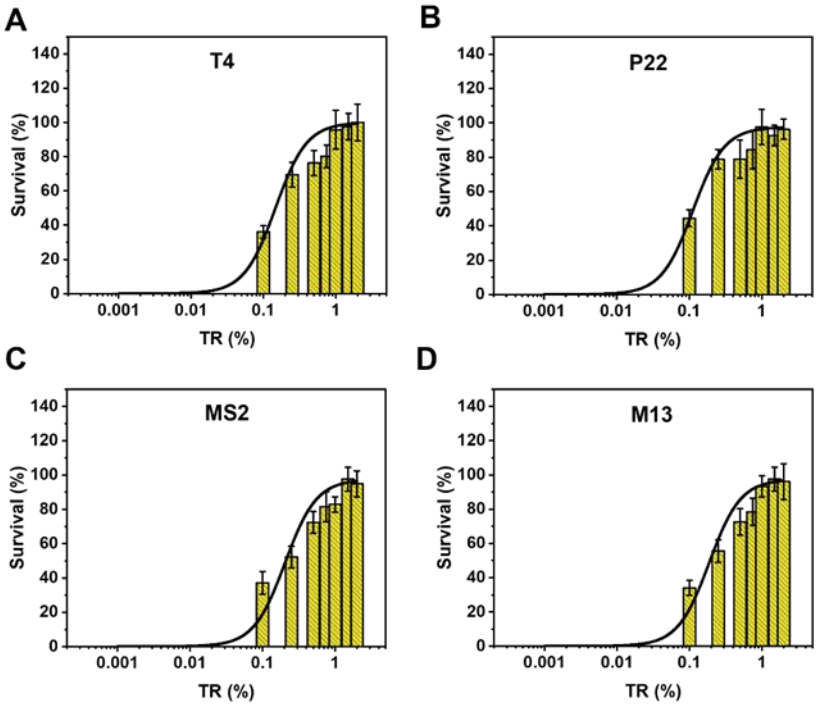

Figure 13. The estimation of EC_{50} values provided by tartrazine (TR) for A) T4, B) P22, C) MS2, D) M13.

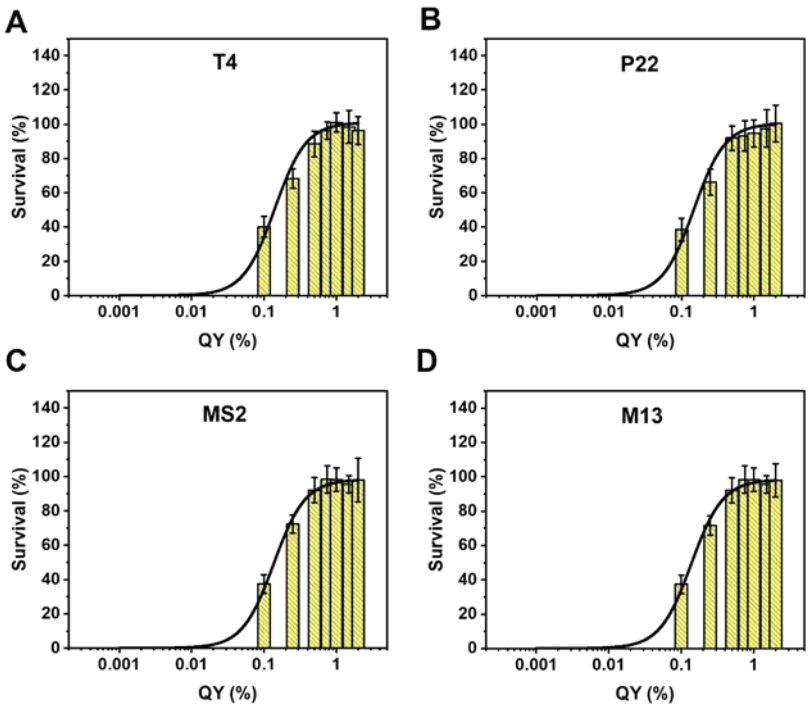

Figure 14. The estimation of EC_{50} values provided by quinoline yellow (QY) for A) T4, B) P22, C) MS2, D) M13.

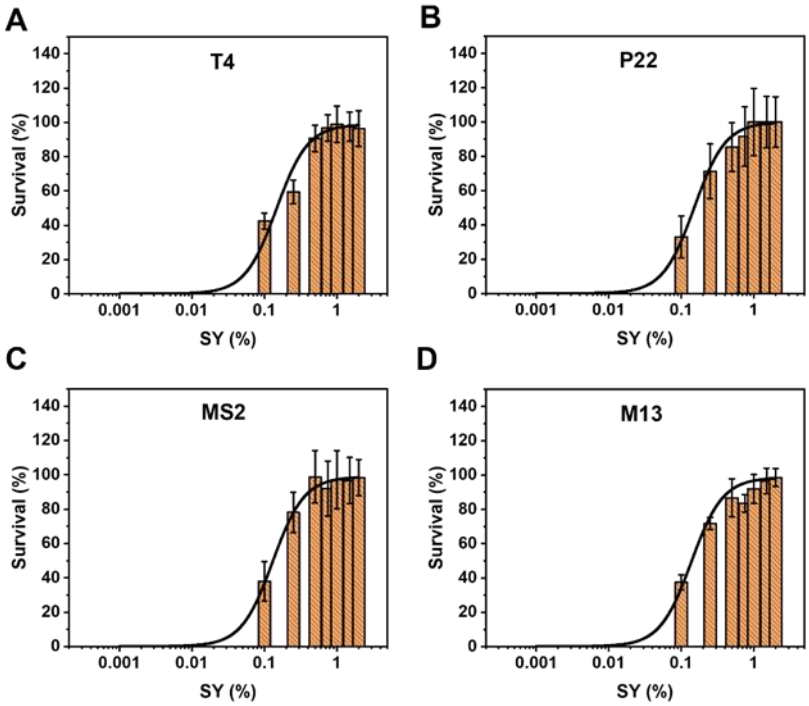

Figure 15. The estimation of EC_{50} values provided by sunset yellow FCF (SY) for A) T4, B) P22, C) MS2, D) M13.

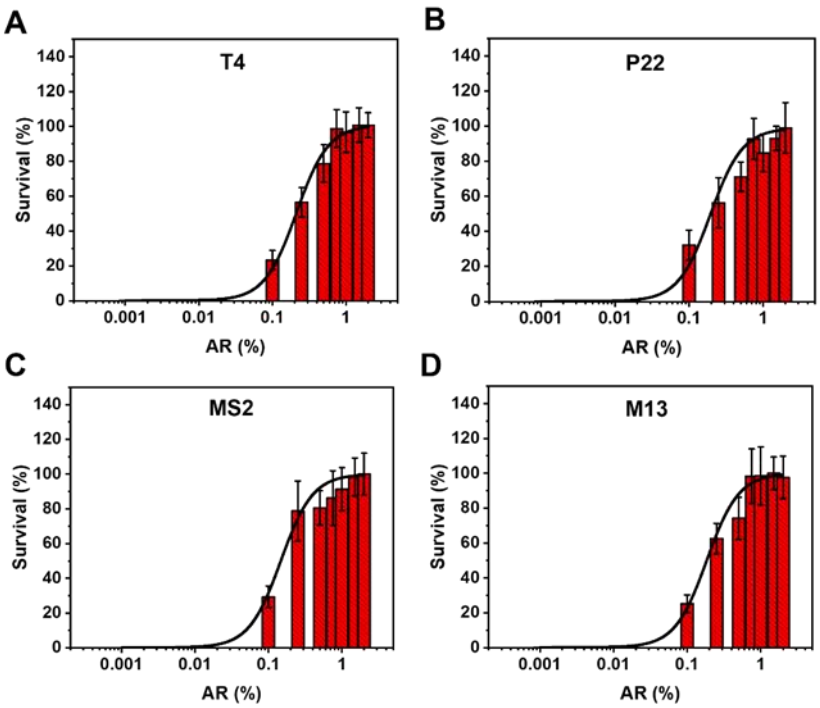

Figure 16. The estimation of EC_{50} values provided by Allura red (AR) for A) T4, B) P22, C) MS2, D) M13.

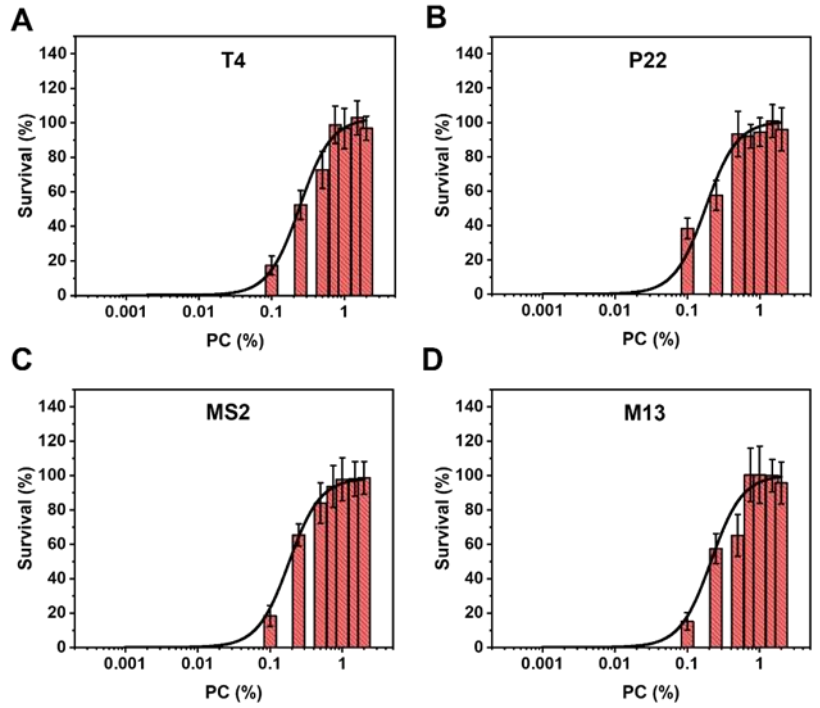

Figure 17. The estimation of EC_{50} values provided by Ponceau 4R (PC) for A) T4, B) P22, C) MS2, D) M13.

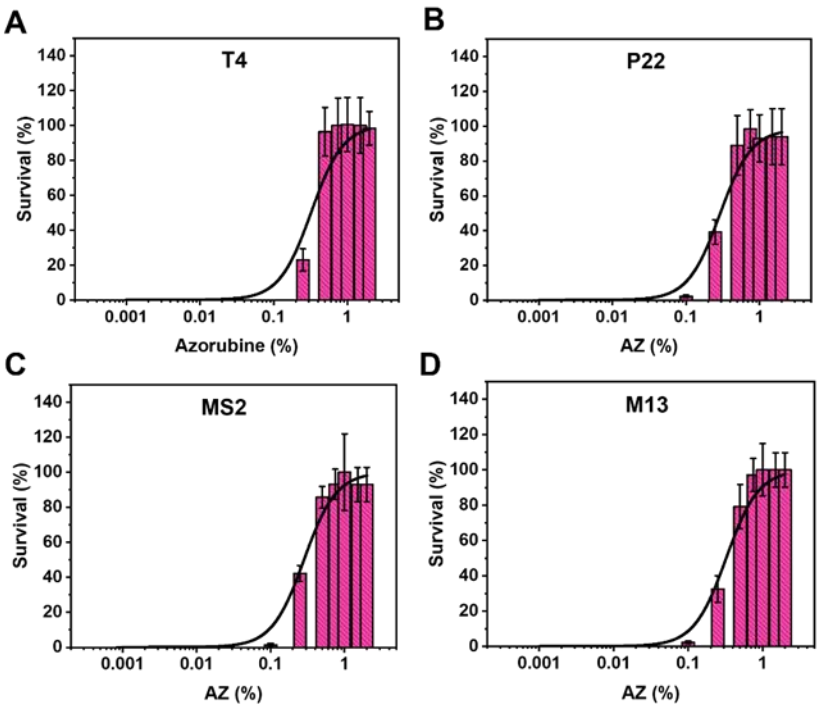

Figure 18. The estimation of EC_{50} values provided by azorubine (AZ) for A) T4, B) P22, C) MS2, D) M13.

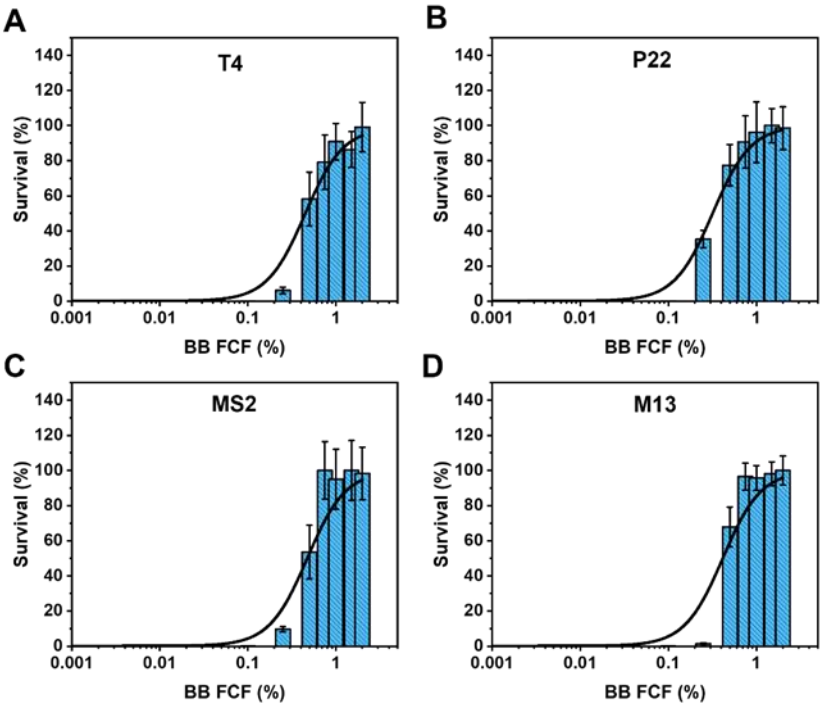

Figure 19. The estimation of EC_{50} values provided by brilliant blue FCF (BB) for A) T4, B) P22, C) MS2, D) M13.

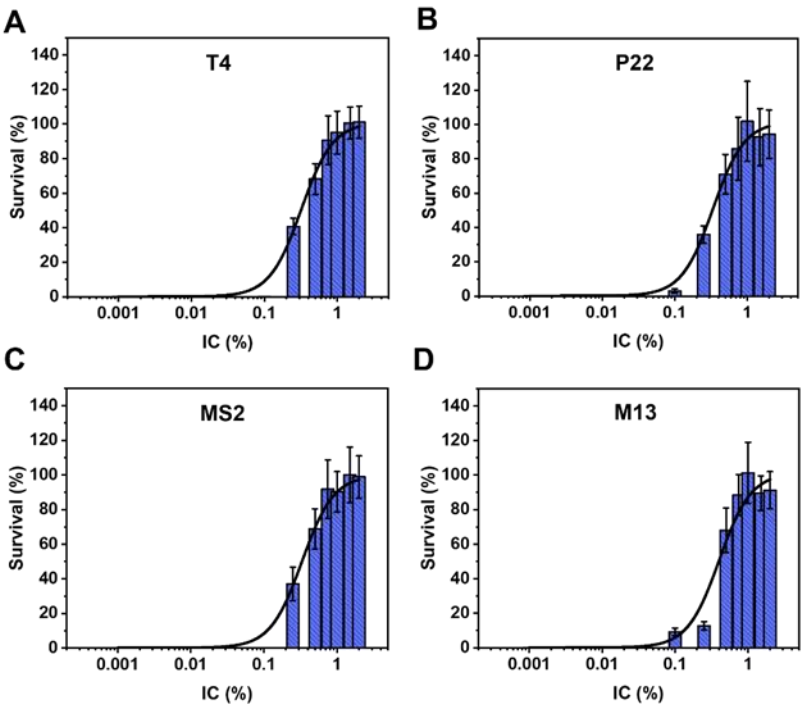

Figure 20. The estimation of EC_{50} values provided by indigocarmine (IC) for A) T4, B) P22, C) MS2, D) M13.

The protection from the adverse effects of UV irradiation appeared universal for all investigated bacteriophages. Moreover, the EC_{50} values of each examined food dye were significantly lower than in the case of Congo red and were as follows: 0.11% for TR, 0.14% for QY, 0.15% for SY, 0.18% for PC, 0.20% for AR, 0.30% for AZ, 0.32% for BB and 0.33% for IC. For CR, these values varied from 0.7% to 1.1% depending on the bacteriophage type. Therefore, all examined food dyes could protect various bacteriophages from UV irradiation just like CR did, but in lower dye concentrations (e.g., about 10x lower in the case of TR).

In the following experiment, the selectivity of the UV protection was verified using representative bacterial strains - *E. coli* BL21, *A. baumannii* ATCC BAA-1605 (Gram-negative bacteria), *B. subtilis* DSM 5547, and *S. aureus* ATCC 44300 (Gram-positive bacteria). The selectivity towards Gram-negative bacteria, but not to Gram-positive bacteria, was expected. Surprisingly, out of all the investigated food dyes, brilliant blue FCF (BB) was the only one that did not exhibit protective properties for Gram-negative bacterial species used in the experiment. The remaining food dyes provided protection against UV irradiation to bacteriophages and bacteria (Gram-positive and Gram-negative) alike (**Figure 21**). Due to this distinctive behavior, BB dye was chosen as the further anti-UV factor.

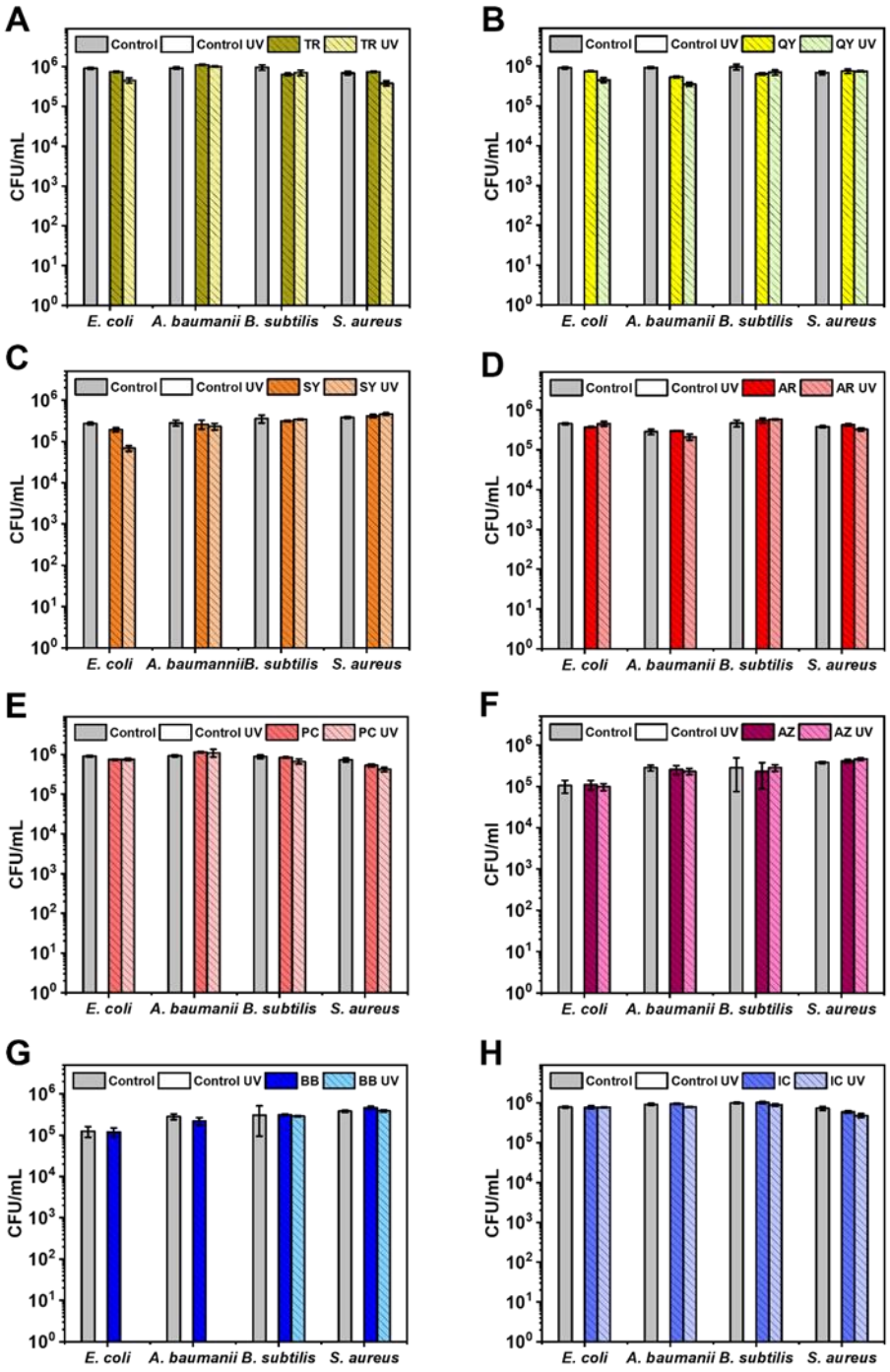

Figure 21. The evaluation of the selective UV-protective properties of the food dyes on bacteria. *E. coli, A. baumannii, B. subtilis*, and *S. aureus* were exposed to the UV irradiation in the presence of A) tartrazine, B) quinoline yellow, C) sunset yellow FCF, D) Allura red, E) Ponceau 4R, F) azorubine, G) brilliant blue FCF, H) indigocarmine.

5.3.3. Explanation of the protection mechanism

CR deactivated enveloped phage Φ6. Literature reports show similar behavior against other enveloped viruses, e.g., HIV and NDV were destabilized in the presence of CR [210]. CR did not negatively affect other tested (non-enveloped) phages (T1, T4,

T7, LR1_PA01, M13, MS2). Similarly, literature reports showed that the dye is harmless to non-enveloped viruses inside a protein matrix (e.g., LdMNPV, HzMNPV) [205,207]. However, these observations weren't summarized nor analyzed previously.

The experiments performed on bacteriophages allowed to summarize and provide some further understanding of the differences in CR action on viruses. In 2010, mild detergent-like interactions of CR with β-amyloid were described [220]. Knowing that the lipid envelope is crucial for the infectivity of enveloped viruses [221] and that detergents generally destabilize lipid-based structures suggested that detergent-like properties of CR might explain the inactivation of enveloped viruses. To confirm that, T4 and Φ6 bacteriophages were incubated in 0.1% (w/v) and 1% (w/v) sodium dodecyl sulfate (SDS, popularly used detergent) solutions in the TM buffer. After 24-hour incubation, bacteriophages were plated on double-layer agar plates with appropriate host bacteria strain. For T4 bacteriophage, SDS at the concentration 0.1% had insignificant effect on the infectivity, while at 1% concentration the decrease in T4 phage titer was < 0.5 log. However, SDS completely inactivated Φ6 regardless of the concentration of the detergent (**Figure 22A-B**). Due to the similarities, most probably the incubation in CR also caused the destabilization of Φ6 lipid envelope (**Figure 22C**). Because of the lack of such envelope, there were no reports on the effects of the detergents (including CR) on non-enveloped viruses (e.g., bacteriophages, baculoviruses).

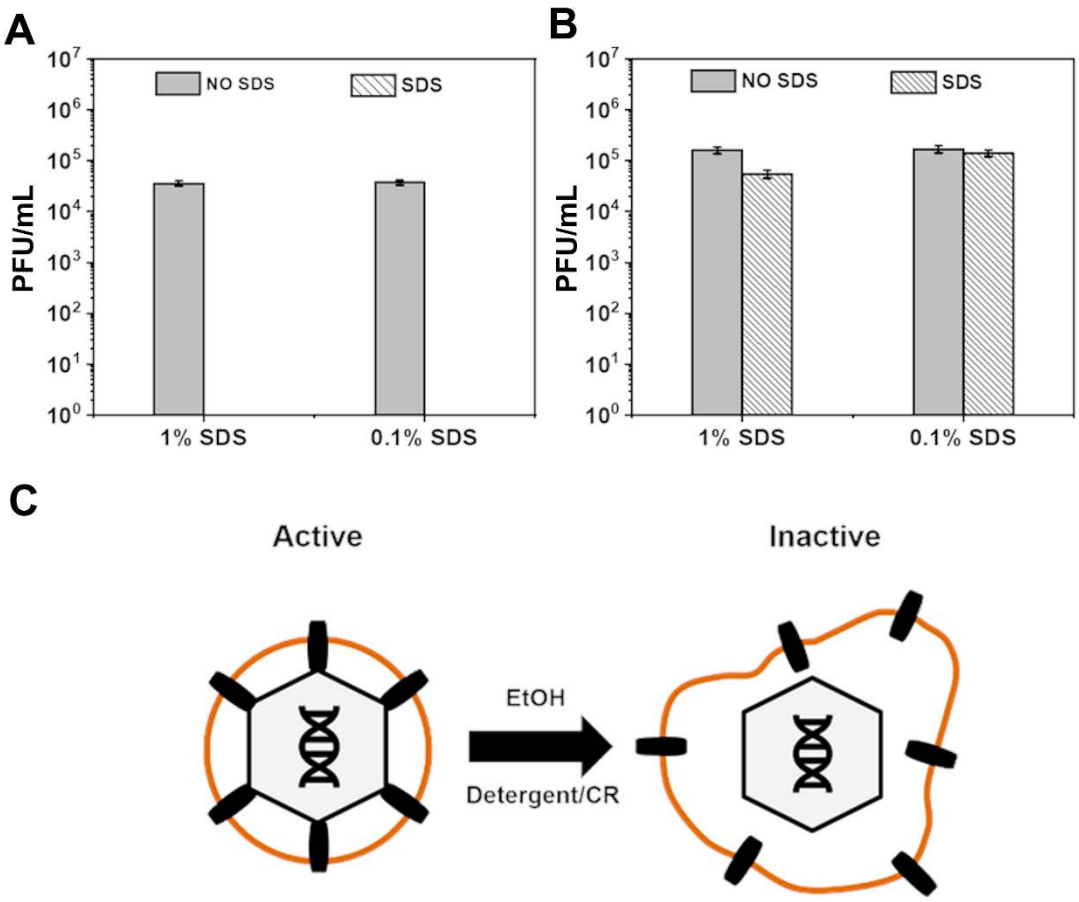

Figure 22. The comparison of the effect of incubation in sodium dodecyl sulfate solution on the representatives of A) enveloped (Φ6) and B) non-enveloped (T4) bacteriophages. C) The proposed mechanism for inactivating enveloped viruses is based on experiments conducted with the Φ6 phage, serving as a surrogate for enveloped eukaryotic viruses. The Congo red dye's detergent-like properties are suggested to induce the destabilization of the viral lipid envelope, a crucial factor for the infectivity of enveloped viruses. This observed effect is comparable to the destabilization caused by other detergents, such as SDS, or ethanol [222].

Another observation from the previous experiments was that the CR did not impact the fitness of Gram-positive and Gram-negative bacteria. Still, it led to the complete eradication of yeast cells. This aligns with the findings that demonstrated the antifungal properties of Congo red. It was shown that the dye binds to the beta-glucans in the chitin cell wall, disturbing further chitin synthesis. This interference results in improper cell separation and leads to the death of both mother and daughter cells [223]. Antifungal activity of CR was also observed for molds, such as *Aspergillus nidulans* and *Aspergillus niger* [224].

Another report also suggested that wall teichoic acids (WTAs) in their cell walls might be crucial to protect Gram-positive bacteria. It was found that CR binds to WTAs; this property is used for the differentiation of biofilm-forming strains. The results from this study suggested that WTAs, exposed in Gram-positive bacteria, might bind

CR molecules at the surface of bacterial cells, which results in improved survival during UV irradiation [225].

Based on the literature and the general application of CR (staining the proteins, particularly amyloids) the interactions of the dye with virion's capsid proteins seemed to explain the observations. Two potential mechanisms explaining CR's protection against UV were examined. The first scenario assumed no specific interactions between CR and virions - the dye in the solution provided a shielding effect by absorbing some UV radiation. Although bacteriophages and bacteria were still exposed to the radiation, the energy uptake was significantly lesser. Due to their smaller size, bacteriophages absorbed lesser, sublethal radiation doses than bacteria and yeasts. Therefore, only the stabilization of phages was observed. This mechanism was termed a "microbial shield".

The second scenario assumed the interaction between CR and the phage virions. The dye molecules bound to the surface of the virion absorbed UV radiation and dissipated the excess energy. CR present at the surface of the capsid absorbed or scattered a significant amount of radiation, so the viral genome was effectively exposed to smaller doses compared to the objects without a CR protective layer. This mechanism was named a "molecular sunscreen". Both of these mechanisms are illustrated in **Figure 23**.

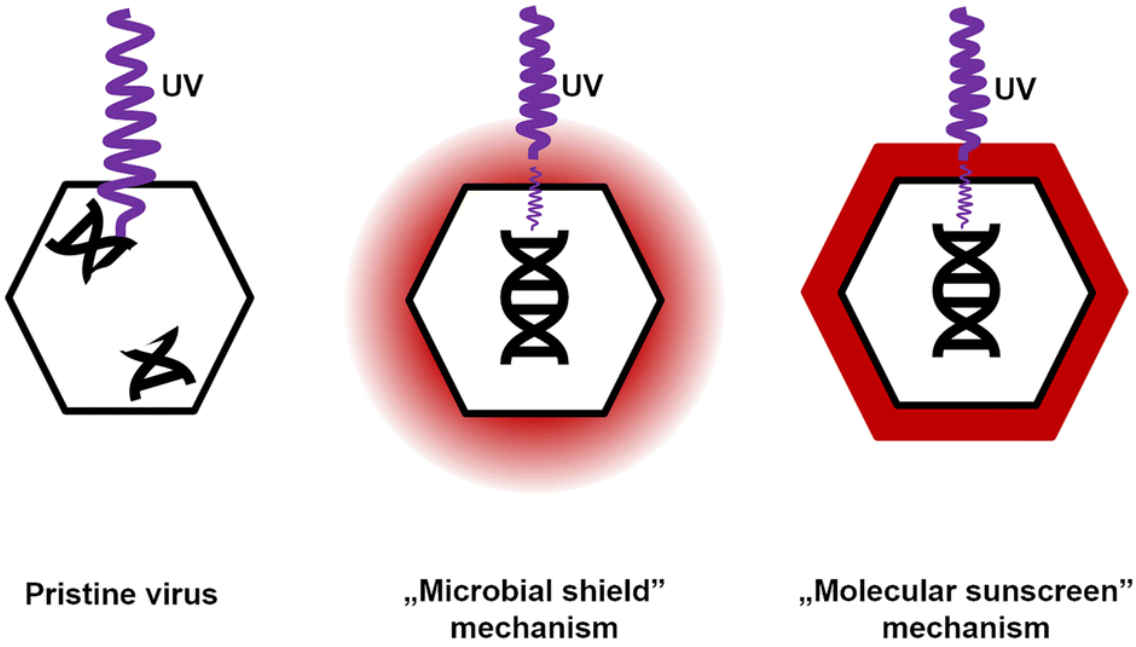

Figure 23. The schematic illustration of the possible mechanisms of UV-protective properties of Congo red for non-enveloped viruses. Based on the experimental results obtained for T1, T4, T7, MS2, M13, and LR1_PA01 phages, the "molecular sunscreen" mechanism, in which the protectant needs to bind to virions, appeared appropriate.

The possibility of CR binding to bacteriophage capsid was first investigated to verify the hypothesis regarding the protection mechanism. All the examined non-enveloped bacteriophages were incubated in CR solution overnight, and then the UV-Vis spectral analysis was performed. The CR solution in TM buffer and PBS buffer solutions were used as a control sample. Additionally, solutions of CR in TM buffer and PBS buffer with the addition of human serum albumin (HSA) were prepared to observe the spectral changes caused by the interactions of CR with globular protein [226,227]. The results of these analyses are presented in **Figure 24**.

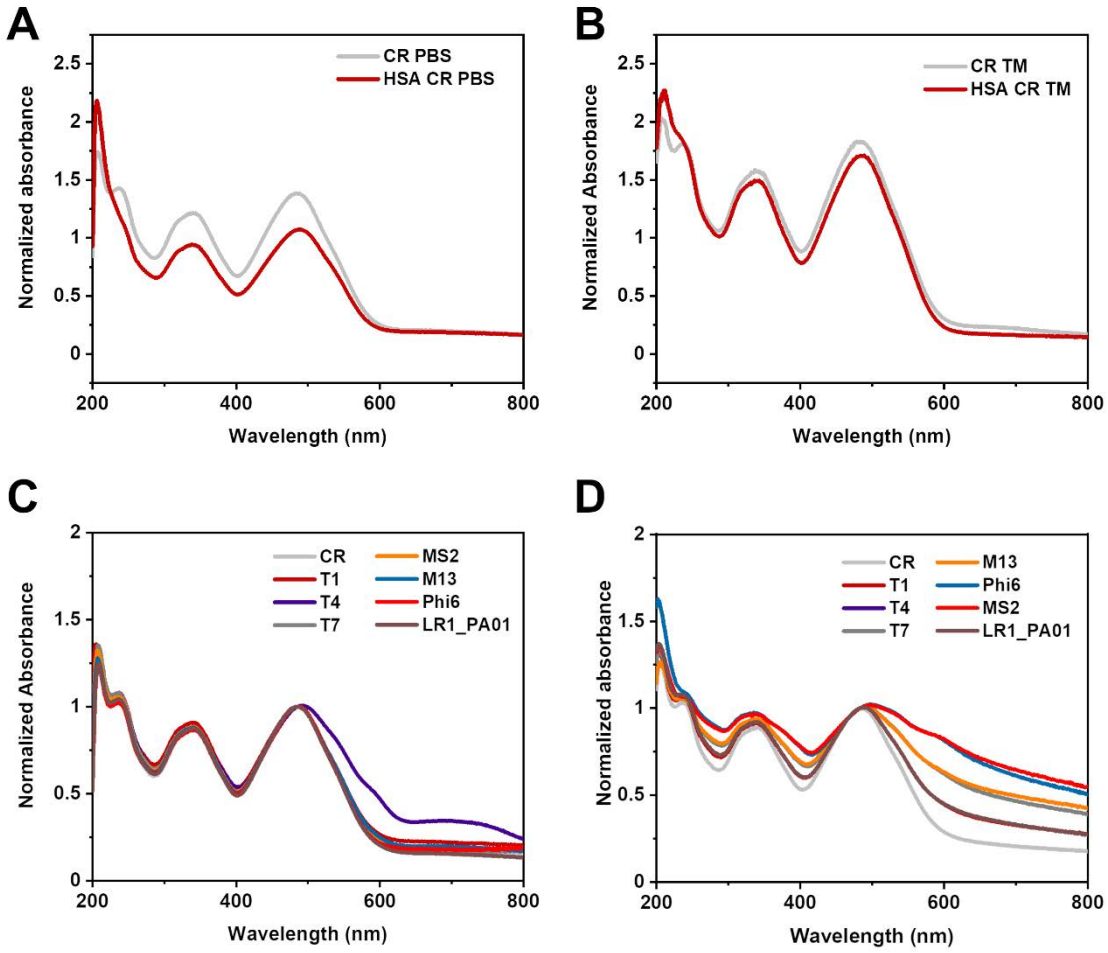

Figure 24. The UV-Vis spectra of Congo red with human serum albumin (HSA) in A) PBS and B) TM buffer. C) UV-vis spectra of 1% CR solution in TM buffer with T1, T4, T7, M13, Φ6, MS2, and LR1_PA01 bacteriophages after 1-minute incubation (normalized for 483 nm), D) UV-Vis spectra of 1% CR solution in TM buffer, with T1, T4, T7, M13, Φ6, MS2 and LR1_PA01 bacteriophages (normalized with respect to 586 nm). A slight shift in the maximum absorption (~490 nm → ~500 nm) was observed in both C) and D). All the measurements were performed after a brief incubation (about 5 minutes).

The spectral analysis revealed a shift in the spectra from about 490 nm to 500 nm in both buffer solutions when HSA was present. This shift was attributed to the formation of a complex between HSA protein and CR. Similar shifts have been

observed in the literature for bovine serum albumin (BSA). The complexation phenomenon was confirmed using various spectroscopic techniques, including UV-Vis spectroscopy, fluorescence spectroscopy, and circular dichroism spectroscopy [227]. Additionally, it is known that in aqueous solutions, serum albumins complexed with CR are favored from a thermodynamic standpoint [226].

Similar changes in CR UV-Vis spectra were observed for bacteriophage suspensions. When phages were present alone in buffers (TM and PBS), they absorbed light only in the range of 230 nm to 280 nm [228]. This was expected, because phage capsids primarily comprised proteins, which generally absorb wavelengths around 230 nm and 260 nm [229]. Upon mixing phages with CR and incubating for 1 minute, a minor shift in the maximum CR absorption was observed from around 490 nm to 500 nm. Such shifts were previously observed by the CR binding to amyloids [230,231]. Protein complexes formed with CR were believed to be exceptionally stable, and thermodynamic models suggested that CR interacts with proteins on various sides in the surrounding basic amino acids, such as lysine and histidine [226].

A spectrophotometric titration of 1% CR solution (in TM buffer) with T4 bacteriophages was performed to confirm CR interaction with bacteriophages. The initial concentration of T4 bacteriophages in the suspension used for titration was 10^7 PFU/mL; phages were added to CR solution in 2 µL portions, increasing the concentration of T4 phages in the solution by 2×10^4 PFU/mL per each portion. Phages were added to reach the final concentration of about 3×10^{10} PFU/mL, and after adding each portion, the UV-Vis spectral analysis of the mixture was performed. For comparison, the absorbance at the wavelength 600 nm was selected since, at this particular value, the absorbance of the bacteriophage was negligible (extinction coefficient $\varepsilon_{T4} \approx 0$). The results illustrated the correlation between phage concentration and absorbance at 600 nm (**Figure 25**).

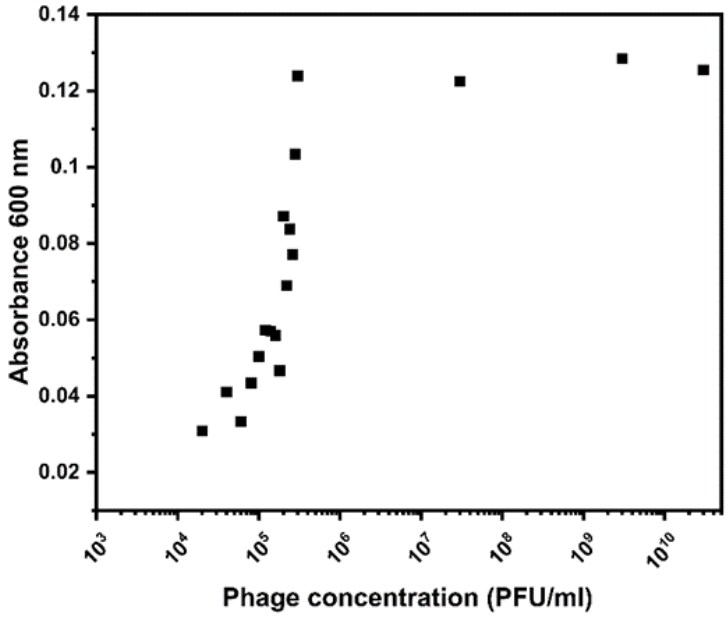

Figure 25. The relation between T4 phage concentration and the absorbance of 1% CR solution. An increase in absorbance value was observed until reaching the phage concentration of about 3 × 10^5 PFU/mL. Above this titer, i.e., at 3 × 10^7, 3 × $10^{9,}$ and 3 × 10^{10} PFU/mL, the absorbance value was similar.

Based on this relation, the binding constant (β) of CR interacting with T4 phages was estimated. For the estimation of the binding constant, Scatchard method [232] with Healy's modification was used [233]. Binding constant β is defined as:

$$\beta = \frac{[S\ CR]}{[CR][S]}$$

where [CR] is the concentration of the free Congo red in equilibrium, [S] is the concentration of unoccupied binding sites (number of all unoccupied sites at all of the bacteriophages per volume), and [SL] is the concentration of occupied binding sites (N_{oc}) (analogically).

$$N = N_{oc} + N_{unoc}$$

where N – an average number of possible binding sites on a bacteriophage, N_{oc} – an average number of occupied binding sites on a bacteriophage, N_{unoc} – an average number of unoccupied binding sites on a bacteriophage.

$$\frac{N_{oc}}{N} = \frac{[S\ CR]}{[S\ CR] + [S]}$$

$$N_{oc} = N\frac{\beta[CR]}{\beta[CR] + 1}$$

The fraction of the ligand bound to the bacteriophage during the titration can be expressed as:

$$f = \frac{A_{obs} - A_{CR}}{A_{max} - A_{CR}}$$

where f stands for the fraction, A_{obs} is the absorbance measured at 600 nm, A_{CR} is the absorbance coming from the free Congo red, and A_{max} represents the maximal absorbance.

To improve the quality of the calculation, the experimental values of measured absorbance were fitted by the exponential function with $R^2 \approx 0.88$. The absorbance of free Congo red was almost equal to the total CR concentration at the beginning and almost 0 at the end of the titration. To minimize the error coming from using one of the estimations (A_{CR0} stands for the absorbance of CR before adding the first portion of bacteriophages):

$$f \approx \frac{A_{obs}}{A_{max}} \text{ or } f \approx \frac{A_{obs} - A_{CR0}}{A_{max} - A_{CR0}}$$

In the function $A_{CR} = A_{CR0} \cdot \left(1 - \frac{[T4]_T}{[T4]_{Tmax}}\right)$, $[T4]_T$ is the total concentration (all forms of T4 and T4-CR_n) of bacteriophage and $[T4]_{Tmax}$ is the total concentration of the added bacteriophage when $A_{obs} \approx A_{max}$.

$$N_{oc} = \frac{f[CR]_T}{[T4]_T}$$

$$\frac{f[CR]_T}{[T4]_T} = N\frac{\beta[CR]}{\beta[CR] + 1}$$

$$[CR] = [CR]_T(1 - f)$$

Hence:

$$\frac{[\boldsymbol{T4}]_T}{\boldsymbol{f}} = \frac{\mathbf{1}}{\boldsymbol{N\beta}(\mathbf{1} - \boldsymbol{f})} + \frac{[\boldsymbol{CR}]_T}{\boldsymbol{N}}$$

where N stands for the average number of possible binding sites on a bacteriophage, f stands for the fraction, and β stands for binding constant.

From the linear regression ($R^2 \approx 0.99$), the binding constant for CR - T4 phage interactions was 1.28×10^4 dm^3/mol, which was lower than the binding constant of CR - bovine serum albumin (BSA) interaction estimated to be 1.947×10^5 dm^3/mol [227]. Compared to CR and the model protein (BSA), the observed lower binding constant between CR and virions could be attributed to viral protein's diverse amino acid

composition or geometric restrictions. In the free BSA experiments, complex formation is not impeded by adjacent macromolecules.

The obtained N value, $2.4 \times 10^{11} \pm 1.59 \times 10^{10}$, was surprisingly high yet in line with the basis of the "molecular sunscreen" mechanism. The mechanism requires a large number of dye molecules to bind to virions' proteins, and CR can bind to multiple sides of the protein (preferably in β-sheet-rich regions). Therefore, the large N-value was consistent based on the proposed nature of phage-CR interactions.

An additional experiment was performed to confirm this mechanism's general applicability. 1 mL of T4 bacteriophage suspensions, initially incubated overnight at 4°C in TM buffer solution, were placed in quartz cuvettes to ensure transparency of the glassware to UV and eliminate the risk of free radical generation from plastic. Another set of quartz cuvettes was positioned on top of the cuvettes. In one sample, the cuvette was left empty. In another, it was filled with 300 µL of TM buffer solution. The third was filled with 300 µL of a 0.5% (w/v) brilliant blue FCF solution. The last set consisted of T4 bacteriophage suspension in 0.5% BB solution (bottom cuvette), with an empty cuvette on top. The quartz cuvettes were securely joined using parafilm and covered with aluminum foil to ensure UV light reached the phage suspension only from above. The UV exposure was performed according to the standard irradiation protocol described previously. Only in the fourth case, i.e., when phages were mixed with protectant, viral activity was retained after the illumination (**Figure 26**).

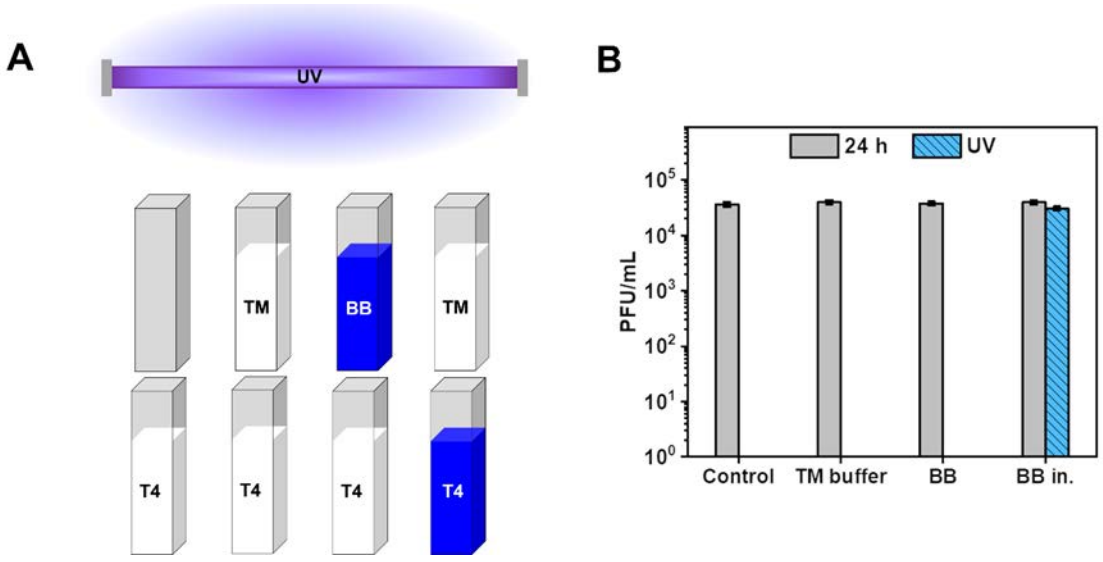

Figure 26. The verification of the possible shielding effect of BB solution. A) The schematic illustration of the experiment. Quartz cuvettes containing T4 phages in TM buffer solution (or 0.5% BB in TM buffer solution) were placed underneath other quartz cuvettes and exposed to UV irradiation. B) T4 phage stability during exposure to UV irradiation. In this experiment,

T4 phages were incubated in the TM buffer solution, and the BB solution was placed right above the phage suspension.

Based on the experimental results, the following evidence supported the hypothesis of “molecular sunscreen” mechanism protection from the UV:

1. Out of the tested dyes, only CR and food dyes protected bacteriophages despite nearly all the examined dyes absorbing radiation from the UV-C spectrum (254 nm). This suggested that only these dyes were likely to interact with certain structures of bacteriophages or at least could form localized gradients of concentration.
2. After incubating with bacteriophages, the UV-Vis spectra of CR exhibited direct shifts at 225 → 230 nm and 490 → 500 nm. Based on literature and experimental findings, these shifts were observed and interpreted as indicative of the binding of CR molecules to viral particles. The same spectral shifts were observed in CR solutions containing 10 μg/mL human serum albumin. Similar shifts in UV-Vis spectra have also been reported for CR binding to β-amyloid fibers [234]. For globular proteins, such as bovine serum albumin (similar to HSA), an additional shift was observed in the UV spectrum towards 225–230 nm [226].
3. CR effectively deactivated Φ6, even without UV radiation, providing clear evidence of its interaction with virions.

   These observations (1 to 3) align with the findings of Shapiro and colleagues [208], who documented CR's protective effect against UV irradiation for *Lymantria dispar* (L.) nuclear polyhedrosis virus (LdMNPV), a baculovirus infecting insects. Their study noted a similar protective effect for another baculovirus, *Heliothis zea* (Boddie), a singly embedded nuclear polyhedrosis virus (HzSNPV). Unlike conventional virions, NPVs (nuclear polyhedrosis viruses) are distinct as they are embedded within the protein polyhedrin matrix [205]. It is plausible that Congo red binds to the surface of baculoviral occlusive bodies, leading to the local accumulation of CR molecules. Eukaryotic viruses lacking such structures were either unaffected or even deactivated by CR [210,211]. Therefore, not only was CR the efficient UV-protectant for bacteriophages, but it was also possible to explain the mechanism behind these properties and the differences in CR effects on enveloped and non-enveloped viruses.
4. CR demonstrated protective effects against UV for Gram-positive bacteria but not for Gram-negative bacteria. This distinction arose from the accumulation of CR

at the surface of Gram-positive bacteria, facilitated by its interaction with cell wall components [225].

5. The spectrophotometric titration of a CR with a T4 bacteriophage suspension demonstrated a correlation between the rise in absorbance at a wavelength of 600 nm and the increasing concentration of bacteriophages. The estimated value of the binding constant between CR and T4 phages is approximately 1.28×10^4 dm^3/mol.
6. The experiment demonstrated that the shielding provided by the brilliant blue (BB) solution didn't significantly affect bacteriophage stability during UV irradiation exposure. Additionally, it was confirmed that the TM buffer, used consistently in the experiments, has a neutral impact on the UV stability protocol. These findings offered another crucial insight, proving that interactions between phage capsid proteins and potentially protective dyes are essential for stabilization during UV exposure (**Figure 26**). This further supports the concept of a "molecular sunscreen" mechanism underlying this protection.

The analysis of the molecular structures of the examined food dyes revealed that the majority of them (TR, SY, AR, PC, AZ) were azo dyes. Considering their protection provided to bacteriophages and Gram-positive bacteria, observed UV-protective properties were probably based on the "molecular sunscreen" mechanism (described in the previous chapter), similar to CR [174]. However, the remaining dyes (QY, IC), including the Gram-negative bacteria-specific brilliant blue FCF (BB), provided similar protection despite being either derivatives of indole (QY, IC) or a triarylmethane dye (BB). In principle, the presence of aromatic rings could explain the UV protection by absorption of large amounts of photons from the UV spectrum [235]. To confirm such a hypothesis, a comparative analysis of this dye with crystal violet (CV), a triarylmethane dye commonly used for staining bacterial cell walls, was performed (**Figure 27**). Crystal violet (CV) was selected for comparison with brilliant blue FCF (BB) due to their structural similarities and similar absorption spectra. In the phage survival protocol using CV, T4 bacteriophage was chosen as the model organism. For the bacteria survival assessment, *E. coli* BL21 and *S. aureus* ATCC 43300 strains were employed. The experiment followed a previously described protocol of UV irradiation.

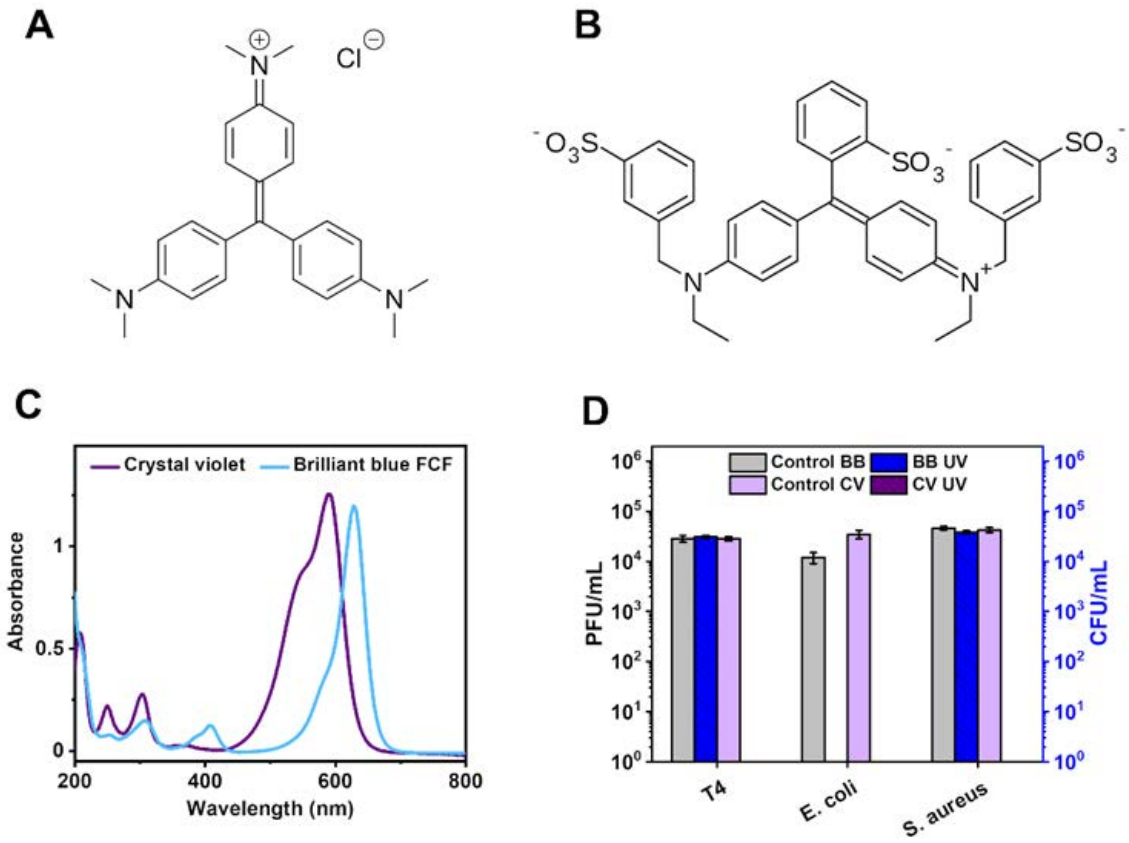

Figure 27. The comparison of two triarylmethane dyes - brilliant blue FCF (BB) and crystal violet (CV). A) The molecular structure of crystal violet, B) The molecular structure of brilliant blue FCF, C) UV-Vis spectra of BB and CV, D) The evaluation of phage/bacteria-protective properties of CV compared to BB.

Besides the additional aromatic rings shared by both dyes, the primary distinction in the molecular structure between brilliant blue FCF (BB) and crystal violet (CV) lies in the presence of three sulfonic groups ($-SO_3^-$) in the structure of BB (**Figure 27A-B**). This was in line with the current state of knowledge; hence, it is known that sulphonic groups bind to protein's protonated amino acid side chains ($-NH_3^+$ in lysine, arginine, and histidine). These interactions are the basis of the protein staining in SDS-PAGE gels using the derivative of brilliant blue FCF – Coomassie brilliant blue R250 and Coomassie brilliant blue G250 [236]. Since the basic amino acids constitute about 10% of the major capsid proteins of T4 phage (gp23 [237] and Hoc [238]), BB had multiple binding sides to the phage capsid.

The UV-Vis spectral analysis demonstrated that both dyes exhibit comparable absorbance in the UV spectrum, particularly at wavelengths around 210 nm and 300 nm. Crystal violet (CV) also displayed an absorption peak at approximately 260 nm. Notably, both dyes show maximum absorbance in the orange light spectrum, with CV peaking at 590 nm and BB at 620 nm (**Figure 27C**).

Despite the similarities in molecular structure and UV-Vis spectra profile, the dyes presented completely different properties in the case of UV protection. Similarly to previous experiments, BB demonstrated protective properties for T4 bacteriophages and the Gram-positive bacterium *S. aureus* while maintaining a neutral effect on Gram-negative bacteria such as *E. coli*. At the same time, CV didn't provide any protection (**Figure 27D**). The comparison of BB and CV provided information on the importance of protein binding for protection from UV irradiation. All the tested UV-protecting dyes have at least one sulphonic group in their molecular structure. For confirmation, quinine was selected (**Figure 10**). Quinine is an excellent UV-absorbent, but does not possess a sulfonic group in its structure. This explained why the addition of quinine did not improve the stability of phages upon irradiation.

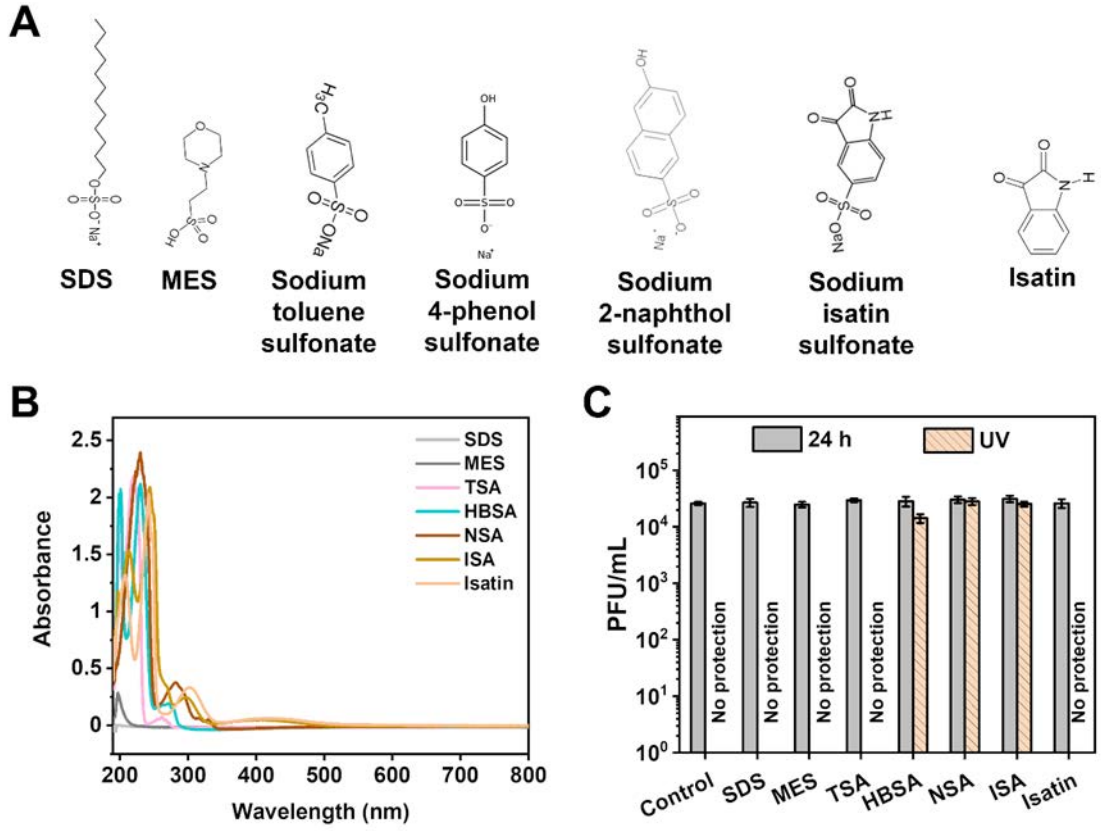

Figure 28. The verification of the importance of the sulfonic group for phage protection from UV irradiation. A) The molecular structures of sodium dodecyl sulfate (SDS), 2-(N-morpholino)ethanesulfonic acid (MES), sodium toluene sulfonate (TSA), sodium 4-hydroxybenzene sulfonate (4-phenol sulfonic acid; HBSA), sodium 2-naphtol-6-sulfonate (NSA), sodium isatin-5-sulfonate(ISA), and isatin, B) The UV-Vis spectra of SDS, MES, toluene sulfonate, 4-hydroxybenzene sulfonate, 2-naphtol-6-sulfonate, isatin-5-sulfonate, and isatin, C) The evaluation of phage protective properties of SDS, MES, toluene sulfonate, 4-hydroxybenzene sulfonate, 2-naphtol-6-sulfonate, isatin-5-sulfonate, and isatin.

The protective properties of sulfonic compounds with different molecular structures were compared to confirm whether the sulfonic group plays a crucial role

in anchoring phages against UV radiation. These compounds included sodium dodecyl sulfate (SDS; Sigma-Aldrich, Saint Louis, Missouri, USA), 2-(N-morpholino)ethanesulfonic acid (MES, Sigma-Aldrich, Saint Louis, Missouri, USA), toluene sulfonic acid (POCH, Gliwice, Poland), 4-hydroxybenzenesulfonic acid (TCI Europe N.V., Zwijndrecht, Belgium), sodium 2-naphthol-6-sulfonate (TCI Europe N.V., Zwijndrecht, Belgium), and sodium isatin-5-sulfonate (Sigma-Aldrich, Saint Louis, Missouri, USA). Isatin (Sigma-Aldrich, Saint Louis, Missouri, USA) was used as a negative control for sodium isatin-5-sulfonate. Before the experiment, acidic compounds such as toluene sulfonic acid and 4-hydroxybenzenesulfonic acid were neutralized using a 0.1M NaOH solution. The analysis included comparing molecular structures, UV-Vis spectra, and protective properties towards T4 bacteriophages (**Figure 28**).

The molecular structures of the examined compounds revealed that SDS and MES were representative of sulfonic compounds with aliphatic chains. Toluene sulfon*a*te, 4-hydroxybenzene sulfonate, 2-naphtol-6-sulfonate, and isatin-5-sulfonate were aromatic sulfonic compounds. Isatin was a derivative of isatin-5-sulfonate, lacking the sulfonic group (SO_3^-) (**Figure 28A**). The analysis of UV-Vis spectra showed that SDS and MES exhibited minimal absorbance across both UV and visible radiation ranges. On the other hand, toluene sulfonate, 4-phenol sulfonate, 2-naphthol-6-sulfonate, isatin-5-sulfonate, and isatin demonstrated significant absorbance in the UV region, particularly at wavelengths of 220 nm and 250 nm. Additionally, 4-phenol sulfonate, 2-naphthol-6-sulfonate, isatin-5-sulfonate, and isatin displayed an absorbance peak at 300 nm. Notably, isatin-5-sulfonate exhibited slightly higher absorbance at 220 nm compared to isatin. 2-naphthol-6-sulfonate did not show absorbance at 220 nm, but its absorbance at 250 nm was relatively higher than that of other compounds. (**Figure 28B**). Despite these variations, all examined aromatic compounds were effective absorbers of UV irradiation.

The results suggested that the effective protection of phages against UV requires three key elements within a compound's molecular structure:

- The presence of a sulfonic group (SO_3^-) anchors the protectant to proteins *via* the $-NH_3^+$ group in the side chain of amino acids.
- An aromatic domain capable of absorbing photons and dissipating the energy.
- An additional hydrophilic group, such as -OH, that facilitates the formation of hydrogen bonds.

Compounds possessing all three features, namely HBSA, NSA, and ISA, effectively countered the adverse effects of UV irradiation. A compelling comparison between ISA and isatin highlighted this point. The sole difference between these molecules is the presence of a sulfonic group in ISA, rendering it effective in our experiments **Figure 28C**). Similarly, indigocarmine, comprising two ISA domains, successfully protected phages against UV.

However, despite containing sulfonic groups, SDS, MES, and TSA failed to protect T4 phages. This demonstrated that merely having a sulfonic group is insufficient for effective protection; other requirements must also be met. SDS and MES did not absorb UV radiation, thus failing to interact with it and influence the results. TSA exhibited maximum absorbance at 230 nm (typical for aromatic rings) and relatively weak absorbance at 254 nm, commonly used for sterilization. However, there was no direct correlation between the extinction coefficient and the degree of protection as long as absorption was non-zero. Furthermore, despite having a similar absorption profile to ISA, isatin did not provide any phage protection, unlike ISA.

This discrepancy suggests that another factor renders TSA ineffective in phage protection. We observed that even a minor structural change - replacing the -CH_3 group (TSA) with the -OH group (HBSA) - yielded markedly different results. It suggested that the potential for hydrogen bond formation represents a third crucial requirement for a compound to protect phages. This effect may be subtle, as illustrated by a comparative analysis of Congo red (an efficient protectant) and methyl orange (no protection) (**Figure 10A**). Congo red contains primary amine groups, whereas methyl orange has a tertiary amine group. Additionally, for biological applications, water solubility serves as an additional criterion. For instance, sulfanilic acid (4-aminobenzenesulfonic acid) was insoluble in the TM buffer.

This investigation identified the simplest molecule capable of protecting bacteriophages from UV irradiation, akin to Congo red and food dyes: 4-hydroxybenzene sulfonate (4-phenol sulfonate).

5.3.4. The application of dye-mediated UV protection in membrane sterilization

The membrane sterilization protocol employed a combination of bacteriophages (LR1_PA01 or T4), UV radiation, and Congo red. Nylon66 syringe filters were a model for simulating the sterilization of bioreactor membranes prone to bacterial biofouling. The contamination of the membranes was mimicked using *P. aeruginosa* PAO1 and

E. coli BL21 (DE3) GFP bacteria. In this experimental design, only Gram-negative bacteria and their phages were examined because Gram-negative bacteria are most frequently responsible for the contaminations in membrane bioreactor (MBR) systems [239,240], and such protocol would most probably be ineffective in the case of Gram-positive bacteria due to their protection by CR. The results are presented in **Figure 29**.

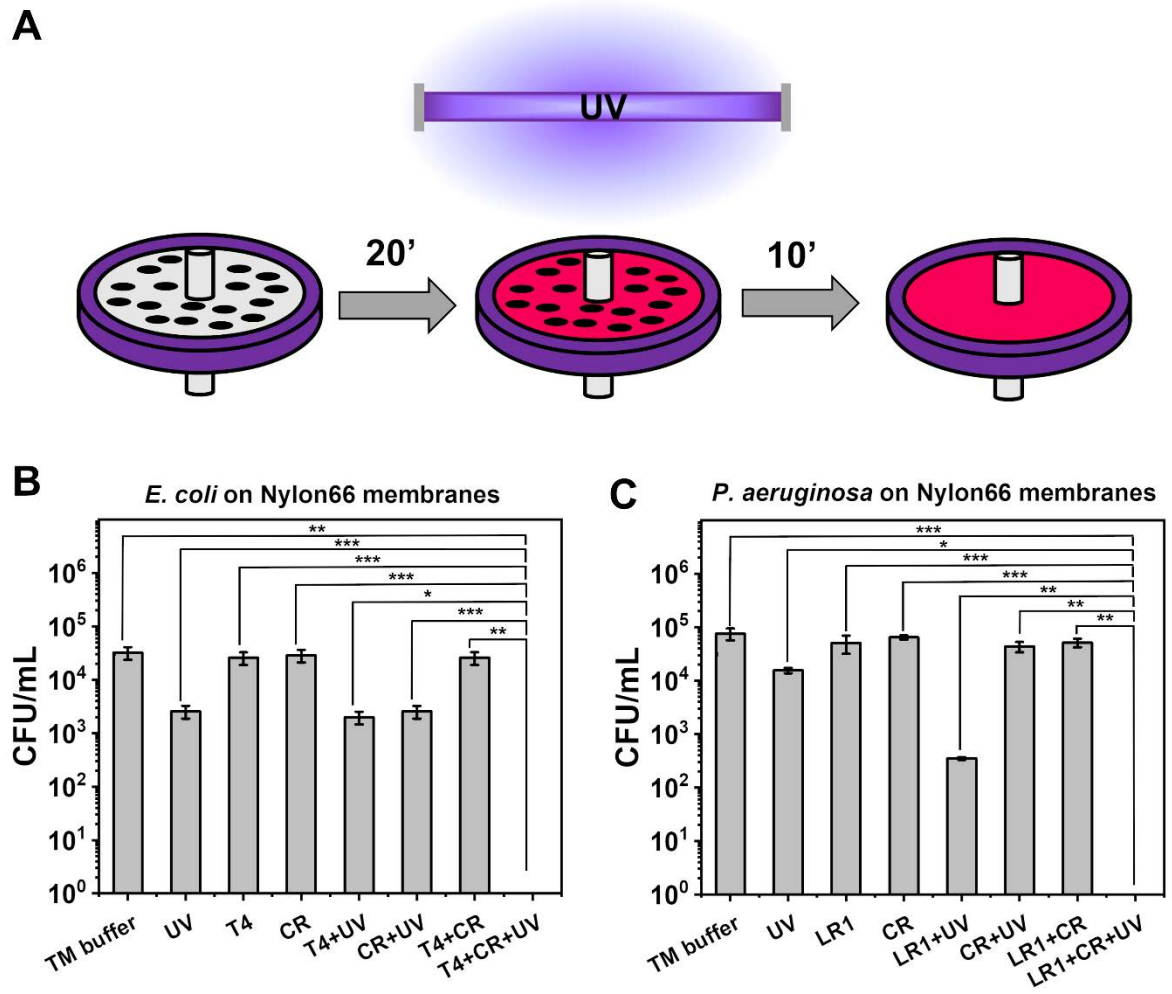

Figure 29. The comparison of the efficacy of bacteriophages, UV radiation, Congo red dye, and their combinations for sterilizing Nylon66 syringe filters from bacterial infections. A) The schematic representation of the experiment. The efficacy of sterilization was performed using B) T4 bacteriophage against *E. coli* BL21, and C) LR1_PA01 bacteriophage against *P. aeruginosa* PAO1, * $p < 0.05$; ** $p < 0.01$; *** $p < 0.001$).

At first, the efficacy of bacteriophages and UV alone against biofouling was confirmed. Both factors resulted in a statistically significant decrease in bacteria, ranging from approximately 0.5 to 1 log reduction. Notably, sterilization with only bacteriophages reduced bacterial counts from 7×10^4 to 5×10^4 CFU/mL and from 3×10^4 to 2×10^4 CFU/mL for T4, demonstrating that the bacteriophage treatment was

less effective than UV sterilization (from 7×10^4 to 2×10^4 CFU/mL; from 3×10^4 to 3×10^3 CFU/mL). For the simultaneous use of phages and UV irradiation, in the T4 phage system, the efficacy was slightly better than for the UV only (from 3×10^4 to 1.5×10^3 CFU/mL); in the LR1_PA01 model, this difference was more significant (from 7×10^4 to 4×10^2 CFU/mL). The most probable explanation is that pristine phages were inactivated during the exposure to the UV. Adding CR to the mixture didn't affect the efficacy of UV- and phage-mediated sterilization; the dye was harmless to bacteria. However, the combination of all three components, namely UV, bacteriophages, and Congo red (CR) ("cleaning mixture"), led to the complete eradication of both *E. coli* and *P. aeruginosa* bacteria (a decrease of bacterial titer from 3×10^4 CFU/mL to below the methods detection limits – 10 CFU/mL). The total cleaning time of approximately 30 minutes added significant value to the UV- and phage-based sterilization protocol.

Following the promising results in the membrane sterilization experiment, the possibility of reusing the "cleaning mixture" was verified. The experimental design was similar to the previous one, but after the final flushing, the suspension containing T4 phages and CR was collected and used for consecutive sterilization. After a brief centrifuging to remove bacterial debris, the sterilization protocol was repeated with the used "cleaning mixture" on newly prepared Nylon66 filters contaminated with bacteria. In total, three cycles of sterilization were performed (**Figure 30**).

The protocol appeared efficient for two consecutive sterilization runs, but the efficacy in bacteria elimination dramatically decreased by the third run. While in the first two cycles, the reduction in bacterial titer was from 2×10^4 CFU/mL to below the limits of detection (~10 CFU/mL), by the third run, the decrease was only from 2×10^4 CFU/mL to 2×10^3 CFU/mL, comparable to the sterilization with UV radiation and bacteriophages simultaneously.

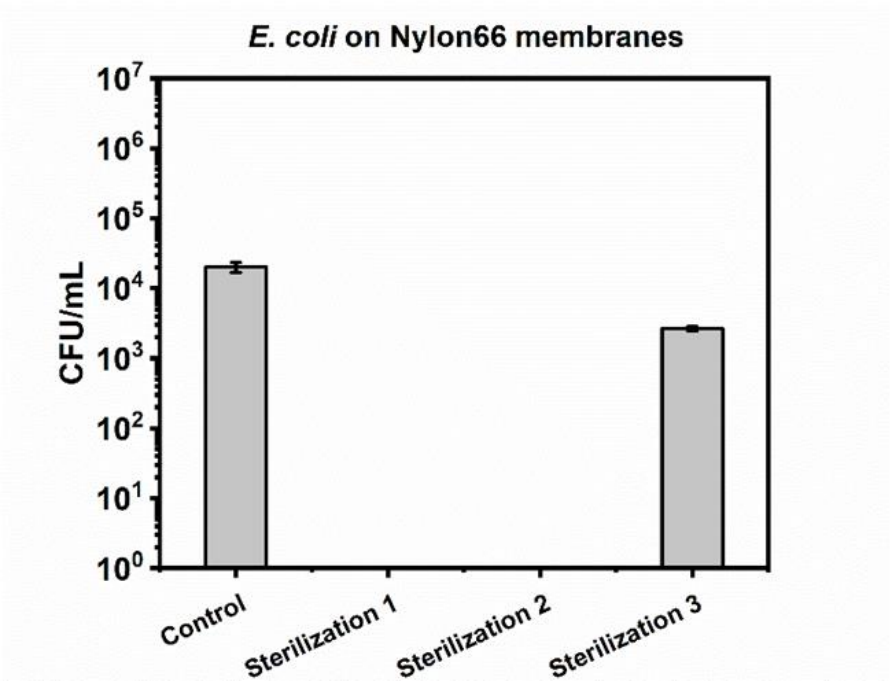

Figure 30. Multiple membrane filter sterilization from *E. coli* BL21 biofouling with the same suspension of T4 bacteriophages with CR in TM buffer and simultaneous UV exposure.

The sterilization protocol using bacteriophages, UV irradiation, and CR was efficient for eliminating bacterial contamination and beneficial for the integrity of the membrane, and the “cleaning mixture” was relatively easy to remove from the experimental system.

To verify the possible penetration of CR through the membranes, affecting their permeate quality, polytetrafluoroethylene (PTFE) syringe filters were filled with CR solution and then rinsed multiple times with water. PTFE has properties similar to polyvinylidene difluoride (PVDF), a frequently used membrane material in MBRs. Following each rinsing step, the solution was transferred to a glass vial, and UV-Vis spectral analyses were conducted to estimate the amount of remaining CR in water (**Figure 31**). Using optical microscopy, the surfaces of PTFE membranes after the incubation with CR were visualized.

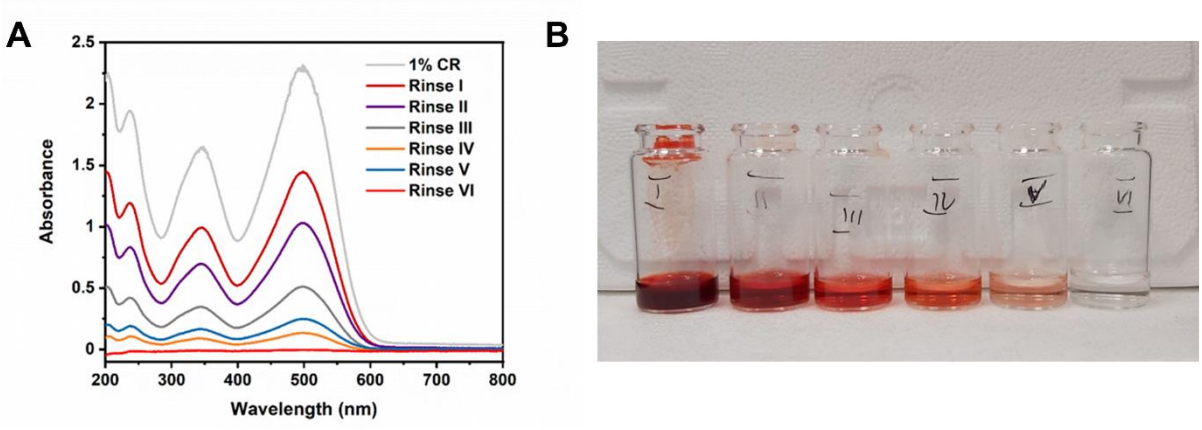

Figure 31. The differences in Congo red content after exposing the PTFE membrane to 1% Congo red solution (1% CR) and after six rinsings. A) The UV-Vis estimation of the amount of CR, with each rinsing, the absorbance value decreased until the background intensity by Rinse VI, B) Organoleptic estimation of the presence of CR in the solution. By Rinse VI, the solution is colorless and transparent, suggesting the presence of trace amounts of CR.

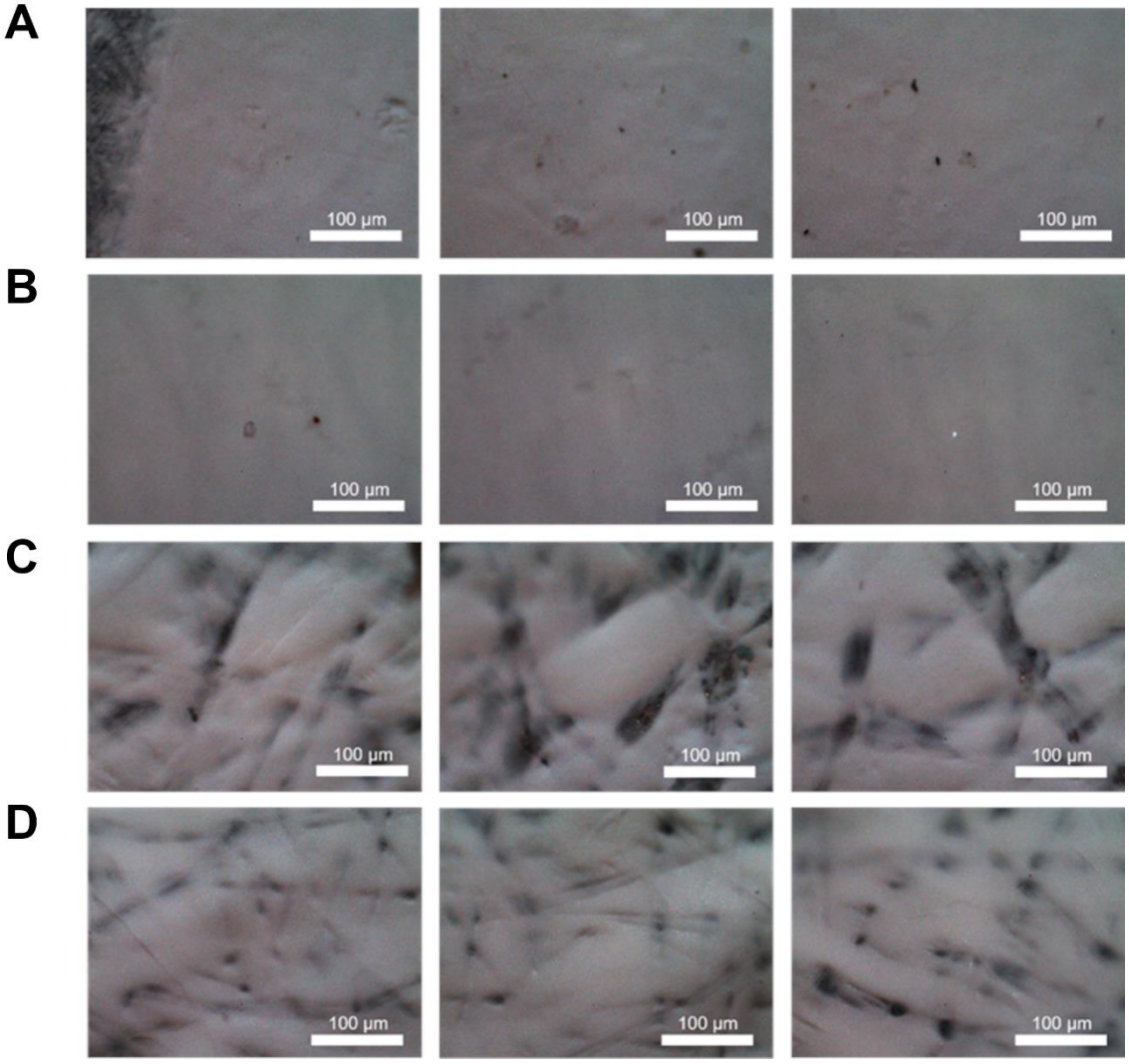

Figure 32. Nylon66 and PTFE membranes are visualized using an optical microscope (10× magnification). A) Nylon66 membrane before the UV exposure, B) Nylon66 membrane after 30 minutes of UV exposition, C) PTFE membrane before the UV exposure, and D) PTFE membrane after 30 minutes of UV exposition.

The optical microscopy observations revealed no significant differences in the PTFE membrane surface structure (**Figure 32**). Combined with the UV-Vis spectral analysis detecting the presence of CR in the rinsed water, the method didn't seem to affect the membrane's integrity.

5.4. Summary

Combining bacteriophages, Congo red, and UV radiation proved effective in sterilizing membrane filters simulating bioreactors. The incorporation of Congo red enabled the concurrent action of UV and phages. The dye functioned as a "molecular sunscreen", safeguarding phages while not protecting Gram-negative bacteria from harmful irradiation. Additionally, its antifungal properties against yeasts added further value for sterilization purposes. These findings led to the proposal of a sterilization protocol that requires only about 30 minutes, suitable for non-enveloped phages and against Gram-negative bacteria.

Moreover, the additional component, CR, is cost-effective and has relatively low cytotoxicity comparable to caffeine. The "cleaning mixture" can be reused, and CR can be removed from aqueous solutions using a previously described protocol. This approach can potentially minimize the use of chemicals in bioreactor membrane sterilization, reducing the risk of chemical release into the environment. Congo red (CR) demonstrated protective effects on non-enveloped phages, including those isolated from the environment, while deactivating the enveloped Φ6 phage. The proposed explanation for the varying effects of CR on different viruses involves the "molecular sunscreen" mechanism. In this mechanism, CR binds to virions, providing local protection, a proposition that was confirmed through experimental evidence.

Additionally, it was proved that food colorants can successfully protect non-enveloped bacteriophages from inactivation by UV irradiation. This protection was specific only in the case of brilliant blue FCF and allowed the simultaneous use of UV and phages to treat infections caused by Gram-negative bacteria. Chapter 7 presents the membrane sterilization experiment in slightly modified system. There, instead of CR, I use the mixture of BB and PVME polymer. This modified protocol is applied to representatives of both Gram-negative and Gram-positive bacterial.

Finally, the experiments on food colorants allowed us to access a larger view of bacteriophage interactions with small molecules and the principles behind the dye-mediated UV protection of bacteriophages. It was found that certain dyes could bind

to the proteins of viral capsid. This binding is specific to basic amino acids with an additional $-NH_3^+$ group that could interact with the $-SO_3^-$ groups in the dye molecules. The aromatic groups absorb the UV radiation photons, limiting the number of these photons that effectively reach the viral genome. In the case of azo dyes, the UV radiation's energy is also absorbed by -N=N- bonds and utilized for isomerization, and despite possessing those functional groups (-N=N- turned out to be optional), the compound used as UV-protectant had to be soluble in water, due to the application in biological systems. This allowed me to explain the mechanism behind the phenomenon and distinguish the simplest feasible molecule of such UV-protectant – 4-hydroxybenzene sulfonate.

CHAPTER 6
Bacteriophage stabilization against elevated temperature

Parts of this chapter constitute research articles:

1. "*Multi-functional phage-stabilizing formulation for simultaneous protection from UV irradiation and elevated temperature",*
   Mateusz Wdowiak, Magdalena Tomczyńska, Quy Ong Khac, Aneta Karpińska, Agnieszka Wiśniewska, Rafał Zbonikowski, Francesco Stellacci, Jan Paczesny*,* submitted,
2. *"Stabilization of virions using acridinyl-flanked poly(ethylene glycol): A promising approach for enhanced viability and therapeutic efficacy*"
   Mateusz Wdowiak, Yurika Nishimura, Patryk A. Mierzejewski, Krzysztof Bielec, Witold Adamkiewicz, Grzegorz Bubak, Agnieszka Wiśniewska, Bartłomiej Bończak, Ryesuke Takeuchi, Shinobu Sato, Toshinari Maeda, Shigeori Takenaka, Satomi Yano, Haruka Ohtani, Kazunori Matsuura, Jan Paczesny, manuscript in preparation.

6.1. The principles of temperature stabilization

Many literature reports indicate that phage formulations experience a significant decrease in virulence at elevated temperatures [241,242]. Notably, some attenuated viruses in vaccine formulations were found to have their potency and infectivity decrease after storage at room temperature [243,244].

Temperature stabilization of bacteriophages is particularly important from the point of view of vaccine formulations. The great variety of vaccines includes vaccines containing attenuated viruses. Even at room temperature, the efficacy of vaccines based on attenuated viruses dramatically decreases [243]. Using the λ bacteriophage model, the Evilevitch group explained the basis of this inactivation virus inactivation by the temperature. The DNA of λ phages undergoes a temperature-induced transition, leading to structure, energy, and mobility changes. The DNA's mobility is restricted when the temperature is below the transition point. This restriction causes a delay or complete prevention of its release, even when the receptor molecule "opens" the capsid [245,246]. The vortex portal, a part of the phage baseplate, was particularly sensitive to this effect. As a result, at 65-70°C, λ phage DNA was prematurely ejected, causing infectivity loss [242,247]. The research on MS2 bacteriophage, which is considered a fine model for rhinoviruses, led to similar observations. At 72°C, MS2 virions burst, releasing genetic material [241], strongly suggesting that such a mechanism of temperature-mediated inactivation is universal among viruses.

As mentioned in the introduction (subchapter 1.4), encapsulation or freeze drying is the most common solution for phage stabilization against elevated temperatures. Neither of these methods would be suitable for agriculture purposes, such as orchard spraying, because powdered bacteriophage formulation wouldn’t still be on the surfaces of fruits or crops. For environmental purposes, polymer-mediated protection seems more suitable. Unfortunately, such formulations are not widely researched, and even though polyethylene glycol-based protocols are commonly used for the thermal stabilization of virus-based vaccines [248], their application for protecting bacteriophages has not been reported. Hence, PEG is frequently used for cosmetic formulations and was also a first-choice compound for polymer-based stabilization protocols. However, in the early stage of the study, it turned out that the protection provided by PEG was limited to particular conditions (temperature, time of exposure).

In fact, in vaccine formulations PEG is used mostly to regulate the immunogenicity, not to improve the stabilization.

To improve the versatility of PEG, a modification by adding the acridine molecules was selected. Acridine is a heterocyclic aromatic compound frequently used in organic synthesis. Due to the fact it's a "flat" molecule, acridine has the potential to intercalate with dsDNA. Hypothetically, such interaction may increase the strength and specificity of the binding to bacteriophages. Acridinyl-flanked PEG (APEG) was the next step in developing the polymer-based temperature stabilization protocol. However, the initial results were slightly better compared to non-modified PEG. Moreover, APEG polymers appeared highly sensitive to light and tended to degrade in Tris buffer solutions. After about a month from the synthesis and suspension, the stabilization rate provided by APEGs was similar to the PEGs of similar molecular mass.

These observations were a motivation for the search for non-conventional, potentially stabilizing polymers. It turned out that thermo-responsive polymers, such as poly(vinyl methyl ether) (PVME), could offer an intriguing alternative to PEG-based temperature stabilization.

6.2. Thermo-sensitive polymers and their application

PVME is classified as a thermo-sensitive polymer and is extensively studied within the poly(vinyl ether) group. Its lower critical solution temperature (LCST) is approximately 36°C, which is close to the physiological temperature of the human body [249]. In aqueous solutions, at this temperature, the equilibrium between hydrophilic interactions with water molecules and the formation of hydrogen bonds between the hydrophobic segments of PVME molecules is disrupted, favoring the creation of hydrogen bonds between polymer molecules. This leads to the dehydration of polymer chains and a reduction in the entropy of the water-PVME system [250]. In effect, above the LCST, PVME undergoes a crosslink-like reaction, causing dehydrated PVME molecules to aggregate, forming a micro-gel-like structure [251]. The process is reversible, and cooling PVME in a water solution below the LCST induces disaggregation back to coiled chains form [252]. This reversible property has been utilized with other thermo-sensitive polymers in various applications such as drug delivery, filtration, and bio separations [249]. Due to its thermo-responsive properties, PVME could enclose bacteriophages in the micro-gel-like structure in elevated temperatures,

stabilizing them against its adverse effects. Such formulation would remain in a liquid form, which could make it suitable for environmental application. Moreover, combining PVME solution with UV-protective dye would potentially protect bacteriophages against all sun-related adverse effects – UV irradiation, temperature, and drying. This chapter describes the experiments verifying the applicative potential of such formulation.

6.3. Results and discussion

6.3.1. Polymer-based stabilization against elevated temperature

The incubation of bacteriophages in PVME solutions, spanning concentrations from 1 ng/mL to 10 mg/mL, revealed that an optimal concentration for virion stabilization is 1 mg/mL (0.1%, approximately 150 μM). At this concentration, the relative survival rate was maximized, showing an approximately 400% of phage activity, compared to the control sample without the addition of the polymer (**Figure 33A**).

The initial experiments confirmed the phage-stabilizing properties of the PVME solution against exposure to high temperatures. These properties were compared with poly(ethylene glycol) (PEG) – a polymeric compound frequently used for stabilizing cosmetic requisites and vaccines, and polyvinyl pyrrolidone (PVP) – a polymeric compound commonly used as a binder in pharmaceutical tablets. This study employed linear PEG with molecular masses of 6.000 or 20.000 Da and PVP with a molecular mass of 20.000 Da (Sigma-Aldrich, Saint Louis, Missouri, USA). Hence, the linear APEG used in this experiment was of 20.000 Da, PEG and PVP of similar molecular mass were used. PVME was of 6.500 Da. Therefore, PEG 6000 (M = 6.000 Da) was used to compare if the polymer chain length affected the stabilization properties.

T4 bacteriophages were subjected to overnight incubation in TM buffer containing PEG, APEG, PVP, or PVME at the following concentrations: 100 nM, 1 μM, 100 μM, and 200 μM. Bacteriophages in the TM buffer alone were used as a control. After the overnight incubation at 4°C, the bacteriophage suspensions were incubated for 3 hours in a water bath set to 65°C and then cooled down (**Figure 33B**).

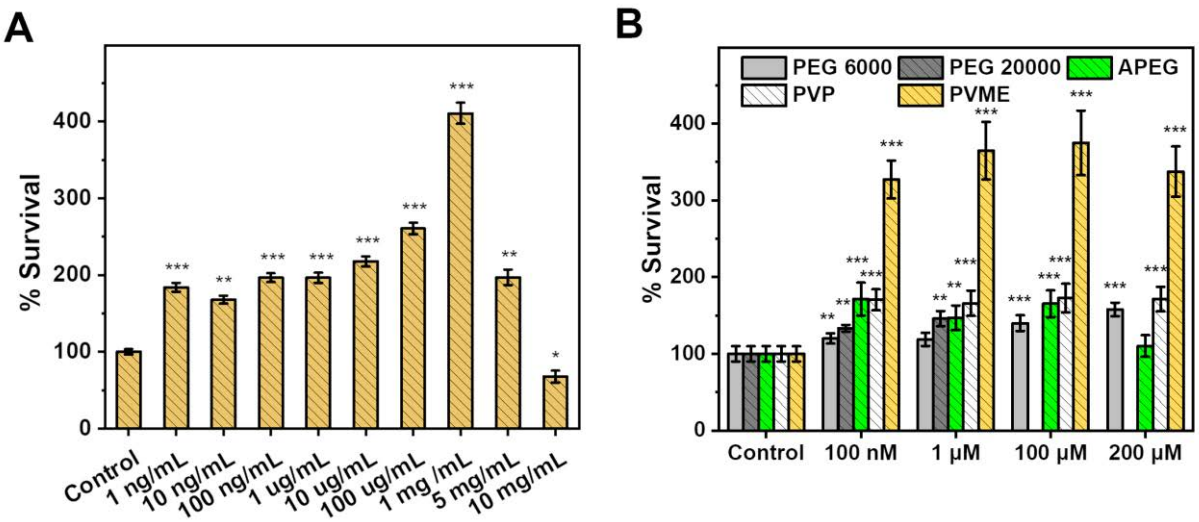

Figure 33. T4 phage stabilization using the PVME solutions. A) The effect of various concentrations of PVME solution on protecting bacteriophages from exposure to elevated temperatures is presented as the relative survival percentage. T4 phages were incubated in a PVME solution (ranging from 1 ng/mL to 10 mg/mL). B) The comparison of phage-stabilization properties of PEG, APEG, and PVME against high temperatures was performed using linear PEG 6000 (M=6.000 Da), PEG 20000 (M = 20.000 Da), APEG (M = 20.000 Da), PVP (M = 20.000 Da), and PVME (M=6.500 Da). T4 bacteriophages were exposed to 3 hours of incubation at 65°C. The statistical analysis was performed using a Student t-test, * $p < 0.05$; ** $p < 0.01$; *** $p < 0.001$.

The results indicated that the PVME solution was significantly more effective in protecting phages against high temperatures than the selected PEG polymer solutions, including the better-performing PEG 6000. Assuming that phage survival in the control samples was 100%, for 100 nM and 1 µM PEG solutions, the survival percentages were approximately 133% and 146%, respectively. However, in higher concentrations (100 µM and 200 µM), the number of active T4 phages dropped below the detection limits of the methods (about 25 PFU/mL), suggesting the possibility of additional phenomena during the incubation at 65°C, potentially involving the aggregation of bacteriophages with PEG 20000. For PEG 6000, the survival rate was ranging from 120% to 160% depending on the concentration. Better stabilization was observed for higher concentrations (100 µM, 200 µM).

As in the preliminary experiment, the APEG polymer was more effective as a temperature-stabilizer than adequate PEG. At 100 nM and 100 µM concentrations, the addition of APEG provided about 170% relative survival (compared to the control sample). Surprisingly, at 1 µM, the stabilization by PEG and APEG was comparable, and at the highest examined concentration (200 µM), no significant stabilization was observed.

For each concentration of PVP, the relative survival percentages were around 170%, indicating that PVP is a better temperature stabilizer than PEG. In 100 nM, 1 μM, and 100 μM, the PVP stabilization rate was similar to APEG. The differences were observed in 200 μM solution, where the stabilizing activity of APEG dramatically dropped, while the PVP activity remained similar. This observation suggested that PVP would be a better and more universal temperature stabilizer than PEG and its derivatives. Moreover, PVP is commercially available and significantly more stable during storage.

However, a significant increase in phage stability was observed in all examined concentrations of PVME – approximately 327% survival in 100 nM, 365% survival in 1 μM, 375% survival in 100 μM, and 338% survival in 200 μM. These results suggest that adding PVME increases the number of active bacteriophages during incubation at high temperatures about 3-4 times compared to the control samples, highlighting PVME as a more efficient temperature protectant than the selected PEGs and PVPs.

The relative survival rate gradually decreased in higher concentrations, reaching a value slightly lower than the control sample at 10 mg/mL (1%, approximately 1.5 mM). Considering these results with the UV-protective properties of food dyes, a BB-PVME formulation (containing 0.5% BB and 0.1% PVME) was prepared and selected for further studies.

6.3.2. Mechanism of PVME-mediated temperature stabilization

PVME belongs to the category of thermo-responsive polymers and is extensively studied within the poly(vinyl ether) class. This interest is primarily due to its lower critical solution temperature (LCST) of approximately 36°C, which is close to the physiological temperature of the human body [249].

In aqueous solutions, at this temperature, the balance shifts from hydrophilic interactions with water molecules to the formation of hydrogen bonds between the hydrophobic segments of PVME molecules. This leads to the dehydration of polymer chains and a reduction in the entropy of the water-PVME system [250]. Crucially, above the LCST, PVME undergoes a reversible crosslink-like reaction. This property has been employed in various applications for drug delivery, filtration, and bio separations with other thermo-sensitive polymers [249].

The initial hypothesis was that PVME could either encase bacteriophages within compact aggregates during incubation at elevated temperatures or adhere to their

surfaces. In either scenario, the polymer would effectively maintain the viral capsid integrity, preventing damage caused by elevated temperatures. However, the cryo-SEM imaging didn't show the presence of the polymer stuck onto the bacteriophages.

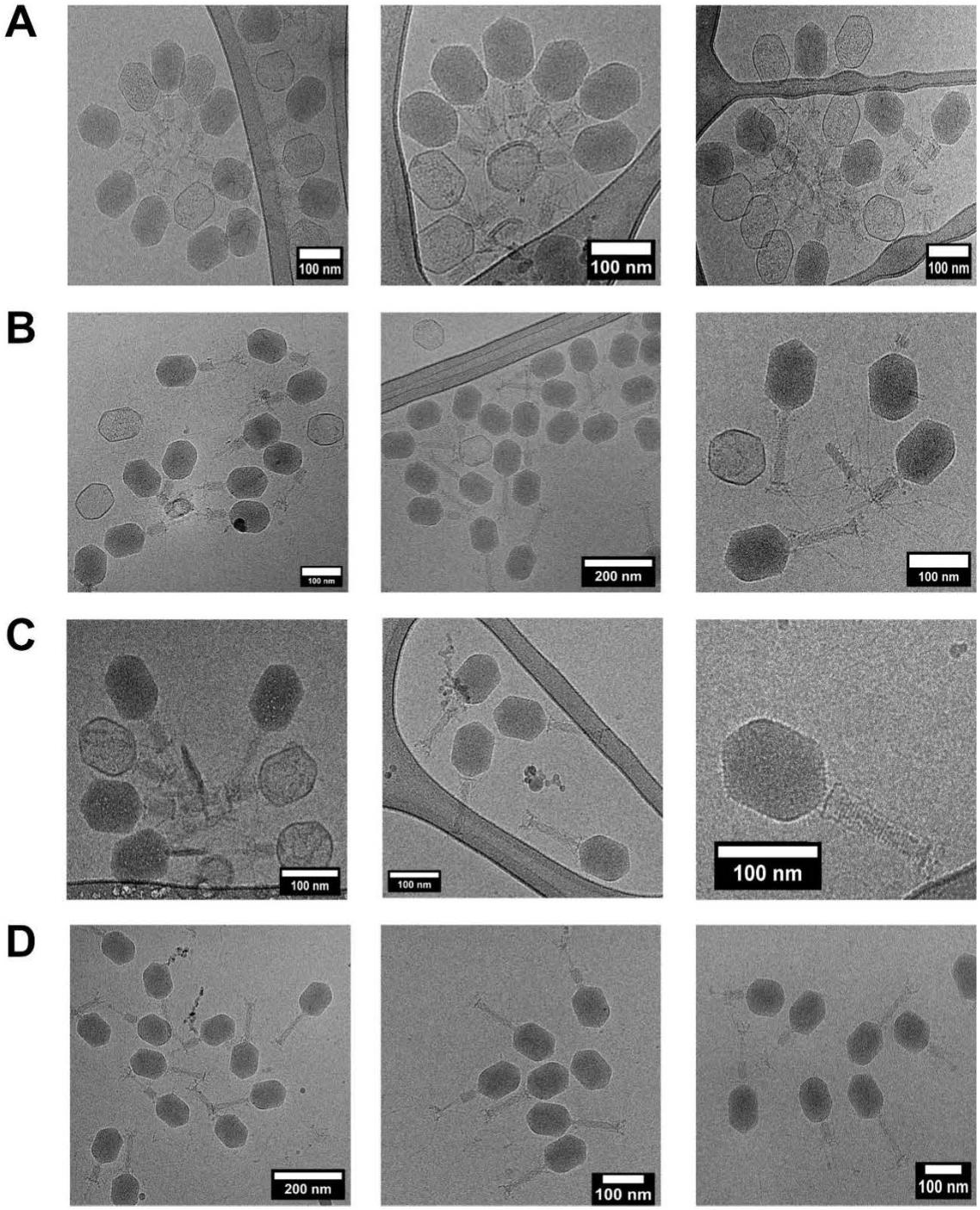

Figure 35. The cryo-EM imaging of the P22 bacteriophages incubated for 3 hours in A) TM buffer at RT, B) TM buffer at 65ºC, C) TM buffer with 0.1% PVME solution at RT, D) TM buffer with 0.1% PVME solution at 65ºC. For each sample, three different images were considered.

Instead, the imaging revealed that during the incubation at elevated temperature, bacteriophages (in the TM buffer) got severely damaged, Numerous

separated heads and sheaths were observed. With the addition of PVME polymer, the number of damaged bacteriophages was significantly reduced (**Figure 35**). The observations confirmed that adding PVME polymer reduced the number of damaged phages during exposure to the elevated temperature. Most probably, the molecules of polymer in the water solution absorb the heat energy and transform it into the energy of chemical bonds.

Differential scanning calorimetry (DSC) was also performed to confirm the repetitive character of PVME phage transition. The DSC measured the heat flow in the PVME solutions preincubated at 65°C for 3 hours. The samples were exposed to either a single cycle or two cycles of incubation. The results are presented in **Figure 36**.

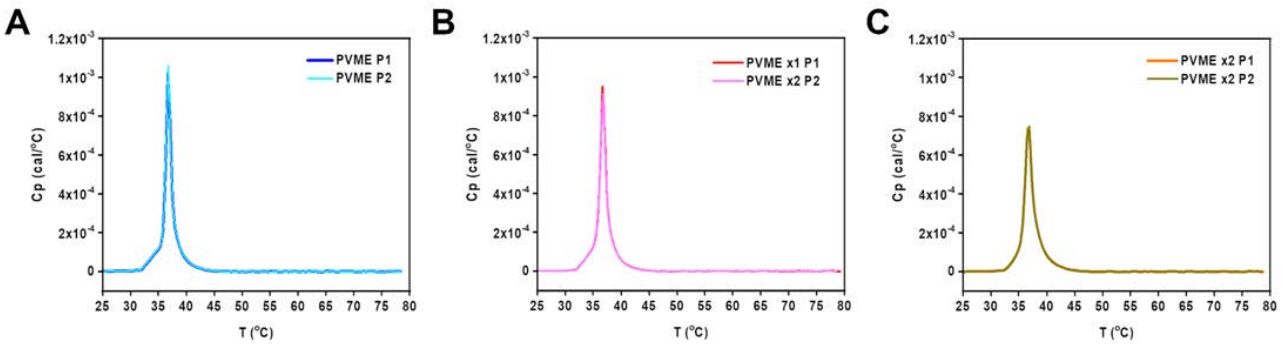

Figure 36. The heat flow in the PVME solutions exposed to A) no pre-incubation, B) a single cycle of incubation (65°C, 3 hours) and cooling, and C) two cycles of incubation and cooling.

In all the samples, an endothermic event occurred at about 36°C, which corresponded to the increase in the heat flow (CP) from 0 to about 1.1 × 10^{-3} cal/°C (**Figure 36A**). Similar events were observed for pre-incubated PVME solutions. However, the increase in heat flow was smaller with each cycle of pre-incubation - 1.0 × 10^{-3} cal/°C for PVME × 1 (**Figure 36B**) and 8.0 × 10^{-4} cal/°C for PVME × 2 (**Figure 36C**). This observation confirmed that the temperature-dependent-aggregation of PVME was a repetitive process. Therefore, the PVME-based formulations can be reused multiple times. However, some PVME molecules remained aggregated or entangled with virion with each heating-cooling cycles. This may negatively affect the stabilizing efficacy of the PVME solution after several heating-cooling cycles.

6.4. Summary

This study was one of the first to compare the efficacy of different, popularly used polymers in bulk solutions for temperature stabilization. PEG and PVP were selected

due to their wide use in drug and cosmetic formulations. The experimental results, however, presented their limited efficacy in phage stabilization. At high concentrations (>100 μM), PEG appeared to have an adverse effect on phage stability, probably due to the increased phage aggregation in the presence of the polymer. This issue was overcome by using APEG (acridine-modified PEG) of the same chain length. The stabilization with APEG had similar efficacy compared to PVP (of similar molecular mass) in the entire range of examined concentrations.

As for PVME, its toxicity has not been extensively studied, primarily because no previous studies have proposed the application of this polymer for biology-related purposes. The Material Safety Data Sheet (MSDS) for PVME suggested that the lowest lethal dose (LDLo) for humans would be about 143 mg/kg of body mass when applied orally. Therefore, PVME seems efficient and safe for humans phage-stabilizer against temperature.

CHAPTER 7

Multimodal phage stabilization from the UV irradiation and elevated temperature using BB-PVME formulation.

Parts of this chapter constitute a research article:

"*Multi-functional phage-stabilizing formulation for simultaneous protection from UV irradiation and elevated temperature"*

Mateusz Wdowiak, Magdalena Tomczyńska, Quy Ong Khac, Aneta Karpińska, Agnieszka Wiśniewska, Rafał Zbonikowski, Francesco Stellacci, Jan Paczesny, submitted.

7.1. The principle of multimodal stabilization

Fire blight, the apple trees (*Malus domestica*) disease caused by bacteria *E. amylovora*, is considered one of the most destructive in the fruit-growing industry. The disease generates annual losses of $100 million in the USA alone [167,253]. To avoid the use of chemical bactericides (harmful to plants and animals) or antibiotics (that may cause the spread of drug resistance among environmental bacteria), bacteriophage-based methods seem the most promising. However, as Chapters 5 and 6 mentioned, phages are easily inactivated by UV irradiation and elevated temperature.

In Chapter 5, I demonstrated that the chemical compounds that possess sulfonic and hydroxyl groups and aromatic rings in their structure can be successfully used as UV-protectants. Among the examined molecules (Congo red, food colorants, derivatives with sulfonic group), brilliant blue FCF dye was selected due to its specificity, efficacy, and low toxicity. The application of BB might solve the problem of bio-accessibility and improve the sterilization protocols combining bacteriophages and UV irradiation in the food industry.

In agriculture and judiciary, where phages are exposed to sunlight, UV-protectants may not be sufficient to counteract all the adverse environmental factors. Sunlight is polychromatic and represents the spectrum of visible light, a range of ultraviolet radiation (UV-A, UV-B), and the radiation from the near-infrared (near-IR) range. The sunlight may cause UV-mediated damage to DNA [171], but IR radiation also plays an important role. UV carries only 6.8%, while IR almost 10x more, i.e., 54.3%, of solar energy. This energy, while in contact with objects and living organisms, manifests as the increase in temperature [254]. Even during my initial experiments, the rapid heating of the sample to over 50°C (within 5-10 minutes) was observed upon exposure to the sunlight. This marked that in the environmental conditions, bacteriophages would simultaneously be exposed to the adverse effects of UV irradiation and temperature.

The results described in Chapter 6 suggested that using PVME at a relatively low concentration (0.1%) can successfully overcome the effects of the elevated temperature. Therefore, I hypothesized that combining BB solution with PVME solution would allow simultaneous protection against UV and elevated temperature. As a result, I tested a BB-PVME formulation in which the components were at the optimal,

experimentally validated concentrations (0.5% BB + 0.1% PVME). The formulation was then introduced for membrane sterilization from bacterial contaminations (similar to CR in Chapter 5). Additionally, I verified if the BB-PVME formulation could preserve food and eliminate bacterial contamination during sunlight exposure. That last experiment simulated the elimination of bacterial plant pathogens in environmental conditions, e.g., in orchards. Finally, there was a need to verify whether the BB-PVME formulation was harmless to mammalian cells. This test was essential; hence, the primary motivation for preparing the BB-PVME formulation was to use it in plant and food protection from bacterial contamination, preferably in environmental conditions under sunlight exposure.

7.2. Results and discussion

7.2.1. Membrane sterilization

Verifying if the formulation would be effective in membrane sterilization protocol, as proposed previously for CR, was vital, hence CR is generally considered as hazardous and potentially carcinogenic. In contrast, BB is a food additive approved by FDA and EDA. Therefore, altering CR with BB possibly allows the use of the "cleaning mixture" for food-related purposes,

The sterilization was performed similarly to the protocol presented in **Figure 29**, with a minor modification of the incubation. In this approach, bacteria were incubated on the surfaces of the syringe filter membranes for 20 minutes. The incubation was followed by 10 minutes of the UV irradiation. Moreover, the protocol was performed on the *E. coli* – T4 phage model and *B. subtilis* – Φ29 bacteriophage model to confirm the specificity towards Gram-negative bacteria. This was to confirm the efficacy of the "cleaning mixture" in dealing with Gram-negative bacteria contaminations.

The sterilization procedure involved a 20-minute incubation in either bacteriophage or control suspensions, followed by 10 minutes of exposure to UV irradiation, resulting in a total sterilization time of 30 minutes. The experiment demonstrated notable outcome variations dependent on the bacterial contaminant species. In the case of *E. coli* (Gram-negative), the BB-PVME formulation had a neutral effect, as anticipated. UV irradiation led to approximately a 3 log reduction in bacterial titer, with a slight improvement when unprotected T4 phages were added. Remarkably, the combination of UV irradiation and T4 phages in the BB-PVME

formulation reduced bacterial titer below the detection limits of the methods (around 10 CFU/mL) (**Figure 37A**).

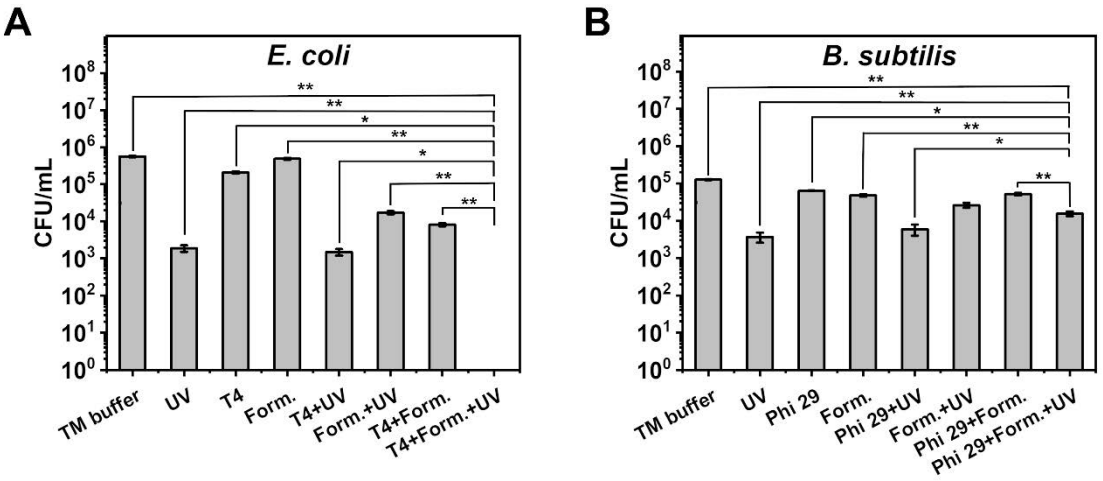

Figure 37. Sterilizing syringe filters against bacterial contaminations using bacteriophages, UV irradiation, and BB-PVME formulation. The efficacy of the sterilization protocol was examined using A) *E. coli* and T4 bacteriophages, B) *B. subtilis* and Φ29 bacteriophages. The statistical analysis was performed in relation to the control sample (TM buffer). Statistical analysis was performed using a Student t-test, * $p < 0.05$; ** $p < 0.01$; *** $p < 0.001$.

For *B. subtilis* (Gram-positive), UV irradiation resulted in almost 2 log reduction in bacteria titer. Similar results were obtained when combining UV and Φ29 bacteriophage. However, applying UV irradiation and Φ29 bacteriophage in the formulation led to only around a 1 log decrease in phage titer, indicating significantly (with $p < 0.01$) worse performance than the effect of UV irradiation alone. This observation aligned with the findings presented in **Figure 21**, which suggested that BB protected UV irradiation for Gram-positive bacteria but not for Gram-negative bacteria. It is also possible that the addition of just bacteriophages affected the irradiation of bacteria. The proteins of phage capsid could absorb or scatter a part of UV irradiation. However, due to the elimination of some bacteria by T4/ Φ29 phages, the estimation of such absobtion/scattering rate would be difficult.

Due to the UV-protective properties specific to Gram-negative bacteria, the application of BB dye appears to be dedicated to prevent contaminations from this type of bacteria. In the following experiments, only Gram-negative bacteria systems were used.

7.2.2. Food preservation

The formulation's efficacy in food sterilization was verified after confirming that the BB-PVME formulation could be successfully applied for membrane sterilization as a non-

hazardous substitute for CR. The lettuce leaves were contaminated with the suspensions of *E. coli* and *S. enterica* (both Gram-negative), i.e., the two most abundant bacteria responsible for contaminating the plant-based food articles. The sterilization procedure involved a 30-minute process, including a 20-minute incubation with bacteriophage (or control) suspensions and a subsequent 10-minute exposure to UV irradiation.

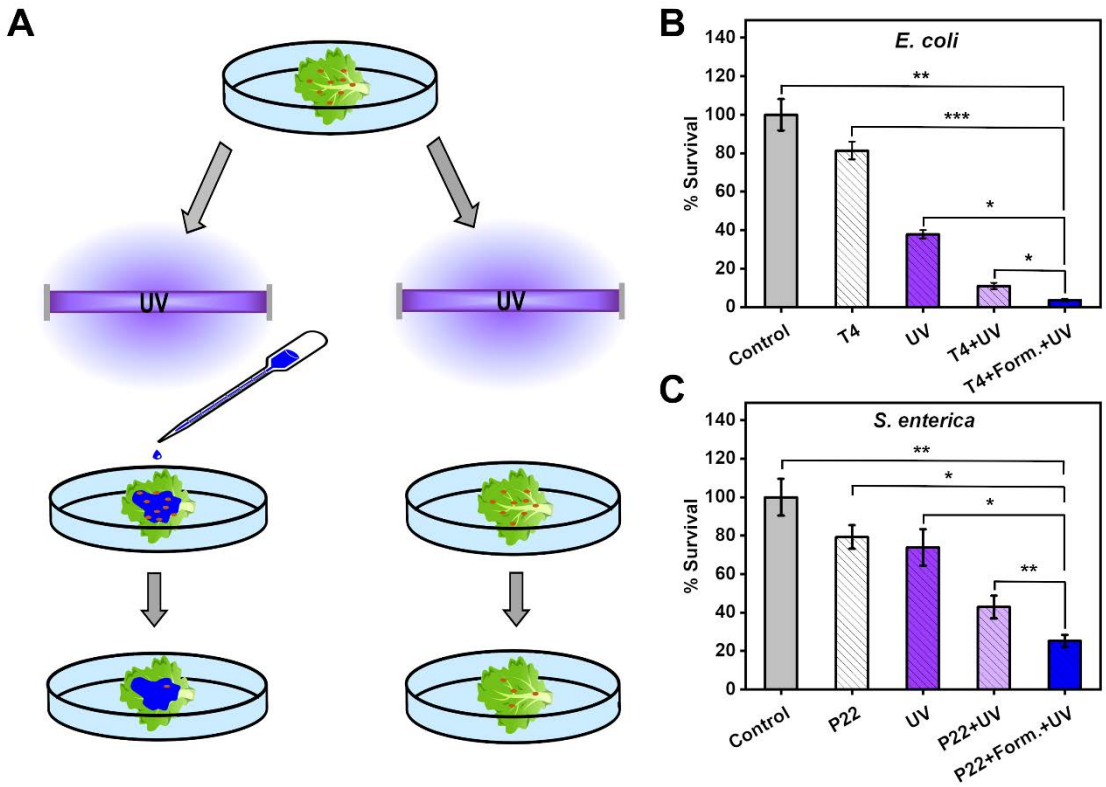

Figure 38. The evaluation of BB-PVME formulation efficacy in plant-based food preservation from bacterial contaminations. A) The schematic illustration of the experiment. Lettuce leaves were contaminated with bacterial suspension and then sterilized using UV irradiation and BB-PVME formulation with B) T4 bacteriophages against the *E. coli* contamination, and C) P22 bacteriophages against the *S. enterica* contamination. The results were presented as the relative percentage of survival, where 100% was the survival in the control sample. Statistical analysis was performed using a Student t-test, * $p < 0.05$; ** $p < 0.01$; *** $p < 0.001$.

The combination of UV irradiation and bacteriophages proved more effective in bacterial elimination, resulting in approximately an 85% reduction for *E. coli* and a 60% reduction for *S. enterica* compared to UV and bacteriophages used separately. Notably, with the incorporation of the phage-protective formulation, the efficacy of this protocol significantly improved for both *E. coli* (**Figure 38B**) – achieving about a 94% reduction in bacterial titer, and *S. enterica* (**Figure 38C**) – reaching about a 75% reduction in bacterial titer within only 30 minutes. These results suggest a promising

potential for using bacteriophages and the formulation for membrane sterilization and applications in the food industry.

7.2.3. BB-PVME formulation protects phages against heat and UV

Finally, to verify if the BB-PVME formulation would be effective under environmental conditions, the T4 bacteriophages and *E. coli* bacteria were exposed to natural and artificial sunlight (using the solar simulator). This was to compare the protective properties of the formulation in both controlled laboratory conditions, simulating the whole spectrum of sunlight and the effects of drying, and during actual sunlight exposure, when the effects of the elevated temperature needed to be considered.

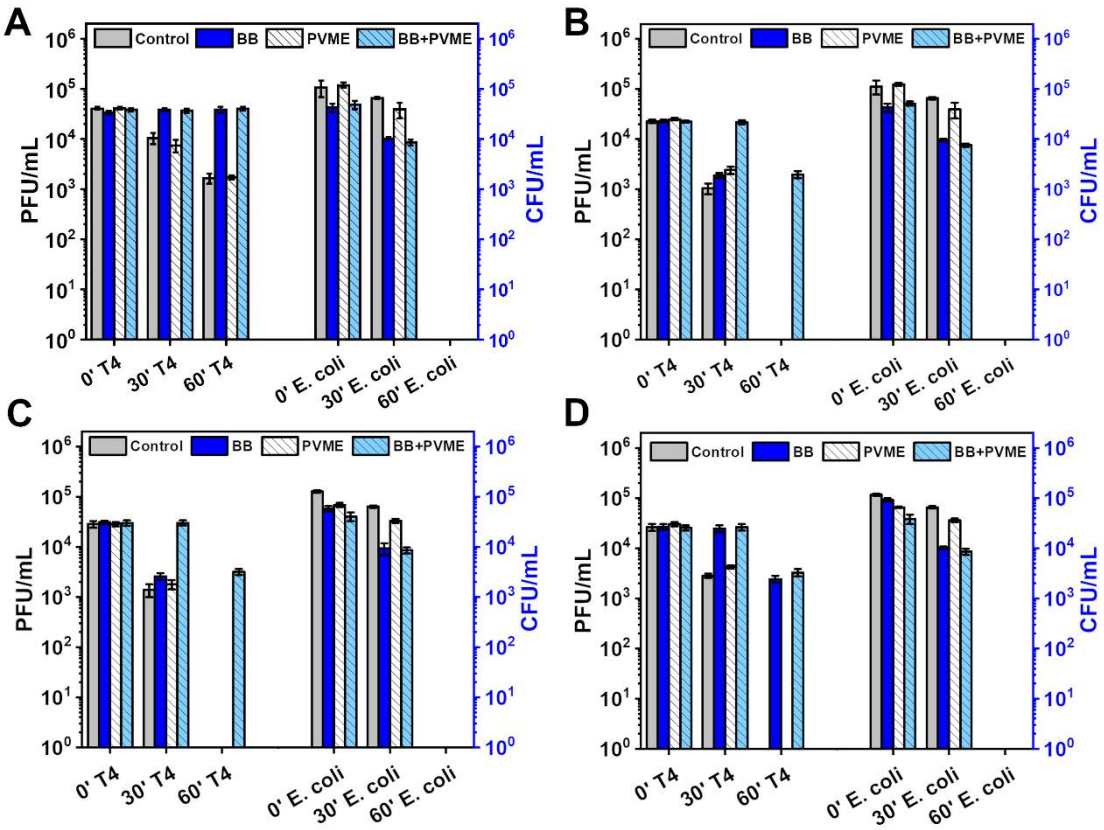

Figure 39. The evaluation of the elimination of bacterial contaminations in the sunlight exposure conditions. T4 bacteriophage and were *E. coli* BL21 suspended in TM buffer, 0.5% Brilliant blue FCF solution, 0.1% PVME solution, and the BB-PVME formulation exposed to A) Artificial sunlight in quartz cuvettes, B) Artificial sunlight on glass Petri dishes, C) Natural sunlight at the UV-index = 4, D) Natural sunlight at the UV-index = 3.

Four experimental protocols were performed and compared. First, phages in closed quartz cuvettes were exposed to a sunlight simulator (**Figure 39A**). An analogous experiment was repeated but for samples placed in open glass Petri

dishes (**Figure 39B**). Finally, phage suspensions were exposed to natural sunlight on two different days (UV-index = 3 - **Figure 39C**; UV-index = 4 - **Figure 39D**).

BB and BB-PVME did not have any significant effect on bacteria. The decrease in bacterial count was approximately similar in the solar simulator and sunlight. After 30 minutes of the experiment, a minor decrease in bacterial titer was observed. The phage-protective additives seemed to promote the elimination of bacteria. While the effect of PVME alone was almost negligible, the decrease in the bacterial titer was about 0.5 log after 30 minutes of exposure in the dye-containing samples. After 60 minutes of exposure, the reduction of bacterial titer was below the method's detection limits in all the samples. This was most likely due to the simultaneous action of three bactericidal factors – UV irradiation, elevated temperature, and bacteriophages.

The survival of bacteriophages showed slight variations depending on the duration of sunlight exposure. Following a 60-minute exposure in the solar simulator (**Figure 39A**), a decrease of about 1.5 log was observed in the control and PVME-containing samples. In dye-containing samples (BB, BB-PVME), the number of active bacteriophages remained similar throughout the incubation. Under sunlight with a UV index of 3 (approximately 75 mW/m^2) (**Figure 39D**), virtually no active phages were observed in the control sample. BB and BB-PVME successfully protected bacteriophage from sunlight exposure, reducing the decrease in phage titer to only 1 log (>4 log in control and PVME samples). However, after 30 minutes, the phage count in BB and BB-PVME was comparable to 0' time point.

The exposure to sunlight with a UV index of 4 (about 100 mW/m^2) (**Figure 39C**) was significantly more devastating to phages. About 1.5 log decrease in the control, BB, and PVME samples was observed after only 30 minutes. BB-PVME formulation successfully protected phages, resulting in almost no reduction in titer. After 60 minutes, a 1 log reduction was observed in the BB-PVME sample. In other samples, the reduction in phage titer was >4 log, inactivating virtually all phages.

The highest bacteriophage activity in the experimental system was observed when the phages were incubated in the BB-PVME formulation. The formulation effectively limited the decrease in bacteriophage titer to approximately 1 log, while in the control sample, such a decrease fell below the detection limits of the methods (around 25 PFU/mL). Although in some experiments, BB alone provided similar protection as the formulation, the protective effect of BB and PVME together was

consistent. Additionally, during exposure to natural sunlight, a rapid increase in the sample's temperature (reaching about 50°C within 5-10 minutes) was noted, making adding a temperature-stabilizing factor beneficial.

Additionally, when the experiment was conducted in glass Petri dishes instead of quartz cuvettes (**Figure 39B**), we observed an additional impact due to the samples drying. This drying effect contributed to a further reduction in bacteriophage titer. Detecting this effect was crucial because, in actual environmental conditions, a bacteriophage suspension would create a thin layer on the sterilized surface, making it susceptible to drying. Including BB-PVME proved advantageous in the experimental design accounting for drying effects (**Figure 39B**). Due to airflow in the solar simulator, samples in glass Petri plates dried during exposure and were later resuspended in the TM buffer solution before titration. After 60 minutes, active bacteriophages were only present in the BB-PVME formulation, indicating its efficacy in protecting from temperature, light, and drying. Both after 30 minutes and 60 minutes, the activity of phages in different samples was comparable to the exposure to UV index = 4 sunlight exposure (**Figure 39C**). Surprisingly, the drying had almost no effect on the survival of bacteria.

7.2.4. Cytotoxicity assay

Hence, the BB-PVME formulation's premise was its food preservation application. The potential cytotoxicity of the formulation was examined to verify if its application wouldn't harm animals (including humans) (**Figure 40**).

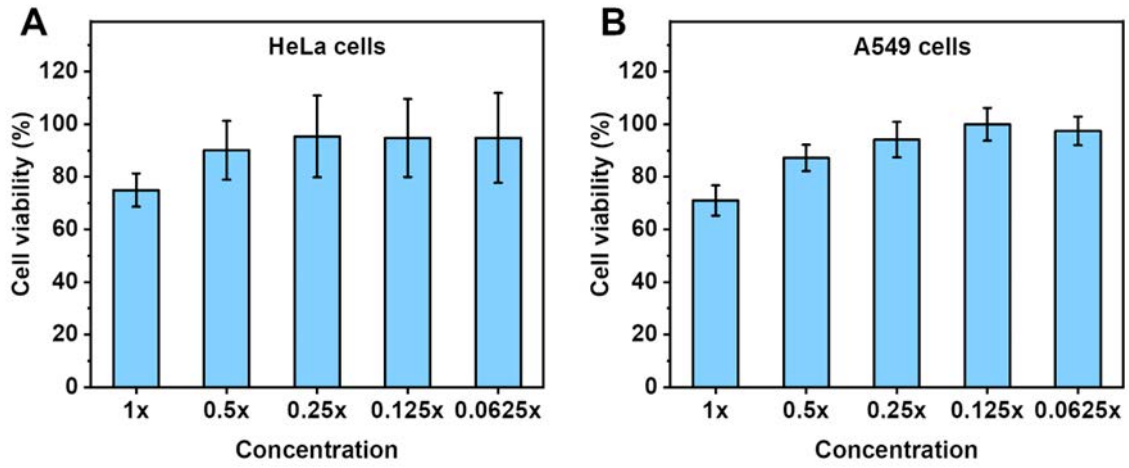

Figure 40. The cytotoxicity assay for the BB-PVME formulation was performed using the MTT protocol, and the results are presented as the percentage of cell viability, with 100% viability

as the control incubated in PBS buffer only. The toxicity of the BB-PVME formulation was assessed on two cell lines: A) HeLa and B) A549.

Cytotoxicity assay was performed on two cell lines - HeLa cells (cervical cancer) and A549 cells (lung cancer), and using the MTT proliferation/metabolic activity protocol. 6 hours of incubation in the optimal concentrations of BB (0.5%) and PVME (0.1%) revealed that the viability of both cell lines was about 70-75%, which was within an acceptable range of cytotoxicity. It is vital to note that human cells wouldn't be directly exposed to the formulation in real-life scenarios, suggesting that the toxicity would likely be significantly lower. BB is generally recognized as a non-toxic dye commonly used for staining various consumables such as candies, soft beverages, and cosmetic products like mouthwash or after-shave products [255]. In animal models, BB did not exhibit fetal toxicity when administered orally [256], and its absorption in the intestines is approximately 0.27%, with the majority of the absorbed dye being excreted from the body through urine [257].

7.3. Summary

Food colorants successfully provided universal UV protection to the non-enveloped bacteriophages. However, among eight examined food dyes, only one – brilliant blue FCF – appeared specific towards Gram-negative bacteria, which was the crucial criterion for its applicational potential. Simultaneously, it was found that thermo-responsive polymer PVME could be successfully used to stabilize bacteriophages in elevated temperature conditions. Due to the efficacy and biocompatibility of both of these substances, a BB-PVME formulation containing the best-performing concentrations of BB and PVME was prepared and applied in the membrane sterilization, food preservation, and sterilization during the sunlight exposure protocols. Proposed methods allowed for the efficient elimination of bacterial contaminations within only 30 minutes (when UV-C radiation (λ = 254 nm) was used), or 60 minutes (during the sunlight exposure). For food preservation, bacteria elimination by up to 95% was noted. Virtually all bacteria were eliminated for the membrane sterilization protocol and the sunlight-mediated sterilization (the titer reduction to below 10 CFU/mL). Therefore, using BB-PVME formulation would allow efficient and quick sterilization procedures to be applied in both enclosed and environmental conditions, which would simultaneously be harmless to the environment and living creatures.

Chapter 8
Summary and conclusions

The main goal of this thesis was to demonstrate the remarkable applicative potential of bacteriophages and to highlight the necessity of efficient phage-stabilization methods to improve the efficacy of bacteriophage-based methods. In this study, I focused on the stabilization against physical factors such as UV irradiation, temperature, and the adverse effects occurring during long-term storage. I used small-molecular compounds (dyes), polymers, and nanocoatings as protectants. I designed their applications for laboratory practice, industrial sterilization, and food preservation. Each chapter concluded a relevant project for bacteriophage-stabilization, including the methodology, mechanism of stabilization, and particular application.

In Chapter 1, I highlighted the importance of novel methods for dealing with bacterial infections related to the rapid spread of drug resistance among microorganisms. I also summarized the current state of the art regarding different methods for phage stabilization, dividing them into physical, chemical, and nanotechnology-based methods.

In Chapter 4, I described the use of gold polyoxoborate (BOA) nanocomposite for the surface modification of plastic labware to improve the long-term storage of bacteriophages. The nanocomposite reduced the phage adsorption onto the walls of the plastic labware and provided additional beneficial antibacterial and antifungal effects.

In Chapter 5, I reported the possibility of using the protein-binding dye (Congo red) to stabilize bacteriophages from the UV irradiation. The addition of the dye was neutral for Gram-negative bacteria and provided additional antifungal activity against selected yeasts. Combining bacteriophage-based studies with the spectroscopic assay, I proposed a “molecular sunscreen” mechanism behind this selective protection. This mechanism additionally explained the differences in the effects of CR towards enveloped and non-enveloped viruses, previously reported in the literature. I confirmed the detergent-like properties of CR and managed to estimate the binding constant of the dye to selected bacteriophages. Eventually, the combination of CR, bacteriophages, and UV irradiation was used to efficiently and rapidly sterilize membrane surfaces, simulating the sterilization in membrane flow bioreactors. Later, I proposed using several food colorants as harmless to humans and environmental alternatives for phage stabilization against UV radiation. Among tested dyes, only brilliant blue FCF (BB) provided a similar selectivity to Congo red; however, at significantly lower concentrations. Digging deeper into the project, I identified the

molecular basis of dye-bacteriophage interactions, confirming the necessity of the presence of sulfonic groups within the structure of a UV-protecting substance. Such molecule anchored to the amine group in the side-chains of basic aminoacids, while it's aromatic part acted as an antenna absorbing the UV radiation. In the case of the azo dyes, additional energy transfer occurs within the azo bond.

In Chapter 6, I proposed using poly(vinyl methyl ether) (PVME) for phage stabilization against elevated temperatures. Adding PVME improved phage survival during the exposure to elevated temperatures by about 400%, performing significantly better than two popularly used polymers – poly(ethylene glycol) and polyvinyl pyrroline. Combining the stabilizing properties of the dye and the polymer in best-performing concentrations, I prepared a BB-PVME formulation that allowed for simultaneous stabilization against UV irradiation and elevated temperature. Surprisingly, the formulation also overcame the adverse effect of drying.

Finally, Chapter 7 described combining the BB-PVME formulation with bacteriophages and UV-irradiation, resulting in the development of rapid and efficient protocols for membrane sterilization, food preservation, and eliminating bacterial contaminations under sunlight exposure.

All the methods used in this study consisted of novel materials or compounds that have never been used for the stabilization of biomolecules. According to the current state of the art, projects described in this thesis were the first to describe dye-mediated protection against the UV on bacteriophages, similar to the application of thermo-responsive polymers for temperature stabilization. I also pinpointed the simplest molecule for stabilization against UV radiation.

These projects demonstrate perfect balance and complementarity between molecular biology and physical chemistry methods in bacteriophage-related research. Bacteriophages are biological entities made of biopolymers (proteins, nucleic acids). Their size, however, determines relatively low concentrations in the stocks (up to 10^{13} virions per mL, effectively femtomolar up to picomolar concentrations), on the verge of the detection limits of standard analytical methods for characterization. Simultaneously, virion's size is significantly larger compared to molecules (including polymers), to large to apply standard molecular techniques, such as the gel electrophoresis. At the same time, virions are too small for direct *in situ* microscopy. Therefore, the direct observation of phage interactions with various entities

is particularly difficult. Even in microbiological research, phages are not observed directly but *via* their interactions with bacterial hosts.

Besides their biological activity, phages undergo the phenomena characteristic of non-animated objects, such as proteins, in colloids. They tend to agglomerate while stored at high concentrations and undergo structural changes when exposed to external factors, such as temperature. The capsids interact with molecules, such as dyes (CR, BB), similarly to globular proteins, *via* the amine groups of aminoacids side chains. The interactions with sulfonic compounds I presented in this thesis were previously described but in the context of phage inactivation. For instance, gold nanoparticles modified with 11-mercapto-1-undecanesulfonic acid (MUS) were selectively binding to T-phages capsids, damaging virions in effect [258]. Similarly to the majority of globular proteins, phages interact with anionic molecules, polymers, and nanoparticles.

To sum up, bacteriophages are exceptional beings of bimodal nature, somehow reminiscent of the mythological Janus, the ancient Roman god of transitions and duality. They are difficult to study using standard analytical methods of physics and chemistry, due to a relatively low number of virions in the samples. On the other hand, methods for molecular biology frequently provide only indirect characterization. For the proper understanding and optimization of phage-related processes, a larger point of view from different fields of science seems essential.

References

(1) Xavier, J. C.; Gerhards, R. E.; Wimmer, J. L. E.; Tria, F. D. K.; Martin, W. F.; Brueckner, J. The Metabolic Network of the Last Bacterial Common Ancestor. *Commun. Biol.* **2021**, *4*, 1–10. https://doi.org/10.1038/s42003-021-01918-4.

(2) Tashiro, T.; Ishida, A.; Hori, M.; Igisu, M.; Koike, M.; Mejean, P.; Takahata, N.; Sano, Y.; Komiya, T. Early Trace of Life from 3.95 Ga Sedimentary Rocks in Labrador, Canada. *Nature* **2017**, *549* (7673), 516–518. https://doi.org/10.1038/nature24019.

(3) Waterworth, S. C.; Isemonger, E. W.; Rees, E. R.; Dorrington, R. A.; Kwan, J. C. Conserved Bacterial Genomes from Two Geographically Isolated Peritidal Stromatolite Formations Shed Light on Potential Functional Guilds. *Environ. Microbiol. Reports* **2021**, *13* (2), 126–137. https://doi.org/10.1111/1758-2229.12916.

(4) Acinas, S. G.; Sánchez, P.; Salazar, G.; Cornejo-castillo, F. M.; Sebastián, M.; Logares, R.; Royo-llonch, M.; Paoli, L.; Sunagawa, S.; Hingamp, P.; Ogata, H.; Lima-mendez, G.; Roux, S.; González, J. M.; Pesant, S.; Bork, P.; Agustí, S.; Gojobori, T.; Vaqué, D.; Gasol, J. M. Deep Ocean Metagenomes Provide Insight into the Metabolic Architecture of Bathypelagic Microbial Communities. *Commun. Biol.* **2021**, *4*, 1–15. https://doi.org/10.1038/s42003-021-02112-2.

(5) Xian, W.; Salam, N.; Li, M.; Zhou, E.; Yin, Y.; Liu, Z.; Ming, Y.; Zhang, X. Network-Directed Efficient Isolation of Previously Uncultivated Chloroflexi and Related Bacteria in Hot Spring Microbial Mats. *Biofilms and Microbiomes* **2020**, No. 4, 1–10. https://doi.org/10.1038/s41522-020-0131-4.

(6) Royo-Llonch, M.; Sanchez, P.; Ruiz-Gonzales, C.; Salazar, G.; Pedros-Alio, C.; M.Sebastian; Labadie, K.; Paoli, L.; Ibarbalz, F. M.; Zinger, L.; Churcheward, B.; Coorginators, T. O.; Chaffron, S.; Eveillard, D.; Karsenti, E.; Sunagawa, S.; Winckler, P.; Karp-Boss, L.; Bowler, C.; Acinas, S. G. Compendium of 530 Metagenome-Assembled Bacterial and Archaeal Genomes from the Polar Arctic Ocean. *Nat. Microbiol.* **2021**, *6*, 1561–1574.

(7) Gong, J.; Qi, J.; Beibei, E.; Yin, Y.; Gao, D. Concentration , Viability and Size Distribution of Bacteria in Atmospheric Bioaerosols under Different Types of Pollution *. *Environ. Pollut.* **2020**, *257*, 1–11. https://doi.org/10.1016/j.envpol.2019.113485.

(8) Dassarma, P.; Antunes, A.; Simões, M. F. Earth's Stratosphere and Microbial Life. *Curr. Issues Mol. Biol.* **2020**, *38* (1), 197–244.

(9) Zheng, T.; Li, W.; Ma, Y.; Liu, J. Sewers Induce Changes in the Chemical Characteristics , Bacterial Communities , and Pathogen Distribution of Sewage and Greywater. *Environ. Res.* **2020**, *187* (May), 109628. https://doi.org/10.1016/j.envres.2020.109628.

(10) Bai, H.; He, L.; Wu, D.; Gao, F.; Zhang, M. Spread of Airborne Antibiotic Resistance from Animal Farms to the Environment : Dispersal Pattern and Exposure Risk. *Environ. Int.* **2022**, *158*, 106927. https://doi.org/10.1016/j.envint.2021.106927.

(11) Dekaboruah, E.; Vasant, M.; Dixita, S.; Anil, C.; Verma, K. Human Microbiome: An Academic Update on Human Body Site Specific Surveillance and Its Possible Role. *Arch. Microbiol.* **2020**, *202* (8), 2147–2167. https://doi.org/10.1007/s00203-020-01931-x.

(12) Nørreslet, L. B.; Agner, T.; Clausen, M. The Skin Microbiome in Inflammatory

Skin Diseases. *Curr. Dermatol. Rep.* **2020**, *9*, 141–151.
(13) Loftus, M.; Al, S.; Hassouneh, D.; Yooseph, S. Bacterial Associations in the Healthy Human Gut Microbiome across Populations. *Sci. Rep.* **2021**, *11*, 1–14. https://doi.org/10.1038/s41598-021-82449-0.
(14) Lehman, C. How Many Bacteria Live on Earth. 2017.
(15) Fouts, D. E.; Matthias, M. A.; Adhikarla, H.; Adler, B.; Amorim-, L.; Berg, D. E.; Bulach, D.; Buschiazzo, A.; Chang, Y.; Galloway, R. L.; Haake, D. A.; Haft, D. H.; Hartskeerl, R. What Makes a Bacterial Species Pathogenic ?: Comparative Genomic Analysis of the Genus Leptospira. *PLoS Negl. Trop. Dis.* **2016**, *10* (2), 1–57. https://doi.org/10.1371/journal.pntd.0004403.
(16) Punina, N. V.; Makridakis, N. M.; Remnev, M. A.; Topunov, A. F. Whole-Genome Sequencing Targets Drug-Resistant Bacterial Infections. *Hum. Genomics* **2015**, *9* (19), 1–20. https://doi.org/10.1186/s40246-015-0037-z.
(17) World Health Organization. Report on the Burden of Endemic Health Care-Associated Infection Worldwide. https://doi.org/http://whqlibdoc.who.int/publications/2011/9789241501507_eng.pdf.
(18) Report, E. technical. *The Bacterial Challenge : Time to React*; European Centre for Disease Prevention and Control and European Medicines Agency.
(19) Grace, D. Burden of Foodborne Disease in Low-Income and Middle-Income Countries and Opportunities for Scaling Food Safety Interventions. In *Food Security*; 2023; pp 1475–1488.
(20) Huang, H.; Wu, K.; Chen, H.; Wang, J.; Chen, L.; Lai, Z.; Lin, S. The Impact of the COVID- Pandemic on Nosocomial Infections : A Retrospective Analysis in a Tertiary Maternal and Child Healthcare Hospital. *Front. Public Heal.* **2023**, *11*, 1–7.
(21) Dadgostar, P. Antimicrobial Resistance: Implications and Costs. *Infect. Drug Resist.* **2019**, *12*, 3903–3910. https://doi.org/10.2147/IDR.S234610.
(22) Arason, V. A.; Sigurdsson, J. A. The Problems of Antibiotic Overuse. *Scand. J. Prim. Health Care* **2010**, *28* (2), 65–66. https://doi.org/10.3109/02813432.2010.487652.
(23) Martin, M. J.; Thottathil, S. E.; Newman, T. B. Antibiotics Overuse in Animal Agriculture : A Call to Action for Health Care Providers. *Am. J. Public Heal.* **2015**, *105* (12), 2409–2410. https://doi.org/10.2105/AJPH.2015.302870.
(24) Centers for Disease Control and Prevention. CDC: 1 in 3 Antibiotic Prescriptions Unnecessary, 2016, 1–2.
(25) Heinemann, J. A. How Antibiotics Cause Drug Resistance. *Drug Discov. Today* **1999**, *4* (2), 72–79.
(26) Matuszewska, M.; Murray, G. G. R.; Ba, X.; Wood, R.; Holmes, M. A.; Weinert, L. A. Stable Antibiotic Resistance and Rapid Human Adaptation in Livestock- -Associated MRSA. *Elife* **2022**, *11*, 1–21.
(27) Saima, S.; Fiaz, M.; Zafar, R.; Ahmed, I.; Arshad, M. *Antibiotics Resistance Mechanism*; 2019. https://doi.org/10.1016/B978-0-12-818882-8.00006-1.
(28) Schneider, C. L. *Bacteriophage-Mediated Horizontal Gene Transfer: Transduction*; 2021.
(29) Koca, O.; Altoparlak, U.; Ayyildiz, A.; Kaynar, H. Persistence of Nosocomial Pathogens on Various Fabrics. *Eurasian J. Med.* **2012**, *44* (1), 28–31. https://doi.org/10.5152/eajm.2012.06.
(30) Waxman, D. J.; Strominger, J. L. Penicillin-Binding Proteins and the Mechanism of Action of β-Lactam Antibiotics. *Annu. Rev. Biochem.* **1983**, *Vol.*

52, 825–869. https://doi.org/10.1146/annurev.bi.52.070183.004141.
(31) Willems, R. P. J.; Dijk, K. van; Vehreschild, M. J. G.; Biehn, L. M.; Ket, J. C. F.; Remmelzwaal, S.; Vanderbroucke-Grauls, C. M. J. E. Incidence of Infection with Multidrug-Resistant Gram- Negative Bacteria and Vancomycin-Resistant Enterococci in Carriers : A Systematic Review and Meta-Regression Analysis. *Lancet Infect. Dis.* **2023**, *23* (6), 719–731. https://doi.org/10.1016/S1473-3099(22)00811-8.
(32) Mancuso, G.; Gaetano, S. De; Midiri, A.; Zummo, S.; Biondo, C. The Challenge of Overcoming Antibiotic Resistance in Carbapenem-Resistant Gram-Negative Bacteria: " Attack on Titan ." *Microorg* **2023**, *11* (8), 1912.
(33) Abavisani, M.; Bostanghadiri, N.; Ghahramanpour, H.; Kodori, M.; Akrami, F.; Fathizadeh, H.; Hashemi, A.; Rastegari-pouyani, M. Colistin Resistance Mechanisms in Gram-Negative Bacteria : A Focus on Escherichia Coli. *Lett. Appl. Microbiol.* **2023**, *76*, 1–13.
(34) De Oliveira, D. M. P.; Forde, B. M.; Kidd, T. J.; Harris, P. N. A.; Schembri, M. A.; Beatson, S. A.; Paterson, D. L.; Walker, M. J. Antimicrobial Resistance in ESKAPE Pathogens. *Clin. Microbiol. Rev.* **2020**, *33* (3). https://doi.org/10.1128/CMR.00181-19.
(35) He, S.; Krainer, K. M. C. Pandemics of People and Plants : Which Is the Greater Threat to Food Security ? *Mol. Plant* **2020**, *13* (7), 933–934.
(36) Dagher, F.; Olishevska, S.; Philion, V.; Zheng, J.; Eric, D. Development of a Novel Biological Control Agent Targeting the Phytopathogen Erwinia Amylovora. *Heliyon* **2020**, *6*, 1–10. https://doi.org/10.1016/j.heliyon.2020.e05222.
(37) Kerr, A. Biological Control of Crown Gall. *Australas. Plant Pathol.* **2016**, *45*, 15–18. https://doi.org/10.1007/s13313-015-0389-9.
(38) Kuek, M.; McLean, S.; Palombo, E. Application of Bacteriophages in Food Production and Their Potential as Biocontrol Agents in the Organic Farming Industry. *Biol. Control* **2022**, *165* (20).
(39) Jonge, P. A. De; Nobrega, F. L.; Brouns, S. J. J.; Dutilh, B. E. Molecular and Evolutionary Determinants of Bacteriophage Host Range. *Trends Microbiol.* **2018**, *27* (1), 51–63. https://doi.org/10.1016/j.tim.2018.08.006.
(40) Lehti, T. A.; Pajunen, M. I.; Skog, M. S.; Finne, J. Internalization of a Polysialic Acid-Binding Escherichia Coli Bacteriophage into Eukaryotic Neuroblastoma Cells. *Nat. Commun.* **2017**, *8*, 1–12. https://doi.org/10.1038/s41467-017-02057-3.
(41) Ackermann, H. W. Phage Classification and Characterization. *Methods Mol. Biol.* **2009**, *501*, 127–140. https://doi.org/10.1007/978-1-60327-164-6_13.
(42) Sharma, S.; Chatterjee, S.; Datta, S.; Prasad, R.; Dubey, D.; Prasad, R. K.; Vairale, M. G. Bacteriophages and Its Applications: An Overview. *Folia Microbiol. (Praha).* **2017**, *62* (1), 17–55. https://doi.org/10.1007/s12223-016-0471-x.
(43) Cochlan, W. P.; Wikner, J.; Steward, G. F.; Smith, D. C.; Azam, F. Spatial Distribution of Viruses, Bacteria and Chlorophyll a in Neritic, Oceanic and Estuarine Environments. *Mar. Ecol. Prog. Ser.* **1993**, *92* (1–2), 77–87. https://doi.org/10.3354/meps092077.
(44) Dion, M. B.; Oechslin, F.; Moineau, S. Phage Diversity, Genomics and Phylogeny. *Nat. Rev. Microbiol.* **2020**, *18* (3), 125–138. https://doi.org/10.1038/s41579-019-0311-5.
(45) Baran, G. J.; Bloomfield, V. A. Tail-fiber Attachement in Bacteriophage T4D

Studied by Quasielastic Light Scattering–Band Electrophoresis. *Biopolymers* **1978**. https://doi.org/10.1002/bip.1978.360170815.
(46) Hay, I. D.; Lithgow, T. Filamentous Phages: Masters of a Microbial Sharing Economy. *EMBO Rep.* **2019**, *20* (6). https://doi.org/10.15252/embr.201847427.
(47) Harper, D. R.; Kutter, E. Bacteriophage: Therapeutic Uses. In *Encyclopedia of Life Sciences*; John Wiley & Sons, Ltd: Chichester, UK, 2003.
(48) Domingo-Calap, P.; Georgel, P.; Bahram, S. Back to the Future: Bacteriophages as Promising Therapeutic Tools. *Hla* **2016**, *87* (3), 133–140. https://doi.org/10.1111/tan.12742.
(49) Jamal, M.; Bukhari, S. M. A. U. S.; Andleeb, S.; Ali, M.; Raza, S.; Nawaz, M. A.; Hussain, T.; Rahman, S. u.; Shah, S. S. A. Bacteriophages: An Overview of the Control Strategies against Multiple Bacterial Infections in Different Fields. *J. Basic Microbiol.* **2019**, *59* (2), 123–133. https://doi.org/10.1002/jobm.201800412.
(50) Mackey, M. C.; Santillán, M.; Tyran-Kamińska, M.; Zeron, E. S. Lecture Notes on Mathematical Modelling in the Life Sciences Simple Mathematical Models of Gene Regulatory Dynamics. **2016**, 87–97. https://doi.org/10.1007/978-3-319-45318-7.
(51) Campbell, A. The Future of Bacteriophage Biology. *Nat. Rev. Genet.* **2003**, *4* (June), 1–7.
(52) Stone, E.; Campbell, K.; Grant, I. Understanding and Exploiting Phage – Host Interactions. *Viruses* **2019**, *11* (6), 1–26.
(53) Paczesny, J.; Richter, Ł.; Hołyst, R. Recent Progress in the Detection of Bacteria Using Bacteriophages: A Review. *Viruses* **2020**, *12* (8). https://doi.org/10.3390/v12080845.
(54) Farooq, U.; Ullah, M. W.; Yang, Q.; Aziz, A.; Xu, J.; Zhou, L.; Wang, S. High-Density Phage Particles Immobilization in Surface-Modified Bacterial Cellulose for Ultra-Sensitive and Selective Electrochemical Detection of Staphylococcus Aureus. *Biosens. Bioelectron.* **2020**, *157* (November 2019), 112163. https://doi.org/10.1016/j.bios.2020.112163.
(55) Machera, S. J.; Niedziółka-Jönsson, J.; Szot-Karpińska, K. Phage-Based Sensors in Medicine: A Review. *Chemosensors* **2020**, *8* (3). https://doi.org/10.3390/CHEMOSENSORS8030061.
(56) Tian, F.; Li, J.; Nazir, A.; Tong, Y. Bacteriophage – a Promising Alternative Measure for Bacterial Biofilm Control. *Infect. Drug Resist.* **2021**, *14*, 205–217. https://doi.org/10.2147/IDR.S290093.
(57) Breaker, R. R.; Banerji, A.; Joyce, G. F. Continuous in Vitro Evolution of Bacteriophage RNA Polymerase Promoters. *Biochemistry* **1994**, *33* (39), 11980–11986. https://doi.org/10.1021/bi00205a037.
(58) Zourob, M. *Recognition Receptors in Biosensors*; 2010. https://doi.org/10.1007/978-1-4419-0919-0.
(59) de Jonge, P. A.; Nobrega, F. L.; Brouns, S. J. J.; Dutilh, B. E. Molecular and Evolutionary Determinants of Bacteriophage Host Range. *Trends Microbiol.* **2019**, *27* (1), 51–63. https://doi.org/10.1016/j.tim.2018.08.006.
(60) Sulakvelidze, A.; Alavidze, Z.; J. Glenn Morris, J. Bacteriophage Therapy. *Antimicrob. Agents Chemother.* **2001**, *45* (3), 649–659. https://doi.org/10.1128/AAC.45.3.649–659.2001.
(61) Summers, W. C. The Strange History of Phage Therapy. *Bacteriophage* **2012**, *2* (2), 130–133. https://doi.org/10.4161/bact.20757.
(62) Lin, D. M.; Koskella, B.; Lin, H. C. Phage Therapy: An Alternative to Antibiotics

in the Age of Multi-Drug Resistance. *World J. Gastrointest. Pharmacol. Ther.* **2017**, *8* (3), 162. https://doi.org/10.4292/wjgpt.v8.i3.162.
(63) Parfitt, T. Georgia: An Unlikely Stronghold for Bacteriophage Therapy. *Lancet* **2005**, *365* (9478), 2166–2167. https://doi.org/10.1016/S0140-6736(05)66759-1.
(64) McCallin, S.; Alam Sarker, S.; Barretto, C.; Sultana, S.; Berger, B.; Huq, S.; Krause, L.; Bibiloni, R.; Schmitt, B.; Reuteler, G.; Brüssow, H. Safety Analysis of a Russian Phage Cocktail: From MetaGenomic Analysis to Oral Application in Healthy Human Subjects. *Virology* **2013**, *443* (2), 187–196. https://doi.org/10.1016/j.virol.2013.05.022.
(65) Goodrinde, L.; Aberdon, S. T. Bacteriophage Biocontrol and Bioprocessing: Application of Phage Therapy to Industry. *Academia* **2003**, *53* (6), 254–262.
(66) Wright, A.; Hawkins, C. H.; Änggård, E. E.; Harper, D. R. A Controlled Clinical Trial of a Therapeutic Bacteriophage Preparation in Chronic Otitis Due to Antibiotic-Resistant Pseudomonas Aeruginosa; A Preliminary Report of Efficacy. *Clin. Otolaryngol.* **2009**, *34* (4), 349–357. https://doi.org/10.1111/j.1749-4486.2009.01973.x.
(67) Dos Santos, C. A.; Seckler, M. M.; Ingle, A. P.; Gupta, I.; Galdiero, S.; Galdiero, M.; Gade, A.; Rai, M. Silver Nanoparticles: Therapeutical Uses, Toxicity, and Safety Issues. *J. Pharm. Sci.* **2014**, *103* (7), 1931–1944. https://doi.org/10.1002/jps.24001.
(68) Jault, P.; Leclerc, T.; Jennes, S.; Pirnay, J. P.; Que, Y.-A.; Resch, G.; Rousseau, A. F.; Ravat, F.; Carsin, H.; Le Floch, R.; Schaal, J. V.; Soler, C.; Fevre, C.; Arnaud, I.; Bretaudeau, L.; Gabard, J. Efficacy and Tolerability of a Cocktail of Bacteriophages to Treat Burn Wounds Infected by Pseudomonas Aeruginosa (PhagoBurn): A Randomised, Controlled, Double-Blind Phase 1/2 Trial. *Lancet Infect. Dis.* **2018**, *19* (January), 35–45. https://doi.org/10.1016/S1473-3099(18)30482-1.
(69) Voelker, R. FDA Approves Bacteriophage Trial. *Jama* **2019**, *321* (7), 638. https://doi.org/10.1001/jama.2019.0510.
(70) Kazi, M.; Annapure, U. S. Bacteriophage Biocontrol of Foodborne Pathogens. *J. Food Sci. Technol.* **2016**, *53* (3), 1355–1362. https://doi.org/10.1007/s13197-015-1996-8.
(71) Pujato, S. A.; Quiberoni, A.; Mercanti, D. J. Bacteriophages on Dairy Foods. *J. Appl. Microbiol.* **2019**, *126* (1), 14–30. https://doi.org/10.1111/jam.14062.
(72) Vonasek, E. L.; Choi, A. H.; Sanchez, J.; Nitin, N. Incorporating Phage Therapy into WPI Dip Coatings for Applications on Fresh Whole and Cut Fruit and Vegetable Surfaces. *J. Food Sci.* **2018**, *83* (7), 1871–1879. https://doi.org/10.1111/1750-3841.14188.
(73) Cadieux, B.; Colavecchio, A.; Jeukens, J.; Freschi, L.; Emond-Rheault, J. G.; Kukavica-Ibrulj, I.; Levesque, R. C.; Bekal, S.; Chandler, J. C.; Coleman, S. M.; Bisha, B.; Goodridge, L. D. Prophage Induction Reduces Shiga Toxin Producing Escherichia Coli (STEC) and Salmonella Enterica on Tomatoes and Spinach: A Model Study. *Food Control* **2018**, *89*, 250–259. https://doi.org/10.1016/j.foodcont.2018.02.001.
(74) Alves, D.; Marques, A.; Milho, C.; Costa, M. J.; Pastrana, L. M.; Cerqueira, M. A.; Sillankorva, S. M. Bacteriophage ΦIBB-PF7A Loaded on Sodium Alginate-Based Films to Prevent Microbial Meat Spoilage. *Int. J. Food Microbiol.* **2019**, *291* (November 2018), 121–127. https://doi.org/10.1016/j.ijfoodmicro.2018.11.026.

(75) Huang, K.; Nitin, N. Edible Bacteriophage Based Antimicrobial Coating on Fish Feed for Enhanced Treatment of Bacterial Infections in Aquaculture Industry. *Aquaculture* **2019**, *502* (September 2018), 18–25. https://doi.org/10.1016/j.aquaculture.2018.12.026.
(76) Sarhan, W. A.; Azzazy, H. M. E. Phage Approved in Food, Why Not as a Therapeutic? *Expert Rev. Anti. Infect. Ther.* **2015**, *13* (1), 91–101. https://doi.org/10.1586/14787210.2015.990383.
(77) Mamane-Gravetz, H.; Linden, K. G.; Cabaj, A.; Sommer, R. Spectral Sensitivity of Bacillus Subtilis Spores and MS2 Coliphage for Validation Testing of Ultraviolet Reactors for Water Disinfection. *Environ. Sci. Technol.* **2005**, *39* (20), 7845–7852. https://doi.org/10.1021/es048446t.
(78) Yang, W.; Cai, C.; Dai, X. Interactions between Virus Surrogates and Sewage Sludge Vary by Viral Analyte: Recovery, Persistence, and Sorption. *Water Res.* **2022**, *210*, 117995. https://doi.org/10.1016/j.watres.2021.117995.
(79) Shirasaki, N.; Matsushita, T.; Matsui, Y.; Urasaki, T.; Ohno, K. Comparison of Behaviors of Two Surrogates for Pathogenic Waterborne Viruses, Bacteriophages Qβ and MS2, during the Aluminum Coagulation Process. *Water Res.* **2009**, *43* (3), 605–612. https://doi.org/10.1016/j.watres.2008.11.002.
(80) Fedorenko, A.; Grinberg, M.; Orevi, T.; Kashtan, N. Survival of the Enveloped Bacteriophage Phi6 (a Surrogate for SARS-CoV-2) in Evaporated Saliva Microdroplets Deposited on Glass Surfaces. *Sci. Rep.* **2020**, *10* (1), 1–10. https://doi.org/10.1038/s41598-020-79625-z.
(81) Havelaar, A. H.; Meulemans, C. C. E.; Pot-Hogeeoom, W. M.; Koster, J. Inactivation of Bacteriophage MS2 in Wastewater Effluent with Monochromatic and Polychromatic Ultraviolet Light. *Water Res.* **1990**, *24* (11), 1387–1393. https://doi.org/10.1016/0043-1354(90)90158-3.
(82) String, G. M.; White, M. R.; Gute, D. M.; Mühlberger, E.; Lantagne, D. S. Selection of a SARS-CoV-2 Surrogate for Use in Surface Disinfection Efficacy Studies with Chlorine and Antimicrobial Surfaces. *Environ. Sci. Technol. Lett.* **2021**. https://doi.org/10.1021/acs.estlett.1c00593.
(83) Raza, S.; Wdowiak, M.; Paczesny, J. An Overview of Diverse Strategies To Inactivate Enterobacteriaceae - Targeting Bacteriophages. *EcoSal Plus* **2023**, 1–22.
(84) Block, K. A.; Trusiak, A.; Katz, A.; Gottlieb, P.; Alimova, A.; Wei, H.; Morales, J.; Rice, W. J.; Steiner, J. C. Disassembly of the Cystovirus Φ{symbol}6 Envelope by Montmorillonite Clay. *Microbiologyopen* **2014**, *3* (1), 42–51. https://doi.org/10.1002/mbo3.148.
(85) Goldsmith, C. S.; Miller, S. E.; Martines, R. B.; Bullock, H. A.; Zaki, S. R. Electron Microscopy of SARS-CoV-2: A Challenging Task. *Lancet* **2020**, *395* (10238), e99. https://doi.org/10.1016/S0140-6736(20)31188-0.
(86) Wdowiak, M.; Paczesny, J.; Raza, S.; Wdowiak, M.; Paczesny, J.; Raza, S. Enhancing the Stability of Bacteriophages Using Physical , Enhancing the Stability Bacteriophages Using Chemical , and Nano - Based of Approaches : A Review Chemical , and Nano-Based Approaches : A Review Pharmaceutics. **2022**.
(87) Bagińska, N.; Grygiel, I.; Orwat, F.; Harhala, M. A.; Jędrusiak, A.; Gębarowska, E.; Letkiewicz, S.; Górski, A.; Matysiak, E. J. Stability Study in Selected Conditions and Biofilm - Reducing Activity of Phages Active against Drug - Resistant Acinetobacter Baumannii. *Sci. Rep.* **2024**, *14*, 1–16.

https://doi.org/10.1038/s41598-024-54469-z.
(88) Brigati, J. R.; Petrenko, V. A. Thermostability of Landscape Phage Probes. *Anal. Bioanal. Chem.* **2005**, *382* (6), 1346–1350. https://doi.org/10.1007/s00216-005-3289-y.
(89) Nobrega, F. L.; Costa, A. R.; Santos, J. F.; Siliakus, M. F.; Van Lent, J. W. M.; Kengen, S. W. M.; Azeredo, J.; Kluskens, L. D. Genetically Manipulated Phages with Improved PH Resistance for Oral Administration in Veterinary Medicine. *Sci. Rep.* **2016**, *6* (May 2017). https://doi.org/10.1038/srep39235.
(90) Olofsson, L.; Ankarloo, J.; Andersson, P. O.; Nicholls, I. A. Filamentous Bacteriophage Stability in Non-Aqueous Media. *Chem. Biol.* **2001**, *8* (7), 661–671. https://doi.org/10.1016/S1074-5521(01)00041-2.
(91) Jończyk-Matysiak, E.; Łodej, N.; Kula, D.; Owczarek, B.; Orwat, F.; Międzybrodzki, R.; Neuberg, J.; Bagińska, N.; Weber-Dąbrowska, B.; Górski, A. Factors Determining Phage Stability/Activity: Challenges in Practical Phage Application. *Expert Rev. Anti. Infect. Ther.* **2019**, *17* (8), 583–606. https://doi.org/10.1080/14787210.2019.1646126.
(92) Hess, K. L.; Jewell, C. M. Phage Display as a Tool for Vaccine and Immunotherapy Development. *Bioeng. Transl. Med.* **2020**, *5* (1), 1–15. https://doi.org/10.1002/btm2.10142.
(93) Van Belleghem, J. D.; Dąbrowska, K.; Vaneechoutte, M.; Barr, J. J.; Bollyky, P. L. Interactions between Bacteriophage, Bacteria, and the Mammalian Immune System. *Viruses* **2019**, *11* (1). https://doi.org/10.3390/v11010010.
(94) Łusiak-Szelachowska, M.; Zaczek, M.; Weber-Dabrowska, B.; Międzybrodzki, R.; Kłak, M.; Fortuna, W.; Letkiewicz, S.; Rogóz, P.; Szufnarowski, K.; Jończyk-Matysiak, E.; Owczarek, B.; Górski, A. Phage Neutralization by Sera of Patients Receiving Phage Therapy. *Viral Immunol.* **2014**, *27* (6), 295–304. https://doi.org/10.1089/vim.2013.0128.
(95) Cisek, A. A.; Dąbrowska, I.; Gregorczyk, K. P.; Wyżewski, Z. Phage Therapy in Bacterial Infections Treatment: One Hundred Years After the Discovery of Bacteriophages. *Curr. Microbiol.* **2017**, *74* (2), 277–283. https://doi.org/10.1007/s00284-016-1166-x.
(96) Ye, Y.; Chang, P. H.; Hartert, J.; Wigginton, K. R. Reactivity of Enveloped Virus Genome, Proteins, and Lipids with Free Chlorine and UV254. *Environ. Sci. Technol.* **2018**, *52* (14), 7698–7708. https://doi.org/10.1021/acs.est.8b00824.
(97) Pinto, F.; Maillard, J. Y.; Denyer, S. P. Effect of Surfactants, Temperature, and Sonication on the Virucidal Activity of Polyhexamethylene Biguanide against the Bacteriophage MS2. *Am. J. Infect. Control* **2010**, *38* (5), 393–398. https://doi.org/10.1016/j.ajic.2009.08.012.
(98) Tanaka, Y.; Yasuda, H.; Kurita, H.; Takashima, K.; Mizuno, A. Analysis of the Inactivation Mechanism of Bacteriophage ΦX174 by Atmospheric Pressure Discharge Plasma. *Conf. Rec. - IAS Annu. Meet. (IEEE Ind. Appl. Soc.* **2012**, *50* (2), 1397–1401. https://doi.org/10.1109/IAS.2012.6373981.
(99) de Vries, C. R.; Chen, Q.; Demirdjian, S.; Kaber, G.; Khosravi, A.; Liu, D.; Van Belleghem, J. D.; Bollyky, P. L. Phages in Vaccine Design and Immunity; Mechanisms and Mysteries. *Curr. Opin. Biotechnol.* **2021**, *68*, 160–165. https://doi.org/10.1016/j.copbio.2020.11.002.
(100) Bazan, J.; Całkosiński, I.; Gamian, A. Phage Displaya Powerful Technique for Immunotherapy: 1. Introduction and Potential of Therapeutic Applications. *Hum. Vaccines Immunother.* **2012**, *8* (12), 1817–1828. https://doi.org/10.4161/hv.21703.

(101) N.G, McCrum, C.P. Buckley, C. B. B. *Principles of Polymer Engineering*; Oxford University Press, 1997.
(102) Lee, J. C.; Timasheff, S. N. The Stabilization of Proteins by Sucrose. *J. Biol. Chem.* **1981**, *256* (14), 7193–7201. https://doi.org/10.1016/s0021-9258(19)68947-7.
(103) He, F.; Woods, C. E.; Litowski, J. R.; Roschen, L. A.; Gadgil, H. S.; Razinkov, V. I.; Kerwin, B. A. Effect of Sugar Molecules on the Viscosity of High Concentration Monoclonal Antibody Solutions. *Pharm. Res.* **2011**, *28* (7), 1552–1560. https://doi.org/10.1007/s11095-011-0388-7.
(104) Walter, T. S.; Ren, J.; Tuthill, T. J.; Rowlands, D. J.; Stuart, D. I.; Fry, E. E. A Plate-Based High-Throughput Assay for Virus Stability and Vaccine Formulation. *J. Virol. Methods* **2012**, *185* (1), 166–170. https://doi.org/10.1016/j.jviromet.2012.06.014.
(105) Alcock, R.; Cottingham, M. G.; Rollier, C. S.; Furze, J.; De Costa, S. D.; Hanlon, M.; Spencer, A. J.; Honeycutt, J. D.; Wyllie, D. H.; Gilbert, S. C.; Bregu, M.; Hill, A. V. S. Long-Term Thermostabilization of Live Poxviral and Adenoviral Vaccine Vectors at Supraphysiological Temperatures in Carbohydrate Glass. *Sci. Transl. Med.* **2010**, *2* (19). https://doi.org/10.1126/scitranslmed.3000490.
(106) Kanta, C.; Siber, G. R.; Leszczynski, J.; Gupta, R. K. Stabilization of Respiratory Syncytial Virus (RSV) against Thermal Inactivation and Freeze-Thaw Cycles for Development and Control of RSV Vaccines and Immune Globulin. **1996**, *14* (15), 1417–1420.
(107) Timasheff, S. N. The Control of Protein Stability and Association by Weak Water Interactions with Water: How Do Solvents Affect These Processes? *Annu. Rev. Biophys. Biomol. Struct.* **1993**, *22*, 67–69.
(108) Wiggan, O.; Livengood, J. A.; Silengo, S. J.; Kinney, R. M.; Osorio, J. E.; Huang, C. Y. H.; Stinchcomb, D. T. Novel Formulations Enhance the Thermal Stability of Live-Attenuated Flavivirus Vaccines. *Vaccine* **2011**, *29* (43), 7456–7462. https://doi.org/10.1016/j.vaccine.2011.07.054.
(109) Harada, L. K.; Jãnior, W. B.; Silva, E. C.; Oliveira, T. J.; Moreli, F. C.; Oliveira Junior, J. M.; Tubino, M.; Vila, M. M. D. C.; Balcão, V. M. Bacteriophage-Based Biosensing of Pseudomonas Aeruginosa: An Integrated Approach for the Putative Real-Time Detection of Multi-Drug-Resistant Strains. *Biosensors* **2021**, *11* (4). https://doi.org/10.3390/bios11040124.
(110) Leung, V.; Szewczyk, A.; Chau, J.; Hosseinidoust, Z.; Groves, L.; Hawsawi, H.; Anany, H.; Griffiths, M. W.; Monsur Ali, M.; Filipe, C. D. M. Long-Term Preservation of Bacteriophage Antimicrobials Using Sugar Glasses. *ACS Biomater. Sci. Eng.* **2018**, *4* (11), 3802–3808. https://doi.org/10.1021/acsbiomaterials.7b00468.
(111) Trempe, J. F.; Morin, F. G.; Xia, Z.; Marchessault, R. H.; Gehring, K. Characterization of Polyacrylamide-Stabilized Pf1 Phage Liquid Crystals for Protein NMR Spectroscopy. *J. Biomol. NMR* **2002**, *22* (1), 83–87. https://doi.org/10.1023/A:1013832422428.
(112) Qi, Y.; Chilkoti, A. Protein-Polymer Conjugation-Moving beyond PEGylation. *Curr. Opin. Chem. Biol.* **2015**, *28*, 181–193. https://doi.org/10.1016/j.cbpa.2015.08.009.
(113) Goodridge, L. Designing Phage Therapeutics. *Curr. Pharm. Biotechnol.* **2010**, *11* (1), 15–27. https://doi.org/10.2174/138920110790725348.
(114) Kim, K. P.; Cha, J. D.; Jang, E. H.; Klumpp, J.; Hagens, S.; Hardt, W. D.; Lee,

K. Y.; Loessner, M. J. PEGylation of Bacteriophages Increases Blood Circulation Time and Reduces T-Helper Type 1 Immune Response. *Microb. Biotechnol.* **2008**, *1* (3), 247–257. https://doi.org/10.1111/j.1751-7915.2008.00028.x.

(115) Viertel, T. M.; Ritter, K.; Horz, H. P. Viruses versus Bacteria-Novel Approaches to Phage Therapy as a Tool against Multidrug-Resistant Pathogens. *J. Antimicrob. Chemother.* **2014**, *69* (9), 2326–2336. https://doi.org/10.1093/jac/dku173.

(116) Resch, G.; Moreillon, P.; Fischetti, V. A. PEGylating a Bacteriophage Endolysin Inhibits Its Bactericidal Activity. *AMB Express* **2011**, *1* (29), 1–5.

(117) Loh, B.; Gondil, V. S.; Manohar, P.; Khan, F. M.; Yang, H.; Leptihn, S. Encapsulation and Delivery of Therapeutic Phages. *Appl. Environ. Microbiol.* **2021**, *87* (5), 1–13. https://doi.org/10.1128/AEM.01979-20.

(118) Malik, D. J.; Sokolov, I. J.; Vinner, G. K.; Mancuso, F.; Cinquerrui, S.; Vladisavljevic, G. T.; Clokie, M. R. J.; Garton, N. J.; Stapley, A. G. F.; Kirpichnikova, A. Formulation, Stabilisation and Encapsulation of Bacteriophage for Phage Therapy. *Adv. Colloid Interface Sci.* **2017**, *249* (May), 100–133. https://doi.org/10.1016/j.cis.2017.05.014.

(119) Gonzalez-Menendez, E.; Fernandez, L.; Gutierrez, D.; Rodríguez, A.; Martínez, B.; Garcíal, P. Comparative Analysis of Different Preservation Techniques for the Storage of Staphylococcus Phages Aimed for the Industrial Development of Phage-Based Antimicrobial Products. *PLoS One* **2018**, *13* (10), 1–14. https://doi.org/10.1371/journal.pone.0205728.

(120) Śliwka, P.; Mituła, P.; Mituła, A.; Skaradziński, G.; Choińska-Pulit, A.; Niezgoda, N.; Weber-Dąbrowska, B.; Żaczek, M.; Skaradzińska, A. Encapsulation of Bacteriophage T4 in Mannitol-Alginate Dry Macrospheres and Survival in Simulated Gastrointestinal Conditions. *Lwt* **2019**, *99* (September 2018), 238–243. https://doi.org/10.1016/j.lwt.2018.09.043.

(121) Briot, T.; Kolenda, C.; Ferry, T.; Medina, M.; Laurent, F.; Leboucher, G.; Pirot, F. Paving the Way for Phage Therapy Using Novel Drug Delivery Approaches. *J. Control. Release* **2022**, *347* (May), 414–424. https://doi.org/10.1016/j.jconrel.2022.05.021.

(122) Pacios-michelena, S.; Rodríguez-herrera, R.; Ramos-gonzález, R.; Ilina, A.; Flores-gallegos, A. C.; Enmanuel, J.; Peña, D. Effect of Encapsulation and Natural Polyphenolic Compounds on Bacteriophage Stability and Activity on Escherichia Coli in Lactuca Sativa L . Var . Longifolia. **2022**, No. February. https://doi.org/10.1111/jfs.13000.

(123) Abdelsattar, A. S.; Abdelrahman, F.; Dawoud, A.; Connerton, I. F.; El-Shibiny, A. Encapsulation of E. Coli Phage ZCEC5 in Chitosan–Alginate Beads as a Delivery System in Phage Therapy. *AMB Express* **2019**, *9* (1). https://doi.org/10.1186/s13568-019-0810-9.

(124) Chadha, P.; Katare, O. P.; Chhibber, S. Liposome Loaded Phage Cocktail: Enhanced Therapeutic Potential in Resolving Klebsiella Pneumoniae Mediated Burn Wound Infections. *Burns* **2017**, *43* (7), 1532–1543. https://doi.org/10.1016/j.burns.2017.03.029.

(125) Sun, W.; Xu, J.; Liu, B.; Zhao, Y. Di; Yu, L.; Chen, W. Controlled Release of Metal Phenolic Network Protected Phage for Treating Bacterial Infection. *Nanotechnology* **2022**, *33* (16). https://doi.org/10.1088/1361-6528/ac4aa7.

(126) Colom, J.; Cano-Sarabia, M.; Otero, J.; Aríñez-Soriano, J.; Cortés, P.; Maspoch, D.; Llagostera, M. Microencapsulation with Alginate/CaCO 3: A

Strategy for Improved Phage Therapy. *Sci. Rep.* **2017**, *7* (September 2016), 1–10. https://doi.org/10.1038/srep41441.
(127) R.P. Patel, M.P. Patel, M. S. Spray Drying Technology: An Overview. *Indian J. Sci. Technol.* **2009**, *2* (5), 44–48.
(128) Lewicki, P. P. Design of Hot Air Drying for Better Foods. *Trends Food Sci. Technol.* **2006**, *17* (4), 153–163. https://doi.org/10.1016/j.tifs.2005.10.012.
(129) Adali, M. B.; Barresi, A. A.; Boccardo, G.; Pisano, R. Spray Freeze-Drying as a Solution to Continuous Manufacturing of Pharmaceutical Products in Bulk. *Processes* **2020**, *8* (6). https://doi.org/10.3390/PR8060709.
(130) H.W.B. Engel, L. Smith, L. G. B. The Preservation of Mycobacteriophages by Means of Freeze Drying. *Am. Rev. Respir. Dis.* **1973**, *109* (5).
(131) Cox, C. S.; Harris, W. J.; Lee, J. Viability and Electron Microscope Studies of Phages T3 and T7 Subjected to Freeze Drying, Freeze Thawing and Aerosolization. *J. Gen. Microbiol.* **1974**, *81* (1), 207–215. https://doi.org/10.1099/00221287-81-1-207.
(132) Shapira, A.; Kohn, A. The Effects of Freeze-Drying on Bacteriophage T4. *Cryobiology* **1974**, *11* (5), 452–464. https://doi.org/10.1016/0011-2240(74)90113-8.
(133) Lyophilization, F.; Merabishvili, M.; Vervaet, C.; Pirnay, J.; Vos, D. De; Verbeken, G.; Mast, J.; Chanishvili, N.; Vaneechoutte, M. Stability of Staphylococcus Aureus Phage ISP After. **2013**, *8* (7), 1–7. https://doi.org/10.1371/journal.pone.0068797.
(134) Dini, C.; de Urraza, P. J. Effect of Buffer Systems and Disaccharides Concentration on Podoviridae Coliphage Stability during Freeze Drying and Storage. *Cryobiology* **2013**, *66* (3), 339–342. https://doi.org/10.1016/j.cryobiol.2013.03.007.
(135) Zhang, Y.; Peng, X.; Zhang, H.; Watts, A. B.; Ghosh, D. Manufacturing and Ambient Stability of Shelf Freeze Dried Bacteriophage Powder Formulations. *Int. J. Pharm.* **2018**, *542* (1–2), 1–7. https://doi.org/10.1016/j.ijpharm.2018.02.023.
(136) Puapermpoonsiri, U.; Ford, S. J.; van der Walle, C. F. Stabilization of Bacteriophage during Freeze Drying. *Int. J. Pharm.* **2010**, *389* (1–2), 168–175. https://doi.org/10.1016/j.ijpharm.2010.01.034.
(137) Petsong, K.; Benjakul, S.; Vongkamjan, K. Optimization of Wall Material for Phage Encapsulation via Freeze-Drying and Antimicrobial Efficacy of Microencapsulated Phage against Salmonella. *J. Food Sci. Technol.* **2021**, *58* (5), 1937–1946. https://doi.org/10.1007/s13197-020-04705-x.
(138) Chang, R. Y. K.; Wallin, M.; Lin, Y.; Leung, S. S. Y.; Wang, H.; Morales, S.; Chan, H. K. Phage Therapy for Respiratory Infections. *Adv. Drug Deliv. Rev.* **2018**, *133*, 76–86. https://doi.org/10.1016/j.addr.2018.08.001.
(139) Ergin, F. Effect of Freeze Drying, Spray Drying and Electrospraying on the Morphological, Thermal, and Structural Properties of Powders Containing Phage Felix O1 and Activity of Phage Felix O1 during Storage. *Powder Technol.* **2022**, *404*, 117516. https://doi.org/10.1016/j.powtec.2022.117516.
(140) Vandenheuvel, D.; Singh, A.; Vandersteegen, K.; Klumpp, J.; Lavigne, R.; Van Den Mooter, G. Feasibility of Spray Drying Bacteriophages into Respirable Powders to Combat Pulmonary Bacterial Infections. *Eur. J. Pharm. Biopharm.* **2013**, *84* (3), 578–582. https://doi.org/10.1016/j.ejpb.2012.12.022.
(141) Ly, A.; Carrigy, N. B.; Wang, H.; Harrison, M.; Sauvageau, D.; Martin, A. R.; Vehring, R.; Finlay, W. H. Atmospheric Spray Freeze Drying of Sugar Solution

with Phage D29. *Front. Microbiol.* **2019**, *10* (MAR), 1–11. https://doi.org/10.3389/fmicb.2019.00488.
(142) Mumenthaler, M.; Leuenberger, H. Atmospheric Spray-Freeze Drying: A Suitable Alternative in Freeze-Drying Technology. *Int. J. Pharm.* **1991**, *72* (2), 97–110. https://doi.org/10.1016/0378-5173(91)90047-R.
(143) Vinner, G. K.; Rezaie-Yazdi, Z.; Leppanen, M.; Stapley, A. G. F.; Leaper, M. C.; Malik, D. J. Microencapsulation of Salmonella-Specific Bacteriophage Felix O1 Using Spray-Drying in a Ph-Responsive Formulation and Direct Compression Tableting of Powders into a Solid Oral Dosage Form. *Pharmaceuticals* **2019**, *12* (1), 1–14. https://doi.org/10.3390/ph12010043.
(144) Carrigy, N. B.; Liang, L.; Wang, H.; Kariuki, S.; Nagel, T. E.; Connerton, I. F.; Vehring, R. Spray-Dried Anti-Campylobacter Bacteriophage CP30A Powder Suitable for Global Distribution without Cold Chain Infrastructure. *Int. J. Pharm.* **2019**, *569*, 1–29. https://doi.org/10.1016/j.ijpharm.2019.118601.
(145) S.S.Y. Leung, T. Parumasivan, F.G. Gao, N.B. Carrigy, R. Vehring, W.H. Finlay, S. Morales, W.J.Warwick, E. Kutter, H.-K. C. Effects of Storage Conditions on the Stability of Spray Dried, Inhalable Bacteriophage Powders. *Int. J. Pharm.* **2017**, *521* (1–2), 141–149. https://doi.org/10.1016/j.ijpharm.2017.01.060.Effects.
(146) Golec, P.; Dabrowski Kamil, K.; Hejnowicz, M. S.; Gozdek, A.; Łoś, J. M.; Wegrzyn, G.; Łobocka, M. B.; Łoś, M. A Reliable Method for Storage of Tailed Phages. *J. Microbiol. Methods* **2011**, *84* (3), 486–489. https://doi.org/10.1016/j.mimet.2011.01.007.
(147) Blanco, E.; Shen, H.; Ferrari, M. Principles of Nanoparticle Design for Overcoming Biological Barriers to Drug Delivery. *Nat. Biotechnol.* **2015**, *33* (9), 941–951. https://doi.org/10.1038/nbt.3330.
(148) Jin, P.; Sha, R.; Zhang, Y.; Liu, L.; Bian, Y.; Qian, J.; Qian, J.; Lin, J.; Ishimwe, N.; Hu, Y.; Zhang, W.; Liu, Y.; Yin, S.; Ren, L.; Wen, L. P. Blood Circulation-Prolonging Peptides for Engineered Nanoparticles Identified via Phage Display. *Nano Lett.* **2019**, *19* (3), 1467–1478. https://doi.org/10.1021/acs.nanolett.8b04007.
(149) Anjum, S.; Ishaque, S.; Fatima, H.; Farooq, W.; Hano, C.; Abbasi, B. H.; Anjum, I. Emerging Applications of Nanotechnology in Healthcare Systems: Grand Challenges and Perspectives. *Pharmaceuticals* **2021**, *14* (8), 1–26. https://doi.org/10.3390/ph14080707.
(150) Jaime, E. A.; Tolibia, S. M.; Rodelo, C. G.; Salinas, R. A.; Galdámez-Martínez, A.; Dutt, A. Interaction of Virus-like Particles and Nanoparticles with Inorganic Materials for Biosensing: An Exciting Approach. *Mater. Lett.* **2022**, *307* (August 2021), 1–5. https://doi.org/10.1016/j.matlet.2021.131088.
(151) Farooq, U.; Yang, Q.; Wajid Ullah, M.; Wang, S. Principle and Development of Phage-Based Biosensors. *Biosens. Environ. Monit.* **2019**, No. August. https://doi.org/10.5772/intechopen.86419.
(152) Wang, D. B.; Cui, M. M.; Li, M.; Zhang, X. E. Biosensors for the Detection of Bacillus Anthracis. *Acc. Chem. Res.* **2021**, *54* (24), 4451–4461. https://doi.org/10.1021/acs.accounts.1c00407.
(153) Paramasivam, K.; Shen, Y.; Yuan, J.; Waheed, I.; Mao, C.; Zhou, X. Advances in the Development of Phage-Based Probes for Detection of Bio-Species. *Biosensors* **2022**, *12* (1). https://doi.org/10.3390/bios12010030.
(154) Ali, Q.; Ahmar, S.; Sohail, M. A.; Kamran, M.; Ali, M.; Saleem, M. H.; Rizwan, M.; Ahmed, A. M.; Mora-Poblete, F.; do Amaral Júnior, A. T.; Mubeen, M.; Ali,

S. Research Advances and Applications of Biosensing Technology for the Diagnosis of Pathogens in Sustainable Agriculture. *Environ. Sci. Pollut. Res.* **2021**, *28* (8), 9002–9019. https://doi.org/10.1007/s11356-021-12419-6.
(155) Sedki, M.; Chen, X.; Chen, C.; Ge, X.; Mulchandani, A. Non-Lytic M13 Phage-Based Highly Sensitive Impedimetric Cytosensor for Detection of Coliforms. *Biosens. Bioelectron.* **2020**, *148* (October 2019), 111794. https://doi.org/10.1016/j.bios.2019.111794.
(156) Wang, Y.; He, Y.; Bhattacharyya, S.; Lu, S.; Fu, Z. Recombinant Bacteriophage Cell-Binding Domain Proteins for Broad-Spectrum Recognition of Methicillin-Resistant Staphylococcus Aureus Strains. *Anal. Chem.* **2020**, *92* (4), 3340–3345. https://doi.org/10.1021/acs.analchem.9b05295.
(157) Witeof, A. E.; McClary, W. D.; Rea, L. T.; Yang, Q.; Davis, M. M.; Funke, H. H.; Catalano, C. E.; Randolph, T. W. Atomic-Layer Deposition Processes Applied to Phage λ and a Phage-like Particle Platform Yield Thermostable, Single-Shot Vaccines. *J. Pharm. Sci.* **2022**, *111* (5), 1354–1362. https://doi.org/10.1016/j.xphs.2022.01.013.
(158) Elsayed, A.; Safwat, A.; Abdelsattar, A. S.; Essam, K.; Makky, S.; El-shibiny, A.; Elsayed, A.; Safwat, A.; Abdelsattar, A. S.; Essam, K. The Antibacterial and Biofilm Inhibition Activity of Encapsulated Silver Nanoparticles in Emulsions and Its Synergistic Effect with E . Coli Bacteriophage. *Inorg. Nano-Metal Chem.* **2022**, *0* (0), 1–11. https://doi.org/10.1080/24701556.2022.2081191.
(159) Abdelsattar, A. S.; Nofal, R.; Makky, S.; Safwat, A.; Taha, A.; El-Shibiny, A. The Synergistic Effect of Biosynthesized Silver Nanoparticles and Phage Zcse2 as a Novel Approach to Combat Multidrug-Resistant Salmonella Enterica. *Antibiotics* **2021**, *10* (6). https://doi.org/10.3390/antibiotics10060678.
(160) Li, L. L.; Yu, P.; Wang, X.; Yu, S. S.; Mathieu, J.; Yu, H. Q.; Alvarez, P. J. J. Enhanced Biofilm Penetration for Microbial Control by Polyvalent Phages Conjugated with Magnetic Colloidal Nanoparticle Clusters (CNCs). *Environ. Sci. Nano* **2017**, *4* (9), 1817–1826. https://doi.org/10.1039/c7en00414a.
(161) Ahiwale, S. S.; Bankar, A. V.; Tagunde, S.; Kapadnis, B. P. A Bacteriophage Mediated Gold Nanoparticles Synthesis and Their Anti-Biofilm Activity. *Indian J. Microbiol.* **2017**, *57* (2), 188–194. https://doi.org/10.1007/s12088-017-0640-x.
(162) Abdelsattar, A. S.; Farouk, W. M.; Mohamed Gouda, S.; Safwat, A.; Hakim, T. A.; El-Shibiny, A. Utilization of Ocimum Basilicum Extracts for Zinc Oxide Nanoparticles Synthesis and Their Antibacterial Activity after a Novel Combination with Phage. *Mater. Lett.* **2022**, *309* (November 2021), 131344. https://doi.org/10.1016/j.matlet.2021.131344.
(163) Manohar, P.; Ramesh, N. Improved Lyophilization Conditions for Long-Term Storage of Bacteriophages. *Sci. Rep.* **2019**, *9* (1), 1–10. https://doi.org/10.1038/s41598-019-51742-4.
(164) Lavenburg, V. M.; Liao, Y. Te; Salvador, A.; Hsu, A. L.; Harden, L. A.; Wu, V. C. H. Effects of Lyophilization on the Stability of Bacteriophages against Different Serogroups of Shiga Toxin-Producing Escherichia Coli. *Cryobiology* **2020**, *96* (June), 85–91. https://doi.org/10.1016/j.cryobiol.2020.07.012.
(165) Duyvejonck, H.; Merabishvili, M.; Vaneechoutte, M.; de Soir, S.; Wright, R.; Friman, V. P.; Verbeken, G.; De Vos, D.; Pirnay, J. P.; Van Mechelen, E.; Vermeulen, S. J. T. Evaluation of the Stability of Bacteriophages in Different Solutions Suitable for the Production of Magistral Preparations in Belgium. *Viruses* **2021**, *13* (5), 1–11. https://doi.org/10.3390/v13050865.
(166) Cui, H.; Yuan, L.; Lin, L. Novel Chitosan Film Embedded with Liposome-

Encapsulated Phage for Biocontrol of Escherichia Coli O157:H7 in Beef. *Carbohydr. Polym.* **2017**, *177* (August), 156–164. https://doi.org/10.1016/j.carbpol.2017.08.137.
(167) Born, Y.; Bosshard, L.; Duffy, B.; Loessner, M. J.; Fieseler, L. Protection of Erwinia Amylovora Bacteriophage Y2 from UV-Induced Damage by Natural Compounds . *Bacteriophage* **2015**, *5* (4), e1074330. https://doi.org/10.1080/21597081.2015.1074330.
(168) Richter, Ł.; Księżarczyk, K.; Paszkowska, K.; Janczuk-Richter, M.; Niedziółka-Jönsson, J.; Gapiński, J.; Łoś, M.; Hołyst, R.; Paczesny, J. Adsorption of Bacteriophages on Polypropylene Labware Affects the Reproducibility of Phage Research. *Sci. Rep.* **2021**, *11* (1), 1–12. https://doi.org/10.1038/s41598-021-86571-x.
(169) Scarascia, G.; Fortunato, L.; Myshkevych, Y.; Cheng, H.; Leiknes, T. O.; Hong, P. Y. UV and Bacteriophages as a Chemical-Free Approach for Cleaning Membranes from Anaerobic Bioreactors. *Proc. Natl. Acad. Sci. U. S. A.* **2021**, *118* (37), 1–9. https://doi.org/10.1073/pnas.2016529118.
(170) Evilevitch, A.; Hohlbauch, S. V. Intranuclear HSV-1 DNA Ejection Induces Major Mechanical Transformations Suggesting Mechanoprotection of Nucleus Integrity. *Proc. Natl. Acad. Sci.* **2022**, *119* (9), 1–12. https://doi.org/10.1073/pnas.2114121119/-/DCSupplemental.Published.
(171) Yoon, J.; Lee, C.; Connor, T. R. O.; Yasui, A.; Pfeifer, G. P. The DNA Damage Spectrum Produced by Simulated Sunlight. *J. Mol. Biol.* **2000**, *299*, 681–693. https://doi.org/10.1006/jmbi.2000.3771.
(172) Martin, M. N.; Basham, J. I.; Chando, P.; Eah, S. Charged Gold Nanoparticles in Non-Polar Solvents : 10-Min Synthesis And. *Langmuir* **2010**, *26* (17), 7410–7417. https://doi.org/10.1021/la100591h.
(173) Rabe, M.; Verdes, D.; Seeger, S. Understanding Protein Adsorption Phenomena at Solid Surfaces. *Adv. Colloid Interface Sci.* **2011**, *162* (1–2), 87–106. https://doi.org/10.1016/j.cis.2010.12.007.
(174) Wdowiak, M.; Mierzejewski, P. A.; Zbonikowski, R.; Bończak, B.; Paczesny, J. Congo Red Protects Bacteriophages against UV Irradiation and Allows for the Simultaneous Use of Phages and UV for Membrane Sterilization. *Environ. Sci. Water Res. Technol.* **2023**. https://doi.org/10.1039/D2EW00913G.
(175) Pardi, N.; Hogan, M. J.; Weissman, D. Recent Advances in MRNA Vaccine Technology. *Curr. Opin. Immunol.* **2020**, *65*, 14–20. https://doi.org/10.1016/j.coi.2020.01.008.
(176) Tregoning, J. S.; Stirling, D. C.; Wang, Z.; Flight, K. E.; Brown, J. C.; Blakney, A. K.; Mckay, P. F.; Cunliffe, R. F.; Murugaiah, V.; Fox, C. B.; Beattie, M.; Tam, Y. K.; Johansson, C.; Shattock, R. J. Formulation , Inflammation , and RNA Sensing Impact the Immunogenicity of Self-Amplifying RNA Vaccines. *Mol. Ther. Nucleic Acid* **2023**, *31*, 29–42. https://doi.org/10.1016/j.omtn.2022.11.024.
(177) Knezevic, I. Stability Evaluation of Vaccines: WHO Approach. *Biologicals* **2009**, *37* (6), 357–359. https://doi.org/10.1016/j.biologicals.2009.08.004.
(178) Wybrańska Katarzyna, Paczesny Jan, Serejko Katarzyna, Sura Karolina, Włodyga Karolina, Dzięcielewski Igor, Jones Samuel T., Śliwa Agnieszka, Wybrańska Iwona, Hołyst Robert, Scherman Oren A., F. M. Gold − Oxoborate Nanocomposites and Their Biomedical Applications Katarzyna Wybran S. *Appl. Mater. Interfaces* **2015**, *7*, 3931–3939. https://doi.org/10.1021/am508979y.
(179) Javed, R.; Zia, M.; Naz, S.; Aisida, S. O.; Ain, N.; Ao, Q. Role of Capping

Agents in the Application of Nanoparticles in Biomedicine and Environmental Remediation : Recent Trends and Future Prospects. *J. Nanobiotechnology* **2020**, *18* (172), 1–15. https://doi.org/10.1186/s12951-020-00704-4.
(180) Bishop, M.; Shahid, N.; Yang, J.; Barron, A. R. Determination of the Mode and Efficacy of the Cross-Linking of Guar by Borate Using MAS 11B NMR of Borate Cross-Linked Guar in Combination with Solution 11B NMR of Model Systems. *Dalt. Trans.* **2004**, 2621–2634.
(181) Davidson, M. *Contemporary Boron Chemistry*; 200AD.
(182) Łyczek, J.; Bończak, B.; Krzymińska, I.; Giżyński, K.; Paczesny, J. Gold – Oxoborate Nanocomposite-Coated Orthodontic Brackets Gain Antibacterial Properties While Remaining Safe for Eukaryotic Cells. *J. Biomed. Mater. Res.* **2023**, No. May 2022, 996–1004. https://doi.org/10.1002/jbm.b.35208.
(183) Leifert, C.; Woodward, S. Laboratory Contamination Management : The Requirement for Microbiological Quality Assurance. *Plant Cell. Tissue Organ Cult.* **1998**, *52*, 83–88.
(184) Garvie, E. I. The Growth of Escherichia Coli in Buffer Substate and Distilled Water. *J. Bacteriol.* **1955**.
(185) Greulich, C.; Braun, D.; Peetsch, A.; Siebers, B.; Ko, M. The Toxic Effect of Silver Ions and Silver Nanoparticles towards Bacteria and Human Cells Occurs in the Same Concentration Range. *RCS Adv.* **2012**, *2*, 6981–6987. https://doi.org/10.1039/c2ra20684f.
(186) Topazio, D.; Moledina, A. Foodborne Antimicrobial Resistance (AMR): An Economic Concern. *Food Agric. Organ. United nations* **2023**, No. September. https://doi.org/10.1016/S2542-5196(19)30130-5.Using.
(187) Wernicki, A.; Nowaczek, A.; Urban-chmiel, R. Bacteriophage Therapy to Combat Bacterial Infections in Poultry. *Virol. J.* **2017**, *14*, 1–13. https://doi.org/10.1186/s12985-017-0849-7.
(188) Huang, K.; Nitin, N. Edible Bacteriophage Based Antimicrobial Coating on Fish Feed for Enhanced.Pdf. *Aquaculture* **2019**, *502*, 18–25.
(189) Skinner, K. A.; Leathers, Æ. T. D. Bacterial Contaminants of Fuel Ethanol Production. *J. Ind. Microbiol. Biotechnol.* **2004**, *9* (1), 401–408. https://doi.org/10.1007/s10295-004-0159-0.
(190) Thomas, K. C.; Hynes, S. H.; Ingledew, W. M. Influence of Medium Buffering Capacity on Inhibition of Saccharomyces Cerevisiae Growth by Acetic and Lactic Acids. *Appl. Environ. Microbiol.* **2002**, *68* (4), 1616–1623. https://doi.org/10.1128/AEM.68.4.1616.
(191) Markets and Markets. *Membrane Bioreactor Market*; 2020.
(192) Membrane Bioreactors: Global Markets.
(193) Porcelli, N.; Judd, S. Chemical Cleaning of Potable Water Membranes: A Review. *Sep. Purif. Technol.* **2010**, *71* (2), 137–143. https://doi.org/10.1016/j.seppur.2009.12.007.
(194) Kimura, K.; Hane, Y.; Watanabe, Y.; Amy, G.; Ohkuma, N. Irreversible Membrane Fouling during Ultrafiltration of Surface Water. *Water Res.* **2004**, *38* (14–15), 3431–3441. https://doi.org/10.1016/j.watres.2004.05.007.
(195) Atamer, Z.; Meike, S.; Neve, H.; Heller, K. J.; Hinrichs, J. Review: Elimination of Bacteriophages in Whey and Whey Products. *Front. Microbiol.* **2013**, *4* (JUL), 1–9. https://doi.org/10.3389/fmicb.2013.00191.
(196) Berovic, M. Sterilisation in Biotechnology. *Biotechnol. Annu. Rev.* **2005**, *11* (SUPPL.), 257–279. https://doi.org/10.1016/S1387-2656(05)11008-4.
(197) Semblante, G. U.; Hai, F. I.; Dionysiou, D. D.; Fukushi, K.; Price, W. E.;

Nghiem, L. D. Holistic Sludge Management through Ozonation: A Critical Review. *J. Environ. Manage.* **2017**, *185*, 79–95. https://doi.org/10.1016/j.jenvman.2016.10.022.
(198) Chang, Y. N.; Wei, F. I. High-Temperature Chlorine Corrosion of Metals and Alloys - A Review. *J. Mater. Sci.* **1991**, *26* (14), 3693–3698. https://doi.org/10.1007/BF01184958.
(199) Sabzevari, S.; Hofman, J. A Worldwide Review of Currently Used Pesticides' Monitoring in Agricultural Soils. *Sci. Total Environ.* **2022**, *812*.
(200) Chang, Q.; Wang, W.; Regev-yochay, G.; Lipsitch, M.; Hanage, W. P. Antibiotics in Agriculture and the Risk to Human Health : How Worried Should We Be ? *Evol. Appl.* **2014**, *8* (3), 240–247. https://doi.org/10.1111/eva.12185.
(201) Melo, A. de; Levesque, S.; S. Moineau. Phages as Friends and Enemies in Food Processing. *Curr. Opin. Biotechnol.* **2018**, *49*, 185–190. https://doi.org/10.1016/j.copbio.2017.09.004.
(202) Połaska, M.; Sokołowska, B. Review Bacteriophages—a New Hope or a Huge Problem in the Food Industry. *AIMS Microbiol.* **2019**, *5* (4), 324–347. https://doi.org/10.3934/microbiol.2019.4.324.
(203) Li, J.; Zhao, F.; Zhan, W.; Li, Z.; Zou, L.; Zhao, Q. Challenges for the Application of Bacteriophages as Effective Antibacterial Agents in the Food Industry. *J. Sci. Food Agric.* **2021**, *102* (2), 461–471. https://doi.org/10.1002/jsfa.11505.
(204) Liu, S.; Quek, S.; Huang, K. Advanced Strategies to Overcome the Challenges of Bacteriophage-Based Antimicrobial Treatments in Food and Agricultural Systems. *Crit. Rev. Food Sci. Nutr.* **2023**, 1–25. https://doi.org/10.1080/10408398.2023.2254837.
(205) Shapiro, M. Congo Red as an Ultraviolet Protectant for the Gypsy Moth (Lepidoptera: Lymantriidae) Nuclear Polyhedrosis Virus. *J. Econ. Entomol.* **1989**, *82* (2), 548–550. https://doi.org/10.1093/jee/82.2.548.
(206) Tom, E. F.; Molineux, I. J.; Paff, M. L.; Bull, J. J. Experimental Evolution of UV Resistance in a Phage. *PeerJ* **2018**, *2018* (7), 1–20. https://doi.org/10.7717/peerj.5190.
(207) Ignoffo, C. M.; Shasha, B. S.; Shapiro, M. Sunlight Ultraviolet Protection of the Heliothis Nuclear Polyhedrosis Virus through Starch-Encapsulation Technology. *J. Invertebr. Pathol.* **1991**, *57* (1), 134–136. https://doi.org/10.1016/0022-2011(91)90053-S.
(208) Shapiro, M.; Shepard, B. M. Relative Efficacies of Congo Red and Tinopal LPW on the Activity of the Gypsy Moth (Lepidoptera : Lymantriidae), Nucleopolyhedrovirus and Cypovirus. *J. Agric. Urban Entomol.* **2008**, *25* (4), 233–243.
(209) Rawal, B. D.; Vyas, G. N. Magnesium-Mediated Reversal of the Apparent Virucidal Effect of Ascorbic Acid or Congo Red Reacted in Vitro with the Human Immunodeficiency Virus. *Biologicals* **1996**, *24* (2), 113–116. https://doi.org/10.1006/biol.1996.0014.
(210) Estupinan, J.; Hanson, R. P. Congo Red and Trypan Blue as Stains for Plaque Assay of Newcastle Disease Virus. *Avian Dis.* **1969**, *13* (2), 330–339. https://doi.org/10.2307/1588501.
(211) Becht, H.; Drzeniek, R. The Effect of Azo Dyes on Myxovirus Neuraminidase and on Virus Multiplication. *J. Gen. Virol.* **1968**, *2* (2), 261–268. https://doi.org/10.1099/0022-1317-2-2-261.
(212) TUBIS, M.; BLAHD, W. H.; NORDYKE, R. A. The Preparation and Use of

Radioiodinated Congo Red in Detecting Amyloidosis. *J. Am. Pharm. Assoc. Am. Pharm. Assoc. (Baltim).* **1960**, *49* (7), 422–425. https://doi.org/10.1002/jps.3030490706.
(213) PETERS, J. M. Factors Affecting Caffeine Toxicity: A Review of the Literature. *J. Clin. Pharmacol. J. New Drugs* **1967**, *7* (3), 131–141. https://doi.org/10.1002/j.1552-4604.1967.tb00034.x.
(214) Vignesh, V.; Shanmugam, G. Removal and Recovery of Hazardous Congo Red from Aqueous Environment by Selective Natural Amino Acids in Simple Processes. *Process Biochem.* **2023**, *127*, 99–111. https://doi.org/10.1016/j.procbio.2023.02.009.
(215) Wang, J.; Cheng, J. Spectroscopic and Molecular Docking Studies of the Interactions of Sunset Yellow and Allura Red with Human Serum Albumin. *J. Food Saf.* **2022**, *43* (2), 1–12. https://doi.org/10.1111/jfs.13030.
(216) Masood, J.; Malik, A.; Mabood, F.; Saeed, M. Molecular Interaction of Sunset Yellow with Whey Protein : Multi-Spectroscopic Techniques and Computational Study. *J. Mol. Liq.* **2022**, *345*. https://doi.org/10.1016/j.molliq.2021.117838.
(217) Reichhardt, C.; Uchida, M.; O'Neil, A.; Li, R.; Prevelige, P. E.; Douglas, T. Templated Assembly of Organic–Inorganic Materials Using the Core Shell Structure of the P22 Bacteriophage. *Chem. Commun.* **2011**, *47*, 6326–6328. https://doi.org/10.1039/c1cc11215e.
(218) Caldeira, J. C.; Peabody, D. S. Stability and Assembly in Vitro of Bacteriophage PP7 Virus-like Particles. *J. Nanobiotechnology* **2007**, *10*, 1–10. https://doi.org/10.1186/1477-3155-5-10.
(219) Buckley, D.; Dharmasena, M.; Wang, H.; Huang, J.; Adams, J.; Pettigrew, C.; Fraser, A.; Jiang, X. Efficacy of Novel Aqueous Photo-Chlorine Dioxide against a Human Norovirus Surrogate , Bacteriophage MS2 and Clostridium Difficile Endospores , in Suspension , on Stainless Steel and under Greenhouse Conditions. *J. Appl. Microbiol.* **2020**, *130*, 1531–1545. https://doi.org/10.1111/jam.14887.
(220) Lendel, C.; Bolognesi, B.; Wahlström, A.; Dobson, C. M.; Gräslund, A. Detergent-like Interaction of Congo Red with the Amyloid β Peptide. *Biochemistry* **2010**, *49* (7), 1358–1360. https://doi.org/10.1021/bi902005t.
(221) Eisenstark, A.; Buzard, R. L.; Hartman, P. S. Inactivation of Phage By Near-Ultraviolet Radiation and Hydrogen Peroxide. *Photochem. Photobiol.* **1986**, *44* (5), 603–606. https://doi.org/10.1111/j.1751-1097.1986.tb04715.x.
(222) Watts, S.; Ramstedt, M.; Salentinig, S. Ethanol Inactivation of Enveloped Viruses: Structural and Surface Chemistry Insights into Phi6. *J. Phys. Chem. Lett.* **2021**, *12* (39), 9557–9563. https://doi.org/10.1021/acs.jpclett.1c02327.
(223) Kopecká, M.; Gabriel, M. The Influence of Congo Red on the Cell Wall and (1 → 3)-β-d-Glucan Microfibril Biogenesis in Saccharomyces Cerevisiae. *Arch. Microbiol.* **1992**, *158* (2), 115–126. https://doi.org/10.1007/BF00245214.
(224) Csillag, K.; Emri, T.; Rangel, D. E. N.; Pocsi, I. PH-Dependent Effect of Congo Red on the Growth of Aspergillus Nidulans and Aspergillus Niger. *Fungal Biol.* **2023**, *127*, 1180–1186. https://doi.org/10.1016/j.funbio.2022.05.006.
(225) Suzuki, T.; Campbell, J.; Kim, Y.; Swoboda, J. G.; Mylonakis, E.; Walker, S.; Gilmore, M. S. Wall Teichoic Acid Protects Staphylococcus Aureus from Inhibition by Congo Red and Other Dyes. *J. Antimicrob. Chemother.* **2012**, *67* (9), 2143–2151. https://doi.org/10.1093/jac/dks184.
(226) de Paula, H. M. C.; Coelho, Y. L.; Agudelo, A. J. P.; Rezende, J. de P.; Ferreira, G. M. D.; Ferreira, G. M. D.; Pires, A. C. dos S.; da Silva, L. H. M.

Kinetics and Thermodynamics of Bovine Serum Albumin Interactions with Congo Red Dye. *Colloids Surfaces B Biointerfaces* **2017**, *159*, 737–742. https://doi.org/10.1016/j.colsurfb.2017.08.036.
(227) Zhang, Y. Z.; Xiang, X.; Mei, P.; Dai, J.; Zhang, L. L.; Liu, Y. Spectroscopic Studies on the Interaction of Congo Red with Bovine Serum Albumin. *Spectrochim. Acta - Part A Mol. Biomol. Spectrosc.* **2009**, *72* (4), 907–914. https://doi.org/10.1016/j.saa.2008.12.007.
(228) Bérces, A.; Egyeki, M.; Fekete, A.; Horneck, G.; Kovács, G.; Panitz, C.; Rontó, G. The PUR Experiment on the EXPOSE-R Facility: Biological Dosimetry of Solar Extraterrestrial UV Radiation. *Int. J. Astrobiol.* **2015**, *14* (1), 47–53. https://doi.org/10.1017/S1473550414000287.
(229) Stefanescu, R.; Brebu, S.; Matei, M.; Risca, I. M.; Surleva, A.; Drochioiu, G. Contribution to Casein Determination by UV Spectrophotometry. *Acta Chem. Iasi* **2017**, *25* (2), 112–126. https://doi.org/10.1515/achi-2017-0011.
(230) Miura, T.; Yamamiya, C.; Sasaki, M.; Suzuki, K.; Takeuchi, H. Binding Mode of Congo Red to Alzheimer's Amyloid β-Peptide Studied by UV Raman Spectroscopy. *J. Raman Spectrosc.* **2002**, *33* (7), 530–535. https://doi.org/10.1002/jrs.869.
(231) Klunk, W. E.; Jacob, R. F.; Mason, R. P. Quantifying Amyloid by Congo Red Spectral Shift Assay. *Methods Enzymol.* **1999**, *309* (1974), 285–305. https://doi.org/10.1016/S0076-6879(99)09021-7.
(232) Scatchard, B. Y. G. The Attractions of Proteins for Small Molecules Abd Ions. *Ann. New York Acad. Sci.* **1949**, No. Sciences, 660–672.
(233) Healy, E. F. Quantitative Determination of DNA-Ligand Binding Using Fluorescence Spectroscopy. An Undergraduate Biochemistry Experiment. *J. Chem. Educ.* **2007**, *84* (8), 1304–1307. https://doi.org/10.1021/ed084p1304.
(234) Yokoyama, K.; Fisher, A. D.; Amori, A. R.; Welchons, D. R.; McKnight, R. E. Spectroscopic and Calorimetric Studies of Congo Red Dye-Amyloid Peptide Complexes. *J. Biophys. Chem.* **2010**, *01* (03), 153–163. https://doi.org/10.4236/jbpc.2010.13018.
(235) Jones, R. N. Some Factors Influencing the Ultraviolet Absorption Spectra of Polynuclear Aromatic. *J. Am. Chem. Soc.* **1945**, *232* (5), 2127–2150.
(236) Krause, R. G. E.; Goldring, J. P. D. Crystal Violet Stains Proteins in SDS-PAGE Gels and Zymograms. *Anal. Biochem.* **2019**, *566*, 107–115.
(237) Parker, M. L.; Christensen, A. C.; Boosman, A.; Stockard, J.; Young, E. T.; Doermann, A. H. Nucleotide Sequence of Bacteriophage T4 Gene 23 and the Amino Acid Sequence of Its Product. *J. Mol. Biol.* **1984**, *180*, 399–416.
(238) Li, Q.; Fokine, A.; Rossmann, M. G.; Rao, V. B. Functional Analysis of the Highly Antigenic Outer Capsid Protein , Hoc , a Virus Decoration Protein from T4-like Bacteriophages. *Mol. Microbiol.* **2010**, *77* (June), 444–455. https://doi.org/10.1111/j.1365-2958.2010.07219.x.
(239) Ayyaru, S.; Choi, J.; Ahn, Y. H. Biofouling Reduction in a MBR by the Application of a Lytic Phage on a Modified Nanocomposite Membrane. *Environ. Sci. Water Res. Technol.* **2018**, *4* (10), 1624–1638. https://doi.org/10.1039/c8ew00316e.
(240) Lee, A.; Elam, J. W.; Darling, S. B. Membrane Materials for Water Purification: Design, Development, and Application. *Environ. Sci. Water Res. Technol.* **2016**, *2* (1), 17–42. https://doi.org/10.1039/c5ew00159e.
(241) Brié, A.; Bertrand, I.; Meo, M.; Boudaud, N.; Gantzer, C. The Effect of Heat on the Physicochemical Properties of Bacteriophage MS2. *Food Environ. Virol.*

2016, *8* (4), 251–261. https://doi.org/10.1007/s12560-016-9248-2.
(242) Bauer, D. W.; Evilevitch, A. Influence of Internal DNA Pressure on Stability and Infectivity of Phage λ. *J. Mol. Biol.* **2015**, *427* (20), 3189–3200. https://doi.org/10.1016/j.jmb.2015.07.023.
(243) Kumru, O. S.; Joshi, S. B.; Smith, D. E.; Middaugh, C. R.; Prusik, T.; Volkin, D. B. Vaccine Instability in the Cold Chain: Mechanisms, Analysis and Formulation Strategies. *Biologicals*. 2014. https://doi.org/10.1016/j.biologicals.2014.05.007.
(244) Pelliccia, M.; Andreozzi, P.; Paulose, J.; D'Alicarnasso, M.; Cagno, V.; Donalisio, M.; Civra, A.; Broeckel, R. M.; Haese, N.; Silva, P. J.; Carney, R. P.; Marjomäki, V.; Streblow, D. N.; Lembo, D.; Stellacci, F.; Vitelli, V.; Krol, S. Additives for Vaccine Storage to Improve Thermal Stability of Adenoviruses from Hours to Months. *Nat. Commun.* **2016**, *7*, 1–7. https://doi.org/10.1038/ncomms13520.
(245) Evilevitch, A. The Mobility of Packaged Phage Genome Controls Ejection Dynamics. *Elife* **2018**. https://doi.org/10.7554/eLife.37345.
(246) Liu, T.; Sae-Ueng, U.; Li, D.; Lander, G. C.; Zuo, X.; Jönsson, B.; Rau, D.; Shefer, I.; Evilevitch, A. Correction: Solid-to-Fluid - Like DNA Transition in Viruses Facilitates Infection (Proc Natl Acad Sci USA (2014) 111, 41, (14675-14680) DOI: 10.1073/Pnas.1321637111). *Proc. Natl. Acad. Sci. U. S. A.* **2015**, *112* (18), E2410. https://doi.org/10.1073/pnas.1506556112.
(247) Freeman, K. G.; Behrens, M. A.; Streletzky, K. A.; Olsson, U.; Evilevitch, A. Portal Stability Controls Dynamics of DNA Ejection from Phage. *J. Phys. Chem. B* **2016**, *120* (26), 6421–6429. https://doi.org/10.1021/acs.jpcb.6b04172.
(248) Hayashi, T.; Nakagawa, F.; Ohno, Y.; Suzuki, Y. Antigen Stabilizing Hydrogels Based on Cyclodextrins and Polyethylene Glycol Act as Type-2 Adjuvants with Suppressed Local Irritation. *Eur. J. Pharm. Biopharm.* **2022**, *181* (June), 113–121. https://doi.org/10.1016/j.ejpb.2022.11.002.
(249) Roy, D.; Brooks, W. L. A.; Sumerlin, B. S. New Directions in Thermoresponsive Polymers. *Chem Soc Rev* **2013**, *42*, 7214–7243. https://doi.org/10.1039/c3cs35499g.
(250) Maeda, Y. IR Spectroscopic Study on the Hydration and the Phase Transition of Poly (Vinyl Methyl Ether) in Water. *Langmuir* **2001**, *17* (6), 1737–1742.
(251) Arndt, K.; Schmidt, T.; Reichelt, R. Thermo-Sensitive Poly (Methyl Vinyl Ether) Micro-Gel Formed by High Energy Radiation. *Polymer (Guildf).* **2001**, *42*, 6785–6791.
(252) Zhang, W. Z.; Chen, X. D.; Luo, W.; Yang, J.; Zhang, M. Q.; Zhu, F. M. Study of Phase Separation of Poly(Vinyl Methyl Ether) Aqueous Solutions with Rayleigh Scattering Technique. *Macromolecules* **2009**, *42*, 1720–1725.
(253) Wallis, A.; Carroll, J.; Cox, K. *Fire Blight*; New York State IPM Program, 2020.
(254) Cho, S.; Jung, M.; Sun, M.; Lee, S.; Kyung, Y.; Hun, D.; Wook, C.; Hyun, K.; Ho, J. Infrared plus Visible Light and Heat from Natural Sunlight Participate in the Expression of MMPs and Type I Procollagen as Well as Infiltration of Inflammatory Cell in Human Skin in Vivo. *J. Dermatol. Sci.* **2008**, *50*, 123–133. https://doi.org/10.1016/j.jdermsci.2007.11.009.
(255) Klimová, Z.; Lucová, M.; Hojerová, J.; Paz, S. Absorption of Triphenylmethane Dyes Brilliant Blue and Patent Blue through Intact Skin , Shaven Skin and Lingual Mucosa from Daily Life Products. *Food Chem. Toxicol.* **2013**, *52*, 19–27. https://doi.org/10.1016/j.fct.2012.10.027.
(256) Aguilar, F.; Dusemund, B.; Galtier, P.; Gilbert, J.; Gott, D. M.; Grilli, S.; Gurtler,

27. https://doi.org/10.1016/j.fct.2012.10.027.
(256) Aguilar, F.; Dusemund, B.; Galtier, P.; Gilbert, J.; Gott, D. M.; Grilli, S.; Gurtler, R.; Konig, J.; Lambre, C.; Larsen, J.-C.; Leblanc, J.-C.; Mortensen, A.; Parent-Massin, D.; Pratt, I.; Rietjens, I. M. C. M.; Stankovic, I.; Tobback, P.; Verguieva, T.; Woutersen, R. A. Scientific Opinion on the Re-Evaluation of Brilliant Blue FCF (E 133) as A. *EFSA J.* **2010**, *8* (11), 1–36. https://doi.org/10.2903/j.efsa.2010.1853.
(257) Brown, J. P.; Dorsky, A.; Enderlin, F. E.; Hale, R. L.; Wright, V. A.; Parkinson, T. M. Synthesis of 14C-Labelled FD & C Blue No. 1 (Brilliant Blue FCF) and Its Intestinal Absorption and Metabolic Fate in Rats. *Food Cosmet. Toxicol.* **1980**, *18*, 1–5.
(258) Richter, Ł.; Paszkowska, K.; Cendrowska, U.; Olgiati, F.; Silva, P. J.; Gasbarri, M.; Guven, Z. P.; Paczesny, J.; Stellacci, F. Broad-Spectrum Nanoparticles against Bacteriophage Infections. *Nanoscale* **2021**, *13* (44), 18684–18694. https://doi.org/10.1039/d1nr04936d.